

**SPATIAL VARIABILITY OF SOIL STRUCTURE AND ITS IMPACT ON
TRANSPORT PROCESSES AND SOME ASSOCIATED LAND QUALITIES**

Ontvangen

28 AUG 1992

IB-CARDE

CENTRALE LANDBOUWCATALOGUS



0000 0490 6836

Promotor: Dr. Ir. J. Bouma
hoogleraar in de bodeminventarisatie en landevaluatie,
speciaal gericht op de (sub)tropen

NN08201, 1532

Peter A. Finke

Spatial variability of soil structure and its impact on transport processes and some associated land qualities

Proefschrift

ter verkrijging van de graad van doctor
in de landbouw- en milieuwetenschappen
op gezag van de rector magnificus,
dr. H.C. van der Plas,
in het openbaar te verdedigen
op dinsdag 22 september 1992
des namiddags te vier uur in de Aula
van de Landbouwuniversiteit te Wageningen

im = 563901

**BIBLIOTHEEK
LANDBOUWUNIVERSITEIT
WAGENINGEN**

Voor mijn vader

STELLINGEN

1. Betrouwbaarheidsintervallen bij resultaten van punttellingen aan slijpplaten kunnen niet direct worden afgeleid van het aantal waarnemingen, wanneer deze waarnemingen op een grid zijn verzameld en ruimtelijk zijn gecorrelleerd.
van der Plas, L. and A.C. Tobi. 1965. A chart for judging the reliability of point counting results. American Journal of Science 263: 87-90.
Dit proefschrift.
2. Generalisatie van fijn-gelaagde gronden tot functionele lagen (mits zorgvuldig gedaan op basis van functionele eigenschappen) vereenvoudigt de simulatie van waterstroming zonder groot kwaliteitsverlies ten opzichte van een volledig gediscrèteerd profiel.
Dit proefschrift.
3. Egalisatie van het bodemoppervlak hoeft niet te leiden tot het afvlakken van de door variogrammen beschreven ruimtelijke structuur van aan de profielopbouw gerelateerde variabelen.
Dit proefschrift.
4. Bij de huidige hoge bemestingsnivo's is variabiliteit van de beschikbaarheid van bodemvocht een belangrijke oorzaak van ruimtelijk variërende oogstopbrengsten.
Dit proefschrift.
5. Het verdient aanbeveling om voorschriften voor maximale bemestingsnivo's niet te baseren op het al dan niet overschrijden van een normwaarde voor de uitspoeling, maar op de kans dat deze normwaarde wordt overschreden, zodat rekening kan worden gehouden met ruimtelijke variabiliteit.
6. Bij het bepalen van lokatie-specifieke bemestingsadviezen voor stikstof, zoals bij "Soil Specific Farming", wordt onvoldoende gerealiseerd dat de reactie van de gewasopbrengst op het stikstofaanbod ook lokatie-specifiek is.
7. Bij de evaluatie van het effect van een lager bemestingsadvies op gewasopbrengsten en stikstofuitspoeling dient rekening te worden gehouden met najlिंगseffecten ten gevolge van de huidige, hoge stikstofbemesting.
Neeteson, J.J. 1989. Effect of reduced fertilizer application rates on yield and nitrogen recovery of sugar beet and potatoes. Neth. J. of Agric. Sci. 37: 227-236.
Dit proefschrift.

8. Bij het opzetten van bemestingsproeven zonder rekening te houden met de natuurlijke variabiliteit van de bodem, zijn duplo's vaak geen duplo's.
9. Als alle Kretenzers leugenaars waren, zou niemand dat weten.
10. It hinders to be drunk while executing a random walk.
11. In de ruimtelijke wetenschappen is het modelleren van de ruimtelijke verdeling van een variabele van grotere praktische relevantie dan het schatten van populatieparameters.
De Gruijter, J.J. en C.J.F. ter Braak. 1990. Model-free estimation from spatial samples: a reappraisal of classical sampling theory. Math. Geol. 22(4): 407-415.
12. Het berekenen van ruimtelijke overschrijdingskansen met behulp van een door (Co-)Kriging geëxpandeerde set gegevens moet worden afgeraden, omdat bij deze expansie verlies van variantie optreedt.
Dit proefschrift.

Stellingen behorend bij het proefschrift 'Spatial variability of soil structure and its impact on transport processes and some associated land qualities'. Peter A. Finke, Wageningen, 22 September 1992.

ABSTRACT

This thesis treats the impact of soil spatial variability on spatial variability of simulated land qualities. A sequence of procedures that were done to determine this impact is described in chapters 2 and 3. The subchapters correspond to seven manuscripts that either have appeared in or have been submitted to peer-reviewed journals.

In chapter 2 attention is paid to methods to inventory spatial variability of soil characteristics related to the structure of the soil. A method was developed to construct confidence intervals to point count results in case of spatial dependency of the point observations on a soil thin section. It was concluded, that confidence intervals obtained following the traditional method by assuming all observations independent, will be much narrower than those where spatial dependency structure is taken into account.

Two other papers in chapter 2 describe a method to translate soil profile descriptions into soil physical input data for computer models that simulate solute flow. The concept of *functional layers* is introduced. A functional layer is a combination of soil layers showing comparable soil physical behaviour related to water flow. The functional layer approach was tested and accepted for examples of disturbed and thinly stratified soils by calculating functional properties of the layer under defined hydrological conditions. When functional layers are established, mapping the thickness, starting depth and type of functional layers provides spatial information about soil physical characteristics. In one paper in chapter 2 the number of necessary observations in this mapping procedure is optimized by application of geostatistical methods and a sequential sampling test.

In chapter three the impact of variability of the structure of the soil on variability of crop yields and nitrate leaching is investigated. One paper describes a field scale empirical study where barley grain yield variability is correlated to variability of soil characteristics and simulated transpiration deficits. Simulation model inputs were obtained using the functional layer approach described in chapter 2. Regression functions based on simulated transpiration deficits only could explain 43% of the variance in yields, which suggested that variability of transpiration may be an important factor causing yield variability. This hypothesis was tested in a next paper in which remote sensing estimates of the leaf area index were used to obtain estimates of the potential transpiration with a high spatial accuracy. Incorporating space- and time series of the leaf area index into a crop growth model resulted in a prediction of yield variability that could explain 39% of measured variability. Variability of plant-available water, expressed by the actual transpiration, is an important factor causing yield variability.

Two papers in chapter three describe how a combined solute flow and crop growth model was used to evaluate the spatial varying effect of fertilizing scenarios. The spatial interpolation method *Disjunctive Kriging* was used to translate spatial variability of simulated nitrate leaching into maps of the probability that a threshold leaching concentration is exceeded. It was also investigated, whether the number of simulations could be minimized using *Disjunctive CoKriging* and available spatial information. It was concluded, that different soil units within one agricultural field showed a different leaching response and crop yield response to identical fertilizer treatments, and that yield variability will increase when fertilizer levels approach the level for maximal production.

WOORD VOORAF

Bij het afronden van dit proefschrift wil ik graag degenen die hebben bijgedragen aan de totstandkoming ervan, hartelijk bedanken.

Op de eerste plaats wil ik mijn ouders bedanken voor de stimulatie tijdens mijn studie en het promotie onderzoek. Het doet mij veel verdriet, dat mijn vader de voltooiing ervan niet meer heeft mogen meemaken. Brit, jou wil ik bedanken voor je geduld en voor je niet aflatende inspanningen mij met beide voeten op de grond te houden.

Graag ook wil ik mijn promotor, Prof. Dr. J. Bouma, hartelijk bedanken voor het geven van impulsen op de juiste momenten, voor het in het zicht houden van de grote lijnen en voor het in contact brengen met de juiste mensen. Johan, zonder deze 'tertiaire arbeidsvoorwaarden' was het een stuk moeilijker geweest.

Bijzonder veel heb ik te danken aan Harry Booltink, in het begin van het onderzoek voor de assistentie bij het veldwerk en gedurende de rest van de tijd voor stimulerende discussies en minstens even stimulerende ongein. Aan Alfred Stein ben ik veel dank verschuldigd voor de begeleiding op het gebied van de geostatistiek, en aan Igor Staritsky voor het lenigen van software behoeften.

Herman Mûcher en Victor Witter, destijds beiden verbonden aan de vakgroep Fysische Geografie en Bodemkunde van de Universiteit van Amsterdam, wil ik hartelijk danken voor de efficiënte en gemoedelijke sfeer waarin we een doctoraal onderzoek uitbouwden tot een publicatie. Mijn mede-auteurs Daan Goense en Willem Jan Bosma wil ik bedanken voor hun bijdragen aan onze gemeenschappelijke manuscripten.

I would like to thank Dr. J. Hutson and Dr. R.J. Wagenet from the Center of Environmental Research, Cornell University, for introducing the LEACHN model to me. I also thank Dr. P. Robert from the Soil Science Department, University of Minnesota, for informing me about the 'Farming by Soil' concepts.

Tevens wil ik Wouter de Boer, Auke Breeuwsma, Mirjam Hack-ten Broeke, Hans Jansen en Jan Kragt (Staring Centrum), Andrea Landman (PAGV) en de bedrijfsleiding van de Prof. van Bemmelenhoeve bedanken voor de flexibele uitwisseling van gegevens en inpassing van verschillende proeven in de bedrijfsvoering. Thanks are due to EC DG-XII, for providing funding and deadlines, which stimulated both the research and its efficiency.

Tenslotte wil ik de studenten Daniel Gimenez, Ingrid Janssen, Max Kuhn, Primoz Marolt en Joost Schoute bedanken voor hun hulp bij veldwerk en gegevensverwerking, en wil ik de medewerkers van de vakgroep Bodemkunde en Geologie bedanken voor de plezierige werkomgeving.

CONTENTS

1	GENERAL INTRODUCTION	3
2	VARIABILITY OF SOIL STRUCTURE	
2.1	Reliability of point counts of pedological properties on thin sections.	13
2.2	Measuring field variability of disturbed soils for simulation purposes.	23
2.3	Obtaining basic simulation data for a heterogeneous field with stratified marine soils.	37
3	IMPACT OF SOIL STRUCTURE VARIABILITY ON TRANSPORT PROCESSES AND CROP YIELDS	
3.1	Differences in Barley grain yields as a result of soil variability.	57
3.2	Integration of remote sensing data in the simulation of spatially variable yield of potatoes.	75
3.3	Field scale variability of soil structure and its impact on crop growth and nitrate leaching in the analysis of fertilizing scenarios.	93
3.4	Application of Disjunctive CoKriging to optimize fertilizer additions on a field scale.	113
	Samenvatting	129
	Curriculum Vitae	131

CHAPTER 1
GENERAL INTRODUCTION

GENERAL INTRODUCTION

Currently, environmental pollution is recognized as a major problem (Briggs and Wilson, 1987, Ministerie van VROM, 1989). Legislation is being developed to minimize the input to the environment of substances that are poisonous to humans (dioxines, heavy metals), that cause acidic precipitation (ammonia-gas) or that cause water pollution (nitrates, biocides) and eutrofiation (phosphates).

Agricultural practices are identified as possible sources of these substances (Anderson *et al.*, 1985; van Breemen *et al.*, 1982; Hallberg, 1986), because high level inputs of fertilizers and biocides onto the soil profile are reported to lead to losses to (ground)water and atmosphere by surface-runoff, volatilization or leaching. In order to successfully implement alternative management schemes that result in less pollution, the range of effects of different management schemes have to be investigated by scenario analysis. Scenario-analysis should be carried out at the scale at which agricultural management operates, which is at farm and field level, because it is the management that can be influenced by legislation. Knowing the effects of management schemes on the field-scale is therefore the most appropriate basis for evaluation of scenarios. Many processes that govern transport, transformation and storage of possible pollutants, take place in the soil and are influenced by soil properties. Since soil properties are variable in space and time, scenario analysis should take into account field variability of relevant soil properties. Processes in the soil leading to leaching or volatilization may be very complex when chemical transformations take place, which is the case with biocides, nitrogen etc. When also the spatial and temporal variation is to be included in the analysis, only by application of computer simulation models scenarios can be analyzed quantitatively (Petach and Wagenet, 1988).

In this thesis, attention is paid to procedures ranging from characterizing soil heterogeneity to scenario analyses by computer simulations. Soil variability is not seen as a nuisance, but as a crucial soil property, enabling realistic field scale scenario-analysis.

In several studies reported in this thesis, (geo-) statistical methods were used for various purposes:

- (1) In the inventory studies, statistical methods were used and developed to optimize the number of samples (Burgess and Webster, 1980; Finke *et al.*, 1992) and to construct confidence intervals in case of spatially dependent observations (Finke *et al.*, 1991).
- (2) In studies analyzing the impact of soil variability on transport processes and crop yields, (geo-) statistics were used to transform data to equal space scales (Finke and Goense, 1992; Finke, 1992a), to analyze fertilizing scenarios in terms of probabilities (Finke, 1992b) and to minimize the number of simulations in scenario-analyses (Finke and Stein, 1992).

In the characterization of soil variability, soil structure was regarded as a key variable, because flow of water and nutrients in the soil is strongly related to soil structure. Soil structure is defined as "the physical constitution of a soil material as expressed by the size, shape and arrangement of the solid particles and voids, including both the primary particles to form compound particles and the compound particles themselves" (Brewer, 1964).

Several studies have been made on how to characterize soil structure variability at different scales and degrees of heterogeneity. Studies also have been made on how to translate this variability to input for simulation models that describe water and solute flow. These studies are reported in chapter 2.

In subchapter 2.1 (Finke *et al.*, 1991), a new method is presented to characterize structure-related micromorphologic features in a thin section in case of spatially dependent point observations on these features. Spatial dependency structure is used to construct confidence intervals to estimated probabilities of illuviation ferri-argillans, pores and ferric nodules (van der Plas and Tobi, 1965).

Subchapter 2.2 (Finke *et al.*, 1992) reports on an investigation on disturbed soils. Soil layers formed by pedogenesis or disturbance, encountered in a soil survey of a sandy area, were translated into a number of functional layers. Functional layers are soil layers that have proven to show comparable behaviour from place to place (Bouma and van Lanen, 1986; Wösten and van Genuchten, 1988). An attractive property of functional layers, is that the thickness and the depth at which they occur can be mapped efficiently. They are used throughout this thesis to generate soil hydraulic characteristics from soil profile descriptions for use in simulation models. Furthermore, in subchapter 2.2 a comparison is made between two sampling methods. One method applies model-based statistics (de Gruijter and ter Braak, 1990; Särndal, 1978), using semivariograms to determine an optimal grid mesh in the mapping survey (Burgess and Webster, 1980). Another method applies design-based statistics (de Gruijter and ter Braak, 1990; Särndal, 1978) to evaluate and minimize the number of observations that have to be made in a survey to obtain a representative dataset (Stein *et al.*, 1989; Wald, 1947). Both methods are combined in a procedure that aims at minimizing sampling costs while maximizing the value of the samples for interpolation purposes.

Subchapter 2.3 (Finke and Bosma, 1993) describes into more detail the procedure to derive functional layers from soil profile descriptions. The soil structure of a heterogeneous, thinly stratified marine soil was explicitly used to obtain layers that are non-homogeneous but still recognizable by their over-all structure, which enables the functional layers to be mapped in a conventional soil survey. Simulation techniques were used to obtain functional hydrological properties for these layers, describing the behaviour of these layers during periods of prolonged infiltration and strong evapotranspiration (Wösten *et al.*, 1986). These properties were thereafter used to make a functional distinction between layers, based on their behaviour. This paper offers a novel approach to the problem how to obtain basic simulation data in fine-layered soils.

The inventory of variability of soil characteristics like soil structure is seldom a goal in itself. The effect that field-scale variability has on landqualities and on crop yields, however, can be useful knowledge to anyone that is interested in the implications of soil management. In this thesis, some field-scale studies are described that link soil variability to some landqualities and to crop yields. These studies are reported in chapter 3. Landqualities investigated are moisture availability, nitrogen availability and nitrogen leaching hazard.

In subchapter 3.1 (Finke and Goense, 1992), a field study is presented, in which the observed barley grain yield variability is linked directly to soil variability by multiple regression techniques. Yield variability was also linked to the landquality "moisture availability", by dynamic simulation of the transpiration deficit throughout the growing season on a large number of locations in the field. In these simulations, model input was generated based on profile descriptions and the functional layers.

A transpiration deficit develops during a growing season when the soil can no longer satisfy demand by the plant, which is defined by potential transpiration. The actual transpiration may thus vary over a field when soil hydraulic properties vary sufficiently. However, also the potential transpiration may vary over a field, when the transpiring plant area varies by location. This area can be quantified by the leaf area index. In subchapter 3.2 (Finke, 1992a) remote sensing techniques were applied to estimate the leaf area index variation in space during the growing season. This space-time variation was used as input data for a computer model which dynamically simulated water flow, nitrogen dynamics and potato tuber dry matter production. The objective was to improve the explanation of the amount of variability in final yields. The strength of such a combination of the independent estimation of the leaf area index by remote sensing and computer simulation of dry matter production is, that stress caused by water- and nitrogen deficiencies can be identified. Also, these stress factors can be located in space, which enables corrective location-specific management such as irrigation and fertilization.

To allow simulation of the effect of different management scenarios, a simulation model as described in subchapter 3.2 is not suitable, because the leaf area index is input into the model. The model has been adapted therefore to simulate the leaf area index as a function of climatic data (temperaturesum) and soil dependent factors (availability of water and nitrogen in the rooted zone). After calibration, model performance has been tested by comparing simulated leaf area indexes and simulated crop yields to measurements.

The spatially variable impact of different fertilizing scenarios on simulated nitrate leaching and crop yields is reported in subchapter 3.3 (Finke, 1992b). Effects of soil specific farming (Robert, 1988) and field specific farming for several types and levels of nitrogen application were evaluated for a Dutch agricultural field. In a first scenario-analysis, the impact of application of animal slurry was simulated. Nitrate leaching in the year following an application, expressed as a probability of exceeding a critical value, was used to optimize the amount of manure. In a second scenario-analysis, anorganic nitrogen-fertilization levels were optimized, and the effect of implementation of soil-specific fertilization on crop production and nitrate leaching was evaluated. A novel approach in this study is that the evaluation of scenarios is not only based on simulation outcomes, but also on the probability that these outcomes exceed a critical level, in this case a critical nitrate-concentration in the leaching water. This probability is based on spatial variation of simulation results as well as the results themselves.

Subchapter 3.4 (Finke and Stein, 1992) elaborates on the geostatistical method of disjunctive kriging which was used in subchapter 3.3 to construct the probability of exceeding some selected threshold value. The spatial variation of the property of interest is used in disjunctive kriging to estimate this probability. Another item in this study was to apply cokriging to allow optimization of the number of computer simulations in the scenario analysis.

REFERENCES

- Anderson, G.D., J.J. Opaluch and W.M. Sullivan. 1985. Nonpoint agricultural pollution: pesticide contamination of groundwater supplies. *Am. J. of Agric. Econom.* 67/5: 1238-1243.
- Bouma, J. and H.A.J. van Lanen. 1986. Transfer functions and threshold values: from soil characteristics to land qualities. In: K.J. ter Beek, P.A. Burrough and D.E. McCormack (Eds.), ITC Publication No. 6, Enschede, pp. 106-110.
- van Breemen, N., P.A. Burrough, E.J. Veldhorst, H.F. van Dobben, Toke de Wit, T.B. Ridder and H.F.R. Reijnders. 1982. Soil acidification from atmospheric ammonium sulphate in forest canopy throughfall. *Nature* 299: 548-550.
- Brewer, R. 1964. Fabric and mineral analysis of soils. R.E. Krieger Publ. Comp. Huntington, New York.
- Briggs, D.J. and D. Wilson. 1987. The state of the environment in the European community in 1986. Commission of the European Communities. EUR 10633, Luxembourg, 370 pp.
- Burgess, T.M. and R. Webster. 1980. Optimal interpolation and isarithmic mapping of soil properties. I. The semi-variogram and punctual kriging. *J. Soil Sci.* 31: 314-331.
- Finke, P.A. 1992a. Integration of remote sensing data in the simulation of spatially variable yield of potatoes. In press: *Soil Technology*.
- Finke, P.A. 1992b. Field scale variability of soil structure and its impact on crop growth and nitrate leaching in the analysis of fertilizing scenarios. 1992 Conference of Working Group MV of the ISSS: Operational Methods to Characterize Soil Behavior in Space and Time. July 26-29, 1992, Cornell University, N.Y., U.S.A.
- Finke, P.A. and W.J.P. Bosma. 1993. Obtaining basic simulation data for a heterogeneous field with stratified marine soils. *Hydr. Proc.* 7(2): (in press).
- Finke, P.A. and D. Goense. 1992. Differences in barley grain yields as a result of soil variability. In review *Journal of Agricultural Science*.
- Finke, P.A. and A. Stein. 1992. Application of Disjunctive CoKriging to optimize fertilizer additions on a field scale. Conference of the Working Group on Pedometrics of the ISSS: Developments in Spatial Statistics for Soil Science. September 1-3 1992, Wageningen, The Netherlands.
- Finke, P.A., J. Bouma and A. Stein. 1992. Measuring field variability of disturbed soils for simulation purposes. *Soil Sci. Soc. Am. J.* 56(1): 187-192.
- Finke, P.A., H.J. Múcher and J.V. Witter. 1991. Reliability of point counts of pedological properties on thin sections. *Soil Sci.* 151(3): 249-253.
- de Gruijter, J.J. and C.J.F. ter Braak. 1990. Model-free estimation from spatial samples: A reappraisal of classical sampling theory. *Math. Geol.* 22: 407-415.
- Hallberg, G.R., 1986. From hoes to herbicides, agriculture and groundwater quality. *J. of Soil and Water Conserv.* 41: 357-364.
- Ministerie van VROM, Centrale Directie Voorlichting en Externe Betrekkingen. 1989. Kernpunten uit het Nationaal Milieu Beleidsplan: Een schoon milieu: kiezen of verliezen.
- Petach, M. and R.J. Wagenet. 1988. Integrating and analyzing spatially variable soil properties for land evaluation. In: *Land Qualities in Space and time. Proceedings of a symposium organized by the International Society of Soil Science (ISSS) Wageningen, The Netherlands, 22-26 August 1988: 145-154.*
- Robert, P.C. 1988. Land evaluation at farm level using soil survey information systems.

In: Land Qualities in Space and time. Proceedings of a symposium organized by the International Society of Soil Science (ISSS) Wageningen, The Netherlands, 22-26 August 1988: 299-311.

Särndal, C-E. 1978. Design-based and model-based inference in survey sampling. *Scand. J. Statist.* 5: 27-52.

Stein, A., J. Bouma, S.B. Kroonenberg and S. Cobben. 1989. Sequential sampling to measure the infiltration rate within relatively homogeneous soil units. *Catena* 16: 91-100.

Wald, A. 1947. *Sequential analysis*. John Wiley, New York.

Wösten, J.H.M. and M. Th. van Genuchten. 1988. Using texture and other soil properties to predict the unsaturated soil hydraulic functions. *Soil Sci. A. J.* 52: 1762-1770.

Wösten, J.H.M., M.H. Bannink, J.J. de Gruijter and J. Bouma. 1986. A procedure to identify different groups of hydraulic-conductivity and moisture-retention curves for soil horizons. *J. of Hydr.* 86: 133-145.

CHAPTER 2
VARIABILITY OF SOIL STRUCTURE

CHAPTER 2.1

**RELIABILITY OF POINT COUNTS OF PEDOLOGICAL PROPERTIES ON THIN
SECTIONS**

Published in: *Soil Science* 151(3): 249-253 (1991)

RELIABILITY OF POINT COUNTS OF PEDOLOGICAL PROPERTIES ON THIN SECTIONS

P.A. FINKE ¹, H.J. MÜCHER ², AND J.V. WITTER ²

¹ Department of Soil Science and Geology, Agricultural University, P.O. Box 37, 6700 AA Wageningen, The Netherlands.

² Department of Physical Geography and Soil Science, University of Amsterdam, Dapperstraat 115, 1093 BS Amsterdam, The Netherlands.

ABSTRACT

Point counting of pedological properties on thin sections always starts from the following assumptions: (i) neighbouring counts are spatially independent and (ii) thin sections are representative for the soil horizon under study. We checked the first assumption for some thin section for the following properties: ferric nodules, pores and illuviation ferri-argillans. By using geostatistical methods we find more or less independent observations for two of the three properties that are investigated in this paper with respect to the sampling distance. For one property, i.e. illuviation ferri-argillans, neighbouring observations appeared to be dependent. In the case of dependent observations, a methodology is presented to estimate an equivalent number of independent observations from the sample size and the spatial correlation structure of the observations. A nomogram is presented that yields 95% confidence intervals of estimated probabilities.

KEY WORDS: point counting, micromorphology, binomial distribution, spatial dependency, equivalent numbers.

INTRODUCTION

Thin sections are often studied by soil scientists in order to improve their understanding of pedological processes. Many pedologists look at thin sections in a qualitative sense, but they may also feel the need to quantify the observations. Usually (Daniels *et al.*, 1968; Mùcher *et al.*, 1972; Murphy and Kemp, 1984), a number of point observations is performed on several pedological properties, whereby each observation is properly classified in a binary sense. That is, a property is observed or not observed.

The reliability of the results obtained by point counting has been discussed before. Van der Plas and Tobi (1965) gave a nomogram that yields confidence limits to estimated probabilities to observe some property, given the sample size. Their nomogram is based on the normal approximation of the binomial distribution. Here we will give a substitute for the nomogram supplied in Van der Plas and Tobi (1965). Figure 1 is reproduced from Pearson and Hartley (1970), and gives two-sided 95% confidence intervals for the binomial distribution. The same reference also contains a nomogram for two-sided 99% confidence intervals. As it is not based on the normal approximation, it will yield asymmetric confidence intervals, particularly for small or large values of p .

When counting on thin sections, if the samples are spatially independent one samples from the binomial distribution in order to estimate the probability of observing a certain property. Denote the estimate of p by \hat{p} . Then the following holds:

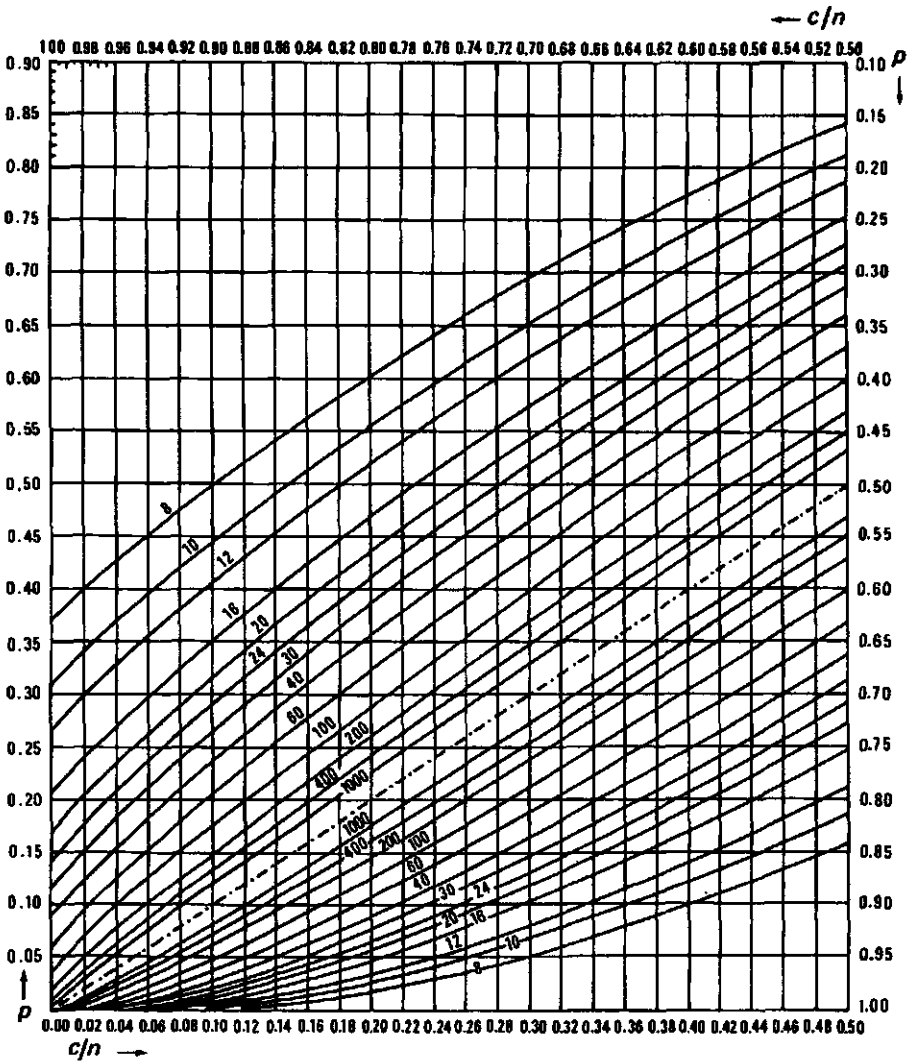


Figure 1 Twosided 95% confidence intervals for estimated probabilities based on the binominal distribution. The numbers printed along the curves indicate the sample size n . If for a given value of the abscissa c/n , p_A and p_B are the ordinates read from (or interpolated between) the appropriate lower and upper curves, then $\Pr\{p_A \leq p \leq p_B\} = 1 - 2\alpha$. Reproduced from Pearson and Hartley (1970).

$$(1) \text{ var}(\hat{p}) = (100 - \hat{p})\hat{p}/n$$

where $\text{var}(\hat{p})$: estimated variance of \hat{p} , n : total number of observations (point counts). According to Van der Plas and Tobi (1965) a 95% confidence interval of the probability p can be constructed as:

$$(2) \hat{p} - 2s < p < \hat{p} + 2s$$

where s : estimated standard deviation of \hat{p} .

Van der Plas and Tobi (1965) themselves mention several restrictions to the use of their nomogram. Firstly, they mention that one thin section might not be representative for a given soil section (see also Murphy, 1983). In such case, several thin sections may be analysed. As pointed out by Murphy (1983) and Mc Keague *et al.* (1980), there may also be a significant operational error, caused by misidentification and other inaccuracies. Secondly, observations are assumed to be independent. Because of this they state, that the "point distance chosen should be larger than the largest grain fraction that is to be included in the analysis". As we now know from geostatistics, however, spatial dependence is often exercised over multiple length scales (see for instance Journel and Huijbregts, 1978). This implies that, in the context of point counting, the distance beyond which properties are independent, will generally be much longer than the dimensions of the studied properties. In our opinion, when counting on thin sections, one should strive to have independent observations. Only in that case one can easily construct confidence intervals.

The objectives of this paper are:

- (i) to estimate for some particular soil properties the distance beyond which observations may be considered to be independent, and to compare these distances with the length dimensions of the properties involved; and
- (ii) to present a method for estimating the equivalent number of independent observations, n_{eq} , when observations are dependent. Then, Figure 1 can still be used, however, with n_{eq} instead of n .

In this paper we will not pay attention to the operator error, and we will assume that the thin section is representative for the soil horizon to which it belongs. Also we will confine ourselves to systematic sampling, because of its ease of implementation, although a stratified sampling design is usually more efficient (Bellhouse, 1981).

GEOSTATISTICAL CONCEPTS

When studying the degree of dependency between observations on a particular property made at several locations, use can be made of the theory of geostatistics. For a thorough background to the field, reference is made to Journel and Huijbregts (1978), Ripley (1981) and Davis (1986). Here we will apply the geostatistical concept of the "semi-variogram", which expresses the dependency between observations as a function of the mutual distance.

When n observations have been made at a mutual distance h , the semi-variance γ can be

estimated by:

$$(3) \quad \gamma(h) = \sum_{i=1}^{n(h)} (Z(x_i) - Z(x_i+h))^2 / (2n(h))$$

where $Z(x_i)$ is the observed value at location x_i .

If semi-variances are calculated for different values of h , the results can be plotted in the form of an experimental semi-variogram. A model can be fitted to the discrete points in the semi-variogram, for instance, the exponential model (Journel and Huijbregts, 1978):

$$(4) \quad \gamma(h) = \begin{cases} C+a(1-\exp(-bh)) & \text{if } h \neq 0 \\ 0 & \text{if } h = 0 \end{cases}$$

where $C + a$: maximum semi-variance ("sill"), C : semi-variance at h close to 0, b : parameter related to the "range".

In case of dependency of neighbouring observations, the semi-variogram exhibits a (slow) rise to some limiting value, the so called "sill". The distance at which the sill is reached, is called the "range". Observations at mutual distances exceeding the range may be considered to be spatially independent. At the origin the semi-variogram may show a discontinuity due to small-scale variability and/or measurement errors.

If observations are dependent, it is intuitively clear, that there is some loss of information, meaning that the equivalent number of independent observations is less than the actual sample size. When n dependent samples are taken, the equivalent number of observations, n_{eff} , is given by (Barnes, 1988):

$$(5) \quad n_{\text{eff}} = n_{\text{eff}} \cdot \exp(1 - n_{\text{eff}}/n)$$

where n_{eff} is an heuristic estimate of the effective number of uncorrelated samples, estimated as:

$$(6) \quad n_{\text{eff}} = 1' R^{-1} 1$$

where R is the sample-to-sample correlation matrix, and 1 is a vector of ones. The correlation coefficient in Eq. (6) can be estimated from the fitted variogram model as (Journel and Huijbregts, 1978):

$$(7) \quad r(h) = 1 - \gamma(h)/(C+a)$$

Thus by fitting a semi-variogram model to the estimated semi-variances, the equivalent number of observations can be conveniently estimated by Eqs. (5) and (6), upon inserting values of $r(h)$ as estimated by Eq. (7).

METHODS

Counts have been performed on one vertical thin section considered representative for the Bt2-argillic horizon in a pedon classified as an Ultic Palexeralf (Soil Survey Staff, 1970). All counts have been performed by one person. Properties considered in this study were

ferric nodules, illuviation ferri-argillans, and pores. A Leitz Orthoplan polarisation microscope with a magnification of about 80 times has been used. At this magnification, the objects to be counted were easily recognizable. The counted properties, their dimensions, and a "characteristic dimension" are presented in Table 1.

Table 1 Counted properties with their dimensions and characteristic dimension.

Property	Dimension		Characteristic dimension
	Diameter	Length	
	mm		
Ferric nodules	0.030-2.0	0.030-2.0	0.5
Illuviation ferri-argillans	0.005-0.1	0.005-2.0	0.4
Pores	0.050-4.0	0.050-4.0	0.4

The characteristic dimension is based on a visual impression and should be understood as being the maximum length scale of the property in most cases. So consider it to be a visual expert guess of, say, the 99% point of the distribution of lengths. Thus, it yields a quick estimate of the minimum sampling distance.

From Table 1 it can be concluded that 0.5 mm is a reasonable guess for the minimum sampling distance. Given the dimensions of the thin section studied, about 45*70 mm, this yielded 11390 observations.

RESULTS AND DISCUSSION

The estimated probabilities \hat{p} (which can be regarded as estimates of volume contributions) and their 95% confidence intervals, based on Fig. 1 as well as on the nomogram in Van der Plas and Tobi (1965) are given in Table 2.

Table 2 Estimated probabilities \hat{p} of observing a certain property and 95% confidence intervals.

Property	\hat{p} (%)	95% confidence interval
Ferric nodules	2.05	1.1-3.1
Illuviation ferri-argillans	4.64	3.6-5.6
Pores	8.63	7.6-9.6

Both Fig. 1 and the nomogram are not easy to read for this combination of sample size and probability, but they both suggest the confidence interval to be 2% wide. These confidence intervals are based on the assumption that all observations are independent.

In order to check the assumption of independence, semi-variograms have been estimated in the usual way for a single realization (Journel and Huijbregts, 1978). These are presented in Fig. 2. For mutual distances in excess of half the maximum distance occurring within the thin section, the semi-variogram can only be very inaccurately estimated

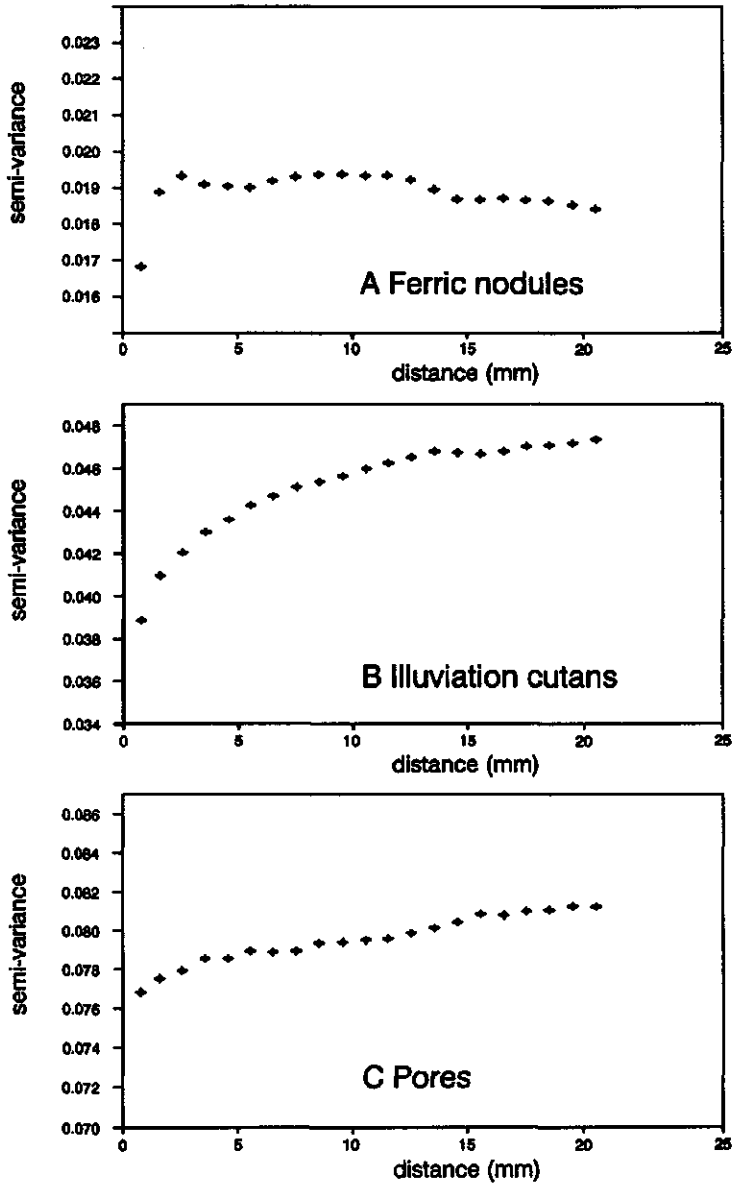


Figure 2 Semi-variograms for Ferric nodules (A), Illuviation ferri-argillans (B), and Pores (C).

(Journel and Huijbregts, 1978). Here only mutual distances smaller than half the smallest length of the thin section have been considered. Thus, the semi-variogram has been plotted for mutual distances less than 20 mm. The semi-variograms indicate that spatial

dependence is very weak or absent for ferric nodules and pores, since the range approximately equals the mesh width (0.5 mm). For illuviation ferri-argillans there is a definite, though weak, spatial dependence.

EXAMPLE

To illustrate the procedure presented in this paper, an example is given, using the point counting results on illuviation ferri-argillans. The estimated volume contribution of illuviation ferri-argillans is $\hat{p} = 4.64\%$ (Table 2). If this estimate was based on $n=1000$ observations, Fig. 1 would yield a 95% confidence interval of $3.5\% \leq p \leq 6.5\%$ when observations would be regarded as independent. The equivalent number of independent observations, calculated using Eqs. (5), (6) and (7), would be $n_{eq}=65$.

Because of the slow decay of the correlation function, the decrease in equivalent number is quite drastic. Using n_{eq} instead of n would yield a 95% confidence interval of $1.5\% \leq p \leq 14.0\%$. The greater width of this interval shows the magnitude of the uncertainty introduced by regarding all observations independent.

CONCLUSIONS

When analysing point counts from thin sections one always starts from the following assumptions:

- (1) neighbouring counts are independent;
- (2) the thin section which is studied is representative for a given soil horizon or rock section.

We confined ourselves to commenting on the first assumption. The representiveness of various thin sections for a given soil horizon will be the subject of a further investigation.

The practical rule by Van der Plas and Tobi (1965) that "the point distance chosen should be larger than the largest grain fraction to be included in the analysis" does result in approximately independent observations. Still, the drop in equivalent sample size because of dependence of observations can be very substantial, as is seen with the illuviation ferri-argillans. Thus, confidence intervals obtained by using Fig. 1 will generally yield a too optimistic view. In case a considerable dependence is expected or feared, it might be useful to check the validity of the assumption of independence. This can be done by estimating semi-variances, and comparing the mesh-width with the range of the fitted variogram. If observations are dependent, an equivalent number of independent observations can be calculated. This equivalent number can then be used to calculate confidence intervals by using the provided nomogram (Fig. 1).

REFERENCES

- Barnes, R.J., 1988. Bounding the required sample size for geologic site characterisation. *Mathematical Geology* 20:477-490.
- Bellhouse, D.R., 1981. Area estimation by point-counting techniques. *Biometrics* 37: 303-312.
- Daniels, R.B., E.E. Gamble, L.J. Bartelli *et al.* 1968, Application of the point count method to problems of soil micromorphology. *Soil Science*, 106: 149-152.
- Journel, A.G., and Ch.J. Huijbregts, 1978. *Mining geostatistics*. Academic Press, New York.
- Mc Keague, J.A., R.K. Guertin, K.W.G. Valentine, J. Bélisle, G.A. Bourbeau, A. Howell, W. Michlyna, L. Hopkins, F. Pegé, and L.M. Bresson, 1980. Note. Estimating illuvial clay in soils by micromorphology. *Soil Science* 129: 386-388.
- Mücher, H.J., T. Carballas, F. Guitián Ojea, P.D. Jungerius, S.B. Kroonenberg and M.C. Villar, 1972. Micromorphological analysis of effects of alternating phases of landscape stability and instability on two soil profiles in Galicia, N.W. Spain. *Geoderma*, 8: 241-266.
- Murphy, C.P., 1983. Point counting pores and illuvial clay in thin section. *Geoderma* 31: 133-150.
- Murphy, C.P. and R.A. Kemp, 1984. The overestimation of clay and under-estimation of pores in soil thin sections. *J. Soil Sci.* 35: 481-495.
- Pearson, E.S., and Hartley, H.O., 1970. *Biometrika Tables for statisticians*. Volume I, third edition. Cambridge University Press, Cambridge.
- Soil Survey Staff, 1975. *Soil Taxonomy*. US Department of Agriculture, Handbook 436. Washington D.C.
- Van der Plas, L., and A.C. Tobi, 1965. A chart for judging the reliability of point counting results. *American Journal of Science* 263: 87-90.

CHAPTER 2.2

**MEASURING FIELD VARIABILITY OF DISTURBED SOILS FOR SIMULATION
PURPOSES**

Published in: *Soil Science Society of America Journal* 56(1): 187-192 (1992).

MEASURING FIELD VARIABILITY OF DISTURBED SOILS FOR SIMULATION PURPOSES

P.A. FINKE, J. BOUMA AND A. STEIN¹

¹ *Department of Soil Science and Geology, Agricultural University, P.O. Box 37, 6700 AA Wageningen, The Netherlands.*

ABSTRACT

Spatial variation of soil profiles disturbed by levelling was inventoried on a field scale to obtain representative data for simulation purposes. Depth of occurrence, thickness and morphology of functional layers, which are different pedogenetic horizons with comparable soil physical properties, were considered to be regionalized variables. The layers served as carriers of physical information, such as water retention and hydraulic conductivity characteristics and organic matter content. An impression of the variability within each layer was obtained by six fold sampling. Spatial variability, expressed by variations in thickness of functional layers, was inventoried in a two step soil survey.

First, semi-variograms were constructed using data obtained following a nested sampling scheme supplemented by a nugget estimation procedure. Variograms were used to evaluate cost/quality ratios at varying potential grid sampling densities, using the root of the prediction error variance (RPEV) as a measure to compare quality of interpolations. Based on these evaluations and a sequential sampling test, a grid mesh of 12 m was chosen.

Second, a grid soil survey and an independent quality test were done, in which root mean square errors (RMSE) on test points were compared with RPEV. The RPEV to RMSE ratios varied between 0.7 and 1.1 for the sampled grid mesh, and had comparable values for other grid meshes. Estimations on test points by an hypothesized spatial mean based on 26 measurements by a sequential sampling method, produced RMSE-values not significantly different from RMSE-values from kriging interpolations. However, sequential sampling required 26 observations whereas kriging required 153, a saving of 83%.

INTRODUCTION

In the Netherlands a considerable area of agricultural land consists of disturbed soils, due to strong human impact on the landscape extending over several centuries. Usually these soils no longer have their original micro- and mesorelief, so physiographic features cannot be used during mapping. Pedological horizons may be mixed due to the disturbance.

The case study presented deals with a detailed soil survey on a field scale in a leveled landscape originally showing strong microrelief. The area studied is located on Pleistocene coversands near the margin of ice-pushed ridges and has a low topographic position. The purpose of the ongoing research is the prediction on a field scale of water fluxes and, more specifically, of NO₃ leaching as a function of N-inputs, climate and soil, using a simulation model. To predict both average and extreme fluxes and leaching in field plots, knowledge about spatial variation of relevant soil properties is essential.

Characteristics assumed to be relevant were soil texture, structure, macroporosity and organic matter content. These influence the shape of retention and conductivity

characteristics and values of N-transformation coefficients.

Spatial variability of these characteristics was modelled using functional layers as carriers of information (Wösten *et al.*, 1985). A *functional layer* was defined as a layer having a unique combination of texture, structure and organic matter content, resulting in characteristic retentivity and conductivity curves. A functional layer may consist of one or more genetic soil horizons or soil layers. Following this approach, variability of a characteristic between locations depends on: (i) spatial variability of the thickness of the functional layers; and (ii) intrinsic variability of the properties of each functional layer. *Intrinsic variability*, the qualitatively characterized variation within a stratum, in this case a functional layer, is minimized by combining only those horizons into a functional layer that have similar characteristics, as measured at several locations. However, considerable intrinsic variability may remain, for instance in the case of a disturbed layer containing fragments of different origin. Such a layer was analysed in this study for its intrinsic variability in morphology and soil physical characteristics.

The purpose of this study was to determine the number and spacing of observations needed to make predictions of the thickness of each functional layer at a desired level of precision relative to the compartment thickness (5 cm) of the simulation model to be used. *Compartment thickness* is the vertical depth increment used by the simulation model to simulate flow and redistribution of water and solutes by finite differencing techniques. When this level can be reached at reasonable sampling costs, simulations on both sampled and interpolated locations could lead to a reliable simulation map. If this level of precision cannot be realized, only simulations on sampled locations are feasible. In this case, a sufficiently large number of observations would have to be made to obtain a data set accurately representing the spatial variation occurring within the fields studied.

MATERIALS AND METHODS

Soils

In the study area, disturbed soils are present (Fig. 1). Generally, below a well homogenized plow layer, a layer was found that showed strong variation in morphology. Differences in morphology reflected different contributions of A, B and C-horizon material to this layer from place to place. Below this disturbed layer, a Bs, (locally) BC, C, Cg sequence or a Cg-horizon occurred. From these sequences, Entic Haplorthods (Fig. 1) and Aquic Udipsamments could be reconstructed as the soils most likely to have been present before disturbance (Soil Survey Staff, 1975). This is confirmed by de Bakker and Schelling (1986). Disturbing activities in the past have been in chronological order:

- (1) *Levelling*. The toplayer of higher grounds was removed, whereby the profile was truncated down to the Bs-horizon (Functional Layer 3). The material thus obtained was deposited on top of the lower grounds, forming a layer consisting of fragments of A, B- and C material (Functional Layer 2).
- (2) *Plowing*. The upper 30 cm of the profile was plowed regularly, whereby morphological differences still recognizable in layer 2 were smoothed out and Functional Layer 1 was formed.

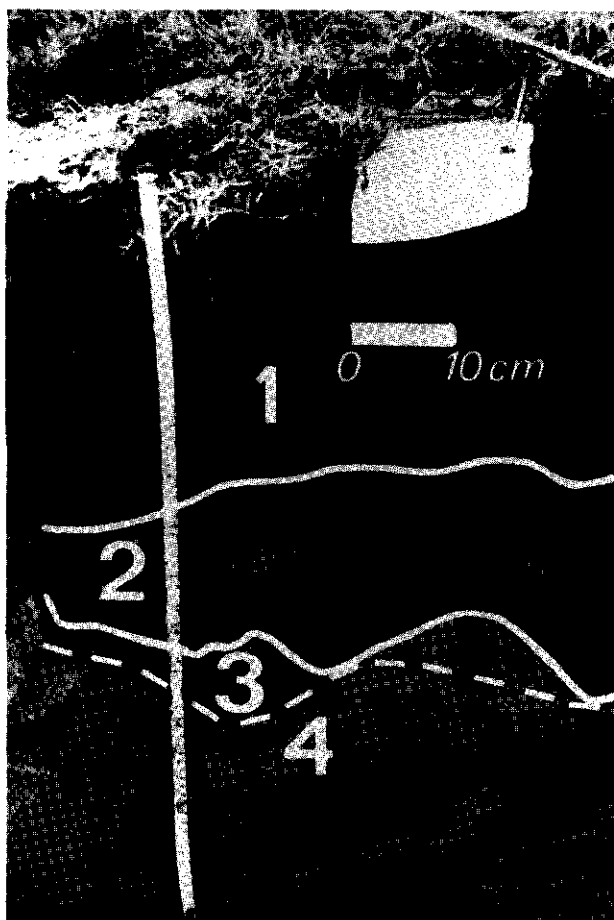


Figure 1 Soil profile and functional layer codes. Codes refer to Table 1.

Soil Physical Measurements

Hydraulic conductivity at and near saturation was measured on undisturbed soil columns in the field using a ring infiltrometer with a horizontal area of 700 cm². In each infiltrometer, tensiometers were installed at two depths to measure the vertical hydraulic head gradient. To measure saturated hydraulic conductivity (K-sat), the soil surface was prepared and water was applied at zero head using a mariotte device. At unit hydraulic head gradient, hydraulic conductivity is proportional to the infiltration rate. Unsaturated conductivity at hydraulic heads in the range between 0 and -4 kPa was determined by applying crusts of hydraulic cement on the soil surface in the ring infiltrometer and measuring infiltration rates at unit head gradient (Bouma *et al.*, 1983). Unsaturated conductivities at higher suctions (to -100 kPa) were determined on undisturbed 300 cm³ samples (taken from the infiltrometer sample), using the one-step outflow method (Doering, 1965; Kool *et al.*, 1985).

Water retention characteristics were determined using one-step outflow data on undisturbed 300 cm³ samples and by measuring moisture release in pressure extractors on disturbed samples.

Functional layers were defined by grouping pedological horizons together that showed comparable physical behaviour, according to functional properties described by Wösten *et al.* (1986).

Sampling

Sampling took place in a number of consecutive steps:

- (1) Soil profile descriptions were collected by augering, following a nested sampling scheme (Webster, 1977). The area was stratified into six equally sized fields, corresponding to the six experimental fields receiving different treatments. Three equally large areas of 360 m² were located at random within each field. Within each area, two clusters of 2 augerings each, having fixed mutual orientations and distances of 8 m were located (Fig. 2). The distance between two samples within one cluster was 2 m.

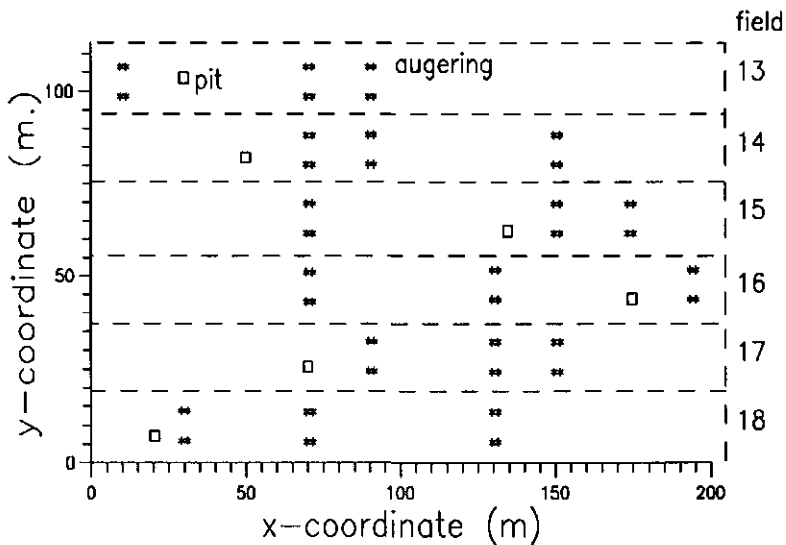


Figure 2 Locations of nested sampling augerings and pits for nugget measurements.

- (2) From the resulting 72 profile descriptions, a number of functional layers were derived in an iterative process including preliminary definition, measurement of water retention and hydraulic conductivity characteristics, determining functional properties, and redefinition.
- (3) Estimations were made of short range- and nugget variances, which can be helpful when choosing the variogram model most appropriate for the study area and the scale of perception. For the estimation of the short range and nugget-variances of

the thicknesses of the various functional layers, a separate sampling procedure was followed. Six pits were dug at randomly chosen locations, one within each field (Fig. 2). The thickness of each functional layer was measured at 5 cm horizontal intervals in each pit. Averaged semi-variances at a lag of 5 cm were considered as nugget, 5 cm being the diameter of the auger used in the nested - and regular grid sampling. The maximal lag covered by the pits was 1 m.

- (4) Construction of variograms for the thickness of each functional layer by fitting transition models (Journel and Huijbregts, 1978) to pit- and augering data. The most appropriate model for each functional layer was selected on a minimal sum-of-squares criterion.
- (5) Collection of soil profile descriptions on a regular grid, the mesh of the grid being derived in a procedure described below.

Quality Criterion

Determination of the spatial distribution of the thickness of the functional layers was to be based on sampling on a rectangular grid. In order to obtain a relation between sampling costs and quality of interpolation maps produced by kriging, this quality was calculated as a function of the grid mesh and the variograms, in a way indicated by Burgess and Webster (1980). A brief description of the underlying concepts is given below. For a more detailed derivation of formulae given, see Corsten (1989) and Stein *et al.* (1988).

In the absence of a trend, the value $y(x_0)$ of a regionalized variable $y(x)$ in an unvisited location x_0 is predicted by a stochastic predictor t (bold-face italic type denotes stochastic variables, bold denotes vectors):

$$(1) \quad t = \mu + \mathbf{g}_0^T \mathbf{G}^{-1} (\mathbf{y} - (\mu \mathbf{1}_n))$$

where μ is the overall mean, \mathbf{g}_0 the n -vector of the semi-variances between point x_0 and n observation points, \mathbf{G} the $n \times n$ -matrix of the semi-variances between observation points, \mathbf{y} a stochastic vector pointing to the observations and $\mathbf{1}_n$ is an n -vector of elements one only.

The variance of the prediction error (the *kriging error*) is given by

$$(2) \quad \text{VAR}(t - y(x_0)) = \mathbf{g}_0^T \mathbf{G}^{-1} \mathbf{g}_0 - x_2 / (\mathbf{1}_n^T \mathbf{G}^{-1} \mathbf{1}_n)$$

where x_2 is the number defined as $x_2 = 1 - \mathbf{g}_0^T \mathbf{G}^{-1} \mathbf{1}_n$ and superscript T indicates a transposed vector.

As is clear from eq. 2, the prediction error variance depends on the variograms and the data configuration only, and not on the actual observations. This makes the prediction error variance a valuable tool in evaluating the quality of an interpolation for varying grid meshes. Gridpoint to gridpoint distances and gridpoint to interpolation point distances are a function of this mesh. In this study, the interpolation point x_0 was located at a maximal average distance from the eight nearest grid locations, which is the most unfavorable place to predict to, except for a location near the border of the area. The prediction error variance was determined for meshes between 1 and 50 m.

Under the assumption that variograms are known, the root of the prediction error variance (RPEV) can be used to construct an approximately 95 % confidence interval $t \pm$

2 RPEV. A confidence interval that was narrow relative to the compartment thickness used in the simulation model (5 cm) was considered appropriate in this study, leading to a quality criterion of RPEV-values < 1.25 cm for each one of the four functional layer thicknesses. The grid mesh associated with this quality criterion determined the sampling costs and thus the economic feasibility.

Sequential Sampling

If quality criteria discussed above cannot be met, the purpose of sampling would become collection of a data set describing the spatial variation of thicknesses of functional layers. To describe variation, an accurate estimate of the mean is essential. Sequential sampling (Wald, 1947; Stein *et al.*, 1989) can be used to stop sampling whenever a sufficiently accurate estimate of the mean is reached, and hence to minimize the number of observations.

The sequential sampling procedure was designed to decide after each additional observation whether sampling should continue. Observations must be stochastically independent. Sampling can stop when a hypothesis $H_0: \mu = \mu_0$ is accepted or is rejected, where μ_0 is the hypothesized mean. Sampling must continue when H_0 remains unproven. If H_0 is rejected, a new hypothesis must be formulated. Testing H_0 is performed by calculating a likelihood ratio, given by Stein *et al.* (1989), and comparing this statistic to an acceptance level $\alpha/(1-\alpha)$ and a rejection level $(1-\alpha)/\alpha$, where α is the probability to decide incorrectly for H_0 . In this study α was set equal to 0.05.

Quality Test

After the grid with the chosen mesh was sampled, 40 additional augerings were made at random locations to obtain an independent measure of the quality of interpolations by kriging. The root mean square error (RMSE) of predictions versus measurements was compared to the root prediction error variance by calculating their ratio. When this ratio equals 1, the predicted interpolation quality agrees with the actual quality. Ratios differing from 1 indicate errors in the estimation of the variograms, or unfavorable data configurations resulting in long lags to prediction points, as may be the case when these points are located near the border of an area. RMSE-values were also used to determine whether a less dense grid would lead to a significant loss in interpolation quality, and to determine whether kriging performed better than estimations by horizontal trend surfaces. Significance was tested using the t-test on difference with paired observations.

RESULTS AND DISCUSSION

Functional Layers

Functional layers derived from profile descriptions collected in the first sampling step are described in Table 1. Characteristic retentivity and conductivity relations and zones of one standard deviation are presented in Fig. 3. These zones from the retentivity curves do not overlap in most cases, which points to relevant differences between the functional layers. Functional Layers 1 and 2 show comparable conductivity relations with overlapping zones, whereas both Functional Layers 3 and 4 differ strongly from the rest. The strong

morphological variation in the layer containing disturbed material did not result in wider one standard deviation zones. Average morphological composition of Functional Layer 2 and standard deviations are presented in Table 2. It was concluded, that, for simulation purposes, the functional layers identified in this study may serve as carriers of physical information when these characteristics are measured elsewhere in identical layers (see also Wösten *et al.*, 1990). In case of presence of a disturbed layer, the functional layer concept still applies.

Table 1 Description of functional layers, relation to horizons and some soil characteristics

layer	description	horizons	texture	structure grade	organic-matter	K-sat av.	CV
1	recent plow layer	1Ap	loamy sand	weak	% 3-4	cm/d 123	% 19
2	disturbed by plowing & levelling	2Abp, 2ABbp, 2BCbp	loamy sand to sand	structure-less	2-4	64	65
3	undisturbed Spodic	2Bsb, 2BCb	sand	structure-less	1-2	119	39
4	coversand	2C, 2Cg	sand	structure-less	0-1	147	41

Table 2 Morphological composition Functional Layer 2, based on data from grid soil survey.

origin of material	average volume	standard deviation
	%	%
A-horizon	61	22
B/BC-horizon	28	20
C-horizon	11	16

Spatial Variability

Variograms of four regionalized variables, the thickness of Functional Layers 1 to 3 and the depth to Functional Layer 4 are presented in Fig. 4. These variograms are based on the nested sampling data and on data from the soil pits where nugget variance was determined. The thicknesses of the plow layer (Functional Layer 1) and Functional Layer 3 show no spatial structure except at very small lags (ranges of variograms are 1.5 and 1 m respectively). This is most likely due to the nature of the disturbance that has affected these layers: plowing and truncation respectively. The thickness of layer 2 and depth to

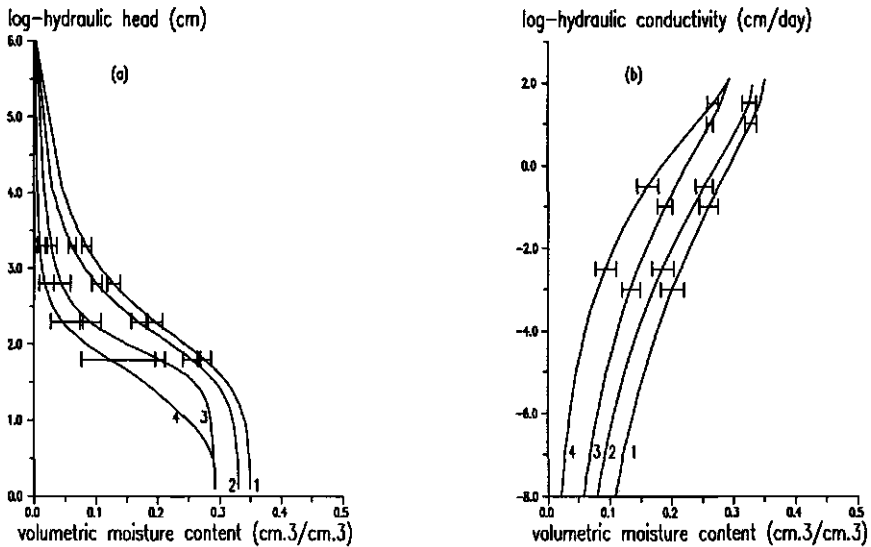


Figure 3 Retention (a) and hydraulic conductivity (b) curves of functional layer 1 to 4. Horizontal bars show zones of 1 standard deviation.

layer 4 show a clear spatial structure. Since layer 4 has been little affected by the levelling activities in the past, its depth relative to the -levelled- soil surface could be expected to show spatial structure. The thickness of layer 2 is a reflection of the former surface relief, because deeper depressions received more infill than shallower depressions. This results in a clear spatial structure in the thickness of Functional Layer 2. It was concluded, that disturbance by levelling does not necessarily lead to absence of spatial structure for the type of variables used in this study.

Relations found between the root of the prediction error variance of the four regionalized variables and the mesh of a potential sampling grid are visualized in Fig. 5. RPEV-values exceeded the criterion, set at 1.25 cm, at grid meshes of 1 m, which would correspond to more than 22000 observations in the area studied. It was concluded, that accurate predictions would not be economically feasible here, and that sampling should aim at collecting a representative data set.

Sequential Sampling

The results of the sequential sampling procedure, presented in Fig. 6, indicated that hypothesized mean values valuable for the whole study area could be accepted after 26 randomly located, spatially independent observations. Hypothesized mean values based on the first 4 measurements were revised for the variables *thickness of Layer 2* and *thickness of Layer 3* after 10 additional measurements. A newly formulated hypothesized mean (H_1) of the thickness of Layer 3, based on 8 measurements, was accepted after 5 additional measurements. The hypothesized mean thickness of Layer 2 was revised and rejected several times, until $H_2: \mu$ layer 2 = 11 cm, based on 20 samples was accepted after 6

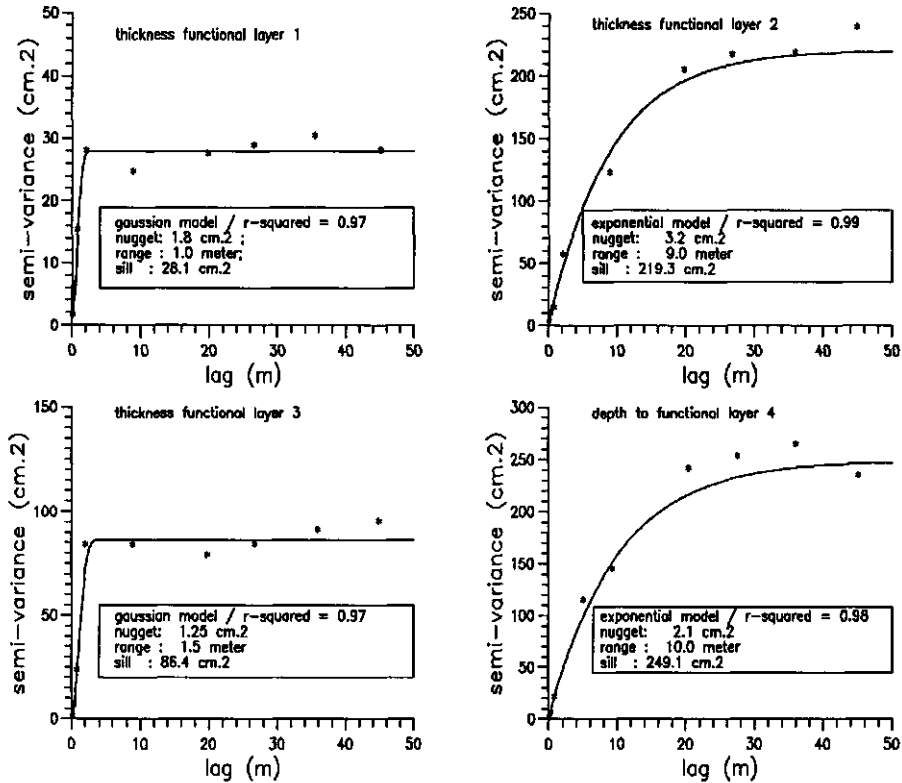


Figure 4 Variograms of thicknesses (a, b, c) or depth to (d) functional layers.

additional samples. Since the study area was divided into 6 experimental fields, it was concluded that 26 augerings should be made on each field. This would correspond to 156 augerings. A grid mesh of 12 m across the whole study area was chosen. At this grid mesh, the 153 observations to be made were known from the variograms to be spatially independent, as their distances exceeded the ranges of the variograms.

Quality of Predicted Values

The RMSE between predicted and measured values and the ratio RPEV/RMSE are presented in Table 3. In general, the RPEV yielded a slightly more optimistic estimate of the average interpolation quality than the RMSE. Ratios varied between 0.7 and 1.1, indicating a reasonably good agreement between predicted and actual quality. By data reduction, RMSE-values were also calculated for grid meshes of 24 and 36 m. The RPEV to RMSE ratios for these grid meshes are comparable. A grid mesh of 24 m performed as well as a grid mesh of 12 m. A grid mesh of 36 m performed significantly (at 95% confidence) worse for the variables *thickness of Layer 3* and *depth to Layer 4*.

Because of spatial independence of the grid observations, kriging predictions were not expected to be better than point estimates based on averaged values obtained from the

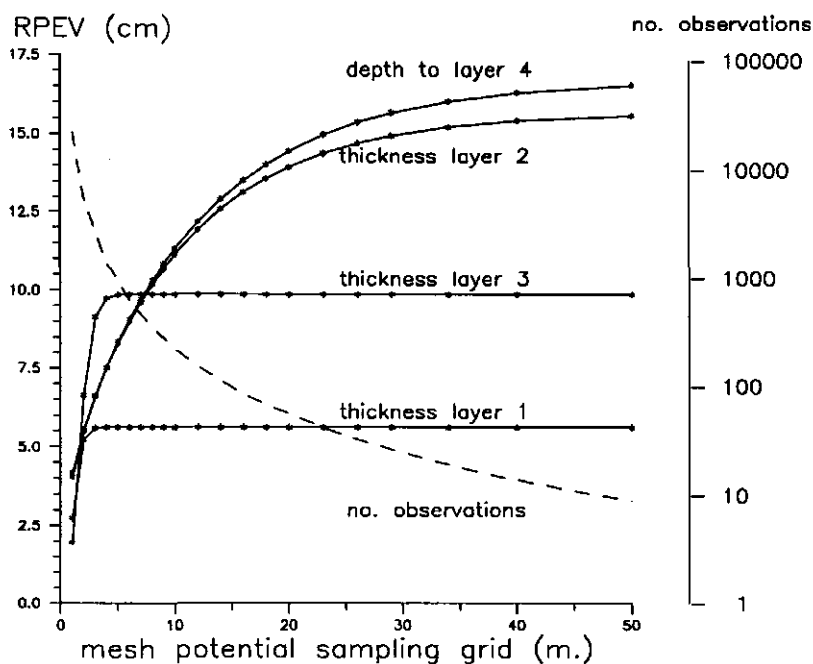


Figure 5 Relations between Prediction Error Variance, the number of grid observations and the mesh of a potential sampling grid.

Table 3 RMSE-values and RPEV/RMSE-ratios for interpolations to an independent test set. RMSE marked with * differ significantly from RMSE with kriging (mesh 12 m.) μ are based on sequential sampling procedure.

Estimation method	no. of observ.	error statistic	thickness of / depth to layer			
			1	2	3	4
kriging mesh=12 m.	153	RMSE (cm)	7	11	14	16
		RPEV/RMSE	0.8	1.1	0.7	0.8
kriging mesh=24 m.	45	RMSE (cm)	7	11	13	16
		RPEV/RMSE	0.8	1.3	0.8	1.0
kriging mesh=36 m.	18	RMSE (cm)	6	12	19*	23*
		RPEV/RMSE	0.9	1.3	0.5	0.7
hypothesized mean	26	RMSE (cm)	7	8	13	12
		μ (cm)	28	11	16	55
		no. obs.	10	26	13	26

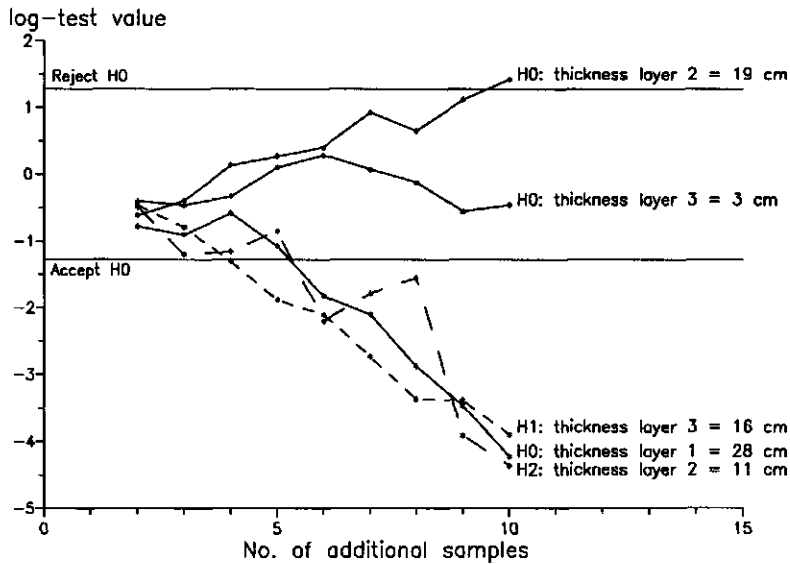


Figure 6 Sequential sampling test results. H_0 -hypotheses are based on 4 observations; H_1 on 8 observations and H_2 on 20 observations.

sequential sampling procedure. The RMSE-values, calculated using hypothesized mean values from the sequential sampling procedure and measured values, did not significantly differ from those of kriging. The sequential sampling procedure however needed 26 random observations, whereas kriging used 153 grid observations, a reduction of 83 % (Table 3).

The difference between RMSE and RPEV may partially be caused by border effects. The RPEV-values are based on interpolation locations surrounded by gridpoints, well away from the borders of the area studied. Some of the test-augerings, however, were located near these borders, causing lags between gridpoints and the prediction point to be greater than normal. This may lead to less accurate predictions and thus RPEV/RMSE ratios smaller than 1. For less dense grid meshes this factor may become more important. Despite possible sources of error, the RPEV/RMSE ratio remained relatively close to 1. This indicates that an evaluation of the prediction error variance for different sampling grids, which is based on variograms, can give a prediction of the quality of the resulting map, which can be used to define the quality of map interpretations.

ACKNOWLEDGEMENT

The authors are grateful to the EC-project EV4V*0098-NL "Nitrate in soils" and the Netherlands Integrated Soil Research Programme for their financial support, and to Ing. H.W.G. Booltink for his assistance.

REFERENCES

- Bakker, H. de and J. Schelling. A system of soil classification for the Netherlands. The higher levels. (In Dutch). 1986. Soil Survey Institute, Wageningen, The Netherlands.
- Bouma, J., C. Belmans, L.W. Dekker and W.J.M. Jeurissen. 1983. Assessing the suitability of soils with macropores for subsurface liquid waste disposal. *J. Environ. Qual.* 12:305-311.
- Burgess, T.M. and R. Webster. 1980. Optimal interpolation and isarithmic mapping of soil properties. I. The semi-variogram and punctual kriging. *J. Soil Sci.* 31:315-331.
- Corsten, L.C.A. 1989. Interpolation and optimal linear prediction. *Statistica Neerlandica* 43, pp.69-84.
- Doering, E.J. 1965. Soil-Water diffusivity by the one-step method. *Soil Sci.* 99:322-326.
- Journel, A.G., and C.J. Huijbregts. 1978. *Mining geostatistics.* Academic Press, New York.
- Kool, J.B., J.C. Parker and M. Th. van Genuchten. 1985. Determining soil hydraulic properties from one step outflow experiments by parameter estimation: I. Theory and numerical experiments. *Soil Sci. Soc. Am. J.* 49:1348-1354.
- Soil Survey Staff. 1975. *Soil taxonomy: A basic system of soil classification for making and interpreting soil surveys.* USDA-SCS Agric. Handb. 436. U.S Gov. Print. Office, Washington DC.
- Stein, A., W. van Dooremolen, J. Bouma, and A.K. Bregt. 1988. Cokriging point data on moisture deficit. *Soil Sci. Soc. Am. J.* 52:1418-1423.
- Stein, A., J. Bouma, S.B. Kroonenberg and S. Cobben. 1989. Sequential sampling to measure the infiltration rate within relatively homogeneous soil units. *Catena* 16:91-100.
- Wald, A. 1947. *Sequential analysis.* John Wiley, New York.
- Webster, R. 1977. *Quantitative and numerical methods in soil classification and survey.* Clarendon Press, Oxford.
- Wösten, J.H.M., J. Bouma and G.H. Stoffelsen. 1985. Use of soil survey data for regional soil water simulation models. *Soil Sci. Soc. Am. J.* 49:1238-1244.
- Wösten, J.H.M., M.H. Bannink, J.J. de Gruijter and J. Bouma. 1986. A procedure to identify different groups of hydraulic-conductivity and moisture-retention curves for soil horizons. *J. of Hydrol.* 86:133-145.
- Wösten, J.H.M., C.H.J.E. Schuren, J. Bouma and A. Stein. 1990. A functional sensitivity analysis of four methods to generate soil hydraulic functions. *Soil Sci. Soc. Am. J.* 54(3): 832-837.

CHAPTER 2.3

OBTAINING BASIC SIMULATION DATA FOR A HETEROGENEOUS FIELD WITH STRATIFIED MARINE SOILS

In press: *Hydrological Processes* 7(2): 000-000 (1993)

OBTAINING BASIC SIMULATION DATA FOR A HETEROGENEOUS FIELD WITH STRATIFIED MARINE SOILS

P.A. FINKE ¹ AND W.J.P. BOSMA ²

¹ *Department of Soil Science and Geology, Agricultural University, Wageningen, The Netherlands.*

² *Department of Soil Science and Plant Nutrition, Agricultural University, Wageningen, The Netherlands.*

ABSTRACT

Thinly stratified sedimentary deposits in a heterogeneous field were investigated to obtain basic physical data for simulation of water flow. A procedure is described which translates a thinly stratified soil profile into a number of functional layers, using functional hydrological properties. A functional layer is defined as a combination of one or more soil horizons, and should (i) be recognizable during a soil survey using an auger and (ii) show significantly different functional hydrological properties when compared to another functional layer. This procedure gave 3 easily recognizable functional layers. Sets of hydrological characteristics of these 3 functional layers were obtained by physical measurements of the soil and by estimation, using textural data for classification into a standard Dutch series.

The performance of several combinations of these sets was tested by comparing simulated and measured soil matric potentials for seven plots during one year. The best simulation results were obtained if measured soil hydraulic characteristics were used for relatively homogeneous functional layers, and if the soil hydraulic characteristics were estimated at each location for the most heterogeneous layer.

KEY WORDS: Layered soils Pedotranfer functions Simulation

INTRODUCTION

Most simulation models which describe solute movement in the unsaturated zone are in essence one dimensional. The study presented forms part of a research in which the spatial variation of landqualities, described as water availability in addition to the availability and leaching hazard of nitrogen, is calculated using simulation models. When a reliable estimation of the spatial variation of, for example, the annual leaching of nitrates must be obtained for an area, multiple model executions must be carried out with the input varying according to the spatial variation of the relevant characteristics occurring in that area. A method is then needed to obtain these relevant characteristics and their variability.

The spatial variation of soil hydraulic characteristics (the water retention and hydraulic conductivity curves) can only be measured at relatively high cost. Soil characteristics that are related to hydraulic characteristics, such as texture, organic matter content and bulk density, are much cheaper to collect. Pedotransfer functions (Bouma and Van Lanen, 1986) that are based on soil characteristics may produce reliable estimations of soil hydraulic characteristics (Vereecken *et al.*, 1989; Wösten *et al.*, 1990). The Dutch Staring database (Wösten, 1987; Wösten and Van Genuchten, 1988) is an example of a national scale soil physical database, in which soil layers are classified into a group according to soil texture and the type of soil horizon. The Staring database distinguishes between

topsoil layers (A horizons) and subsoil layers (B and C horizons) by organic matter content. For each group in the Staring database, average soil hydraulic characteristics are known, which are based on a large number of measurements (Wösten *et al.*, 1987; Wösten, 1987). In the terminology of Bouma and Van Lanen (1986) the Staring database is a "class-pedo transfer-function". Soil layers can be used as carriers of physical information about the soil if they show significantly different hydrological properties compared with other layers and if they show relatively little intrinsic variability (Wösten *et al.*, 1990; Finke *et al.*, 1992). These layers will be referred to as "functional layers" in this paper. Several soil horizons or sediment layers can be combined into a single functional layer if functional hydrological properties are comparable. Functional properties describe the behaviour of a soil layer with respect to water flow under defined boundary conditions. Differently behaving soil layers should be identified because they are likely to contribute to the spatial variation of processes associated with water flow. Functional properties considered here are travel time and height of upward flux (Wösten *et al.*, 1986).

This paper reports about a study in a field where thinly stratified sedimentary deposits are present. Computer simulation of soil water fluxes in these multi-layered soil profiles can become impossible when a finite difference solution is used to solve the Richards equation. Long runs and a large computer memory are needed when every thin soil layer is to be taken into account. It is also difficult to systematically collect soil profile descriptions in the degree of detail required. Purposes of the research reported in this paper were: (i) To test if thinly stratified sedimentary deposits present in the study area could be generalized into a limited number of significantly different functional layers that were also easily recognizable in a regular soil survey; and (ii) to use simulations of the soil water regime for the evaluation of measured and estimated soil hydraulic characteristics by comparison with in situ measurements of pressure heads during a one year period. For comparison purposes, a reference simulation was also carried out for one plot, in which all thin soil layers were considered separately.

MATERIAL AND METHODS

Soils

The study area is located in the Wieringermeer polder in the north-west of The Netherlands. Soil formation is absent, apart from ripening of the upper profile. Before reclamation in 1930, the study area was part of a mud-flat landscape of tidal channels separating shoals. The soil material was deposited during the Calais IV/A transgressive phase (Pons and Van Oosten, 1974) and shows a range in texture between sand and silty clay. The soil is strongly layered, varying from place to place and with depth between a few thin (1 mm to 1 cm) silty clay lenses or layers in a sandy matrix to a few thin sandy layers in a silty clay loam matrix (Fig. 1). Deposited peat fragments are occasionally found in the sandy matrix. The soils were classified as fine-loamy, calcareous, mesic Typic Udifluvents. Layered soils such as these occur widely in alluvial areas in temperal and tropical regions.

The thin layers visible in a vertical section (Fig. 1) cannot be recognized from auger cores in a soil survey. However, combinations of thin layers (layers 2 and 3 in Fig. 1) can be recognized in a soil survey by their marked differences in texture when homogenized. It was investigated whether such combinations of thin layers might serve as functional

layers.

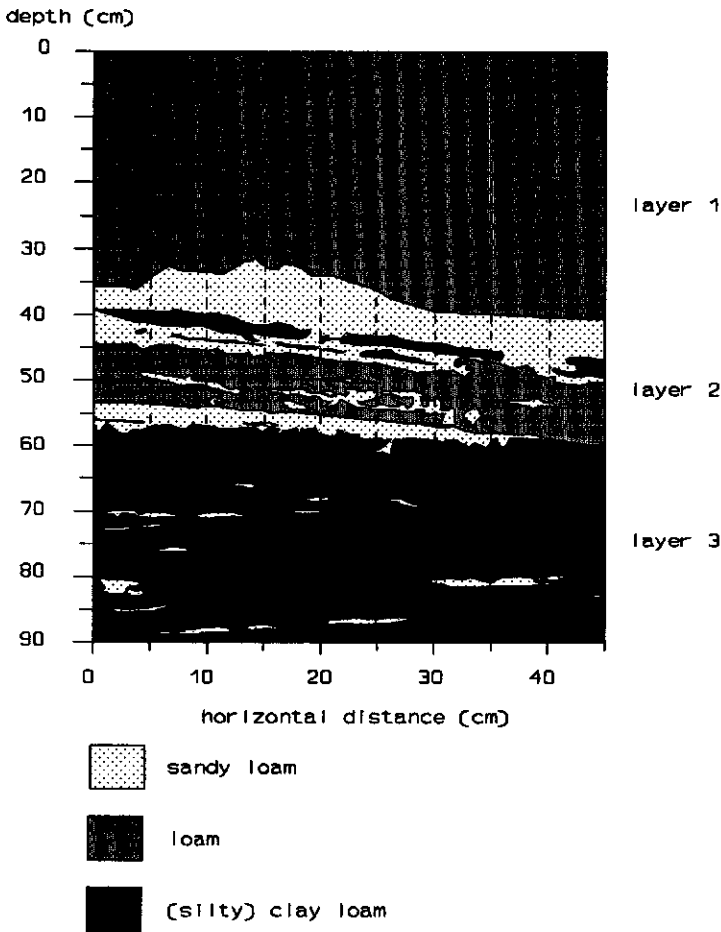


Figure 1 Vertical soil section showing thin layers and lenses. Layer numbers are described in Table 2. Dashed lines indicate vertical sections where thicknesses of thin layers and lenses were measured.

Identification of Functional Layers

To obtain an impression of the variation in soil types and characteristic soil layers in the study area, 93 soil profile descriptions were collected. Based on these descriptions, seven locations were selected which showed a representative range in soil types and characteristic layers for the area. Pits were dug at these locations and detailed profile descriptions were made. Detailed soil profile descriptions (Fig. 1) were translated into a vertical succession of functional layers following the procedure given in Fig. 2. Two successive stages can be distinguished:

In the first stage, a number of preliminary functional layers were identified in vertical

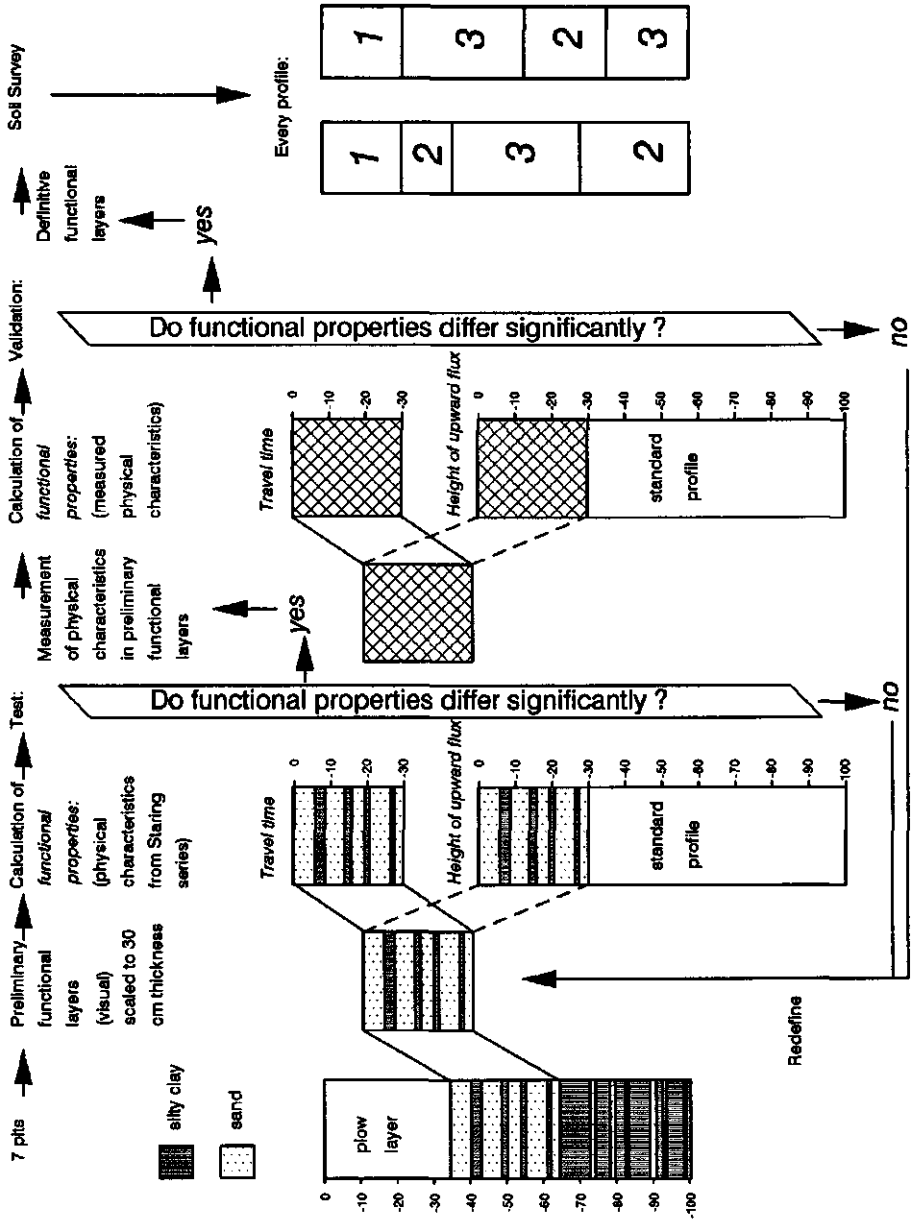


Figure 2 Procedure followed to translate a layered soil profile into functional layers.

sections. These preliminary functional layers should also be recognizable when profile descriptions are less detailed, to allow compatibility with soil survey data in a later stage. The functional properties "Travel time" and "Height of upward flux" (Wösten *et al.*, 1986)

were calculated for each preliminary functional layer using a large number (67) of vertical transects sampled in seven soil pits. These calculations, specified in the next section, were based on hydraulic characteristics from each single thin soil layer encountered in a vertical transect. Hydraulic characteristics were obtained by classifying the texture and type of soil horizon of each thin soil layer into the Staring database. The significance of differences between preliminary functional layers was tested using a t-test on difference of means of calculated functional properties. If differences between preliminary functional layers were significant, the second stage was entered.

In the second stage, the preliminary functional layers were sampled to measure the soil hydraulic characteristics. Functional properties were calculated again, using the measured hydraulic characteristics. If differences between preliminary functional layers were insignificant in a t-test, preliminary functional layer definitions were changed.

If differences between preliminary functional layers were not significant, the definitions were changed. Layers that did not behave differently could then be combined into one new preliminary functional layer. In the extreme example, when differences between layers are small compared with the variability within the layers, the whole soil profile might ultimately be combined into one functional layer.

Travel Time

Travel time is the time needed for infiltrating water to pass a soil layer of a certain thickness. This functional property describes the behaviour of a soil layer during a prolonged moist period as may occur in Dutch winters. In the definition of Wösten *et al.* (1986) it is assumed that all water in the unsaturated zone is mobile, and that flow is characterized by piston flow with unit gradient in a semi-infinite porous medium. In a layered soil however, the assumption of unit gradient flow will not hold. Travel time was calculated as the time needed to displace the total initial water content of the soil profile by infiltration water, using a simulation model and assuming piston flow. Initial and boundary conditions were:

$$\begin{array}{llll}
 (1a) & 0 \leq z \leq L & q = I & t \geq 0 & \text{(stationary flow)} \\
 (1b) & 0 \leq z \leq L & K(\theta) = I & t = 0 & \text{(initial } \theta \text{-profile)} \\
 (1c) & z = L & dH/dz = 1 & t \geq 0 & \text{(free drainage)}
 \end{array}$$

where q is the vertical downward fluxdensity (m/day) at depth z and time t , I is the infiltration rate (m/day), L is the thickness of the preliminary functional layer (m), K is the hydraulic conductivity (m/day), θ is moisture content (m^3/m^3) at a hydraulic conductivity related to I and H is the hydraulic head.

The constant infiltration I was set to the value of the average yearly precipitation surplus, expressed as a daily rate for a winter period of 6 months. For conditions in The Netherlands this daily rate is approximated as $1.4 \cdot 10^{-3}$ m/day. All preliminary functional layers were scaled to a thickness L of 30 cm to allow comparison.

Height of Upward Flux

The height of the upward flux is the distance above the groundwater table that still allows a defined upward flux density. This functional property describes the behaviour of a soil profile during a period without rainfall, when evaporative demand is high. This reflects a possible summer situation in a temperate climate in soils with a shallow water-table. It can be calculated using Darcy's equation for steady, upward, vertical flow:

$$(2) \quad q = -K(1+dh/dz)$$

where dh/dz is the vertical gradient of the soil matric potential (kPa/dm), K is the hydraulic conductivity (m/day) and q is the flux density (m/day). Integration of equation [2] allows the calculation of the height of the upward flux:

$$(3) \quad z_n = -\int_0^{h_n} dh/(1+q/K)$$

where z_n is the vertical distance between the water table and the depth at which a negative pressure head of h_n (kPa) is experienced.

The height of the upward flux is a profile property, and not a property depending on just one layer. This problem was solved by assuming fictional profiles. The lower part of these profiles consists of the least limiting soil material present in the study area (a loam with 18-25 % clay), which is the soil material allowing the largest capillary rise. The upper part of the fictional profiles consists of a functional layer scaled to a thickness of 30 cm. The effect of each layer is thus calculated with the same soil material in the subsoil. The conductivity curve is used to calculate a hydraulic conductivity corresponding to a pressure head that is experienced on a certain depth in the profile. Every thin layer within the preliminary functional layer has its own conductivity curve. To ensure that every thin layer was encountered, small Δh steps were taken while numerically solving integral equation [3]. The height of the upward flux was calculated for all layers in the described fictional profiles, with a defined upward flux density of 0.002 m/day and a pressure head of -50 kPa at the top of the fictional profile.

Soil Physical Measurements

Seven undisturbed soil columns with a diameter and height of 20 cm were taken from each preliminary functional layer. The hydraulic conductivity at and near saturation was measured on these columns using a ring infiltrometer. Tensiometers were installed in each infiltrometer at two depths to measure the vertical gradient of the hydraulic head. The saturated hydraulic conductivity (K_{sat}), was measured by applying water at zero head to the prepared soil surface using a Mariotte device. At hydraulic head gradient of unity, the hydraulic conductivity is proportional to the infiltration rate. The unsaturated conductivity at hydraulic heads in the range between 0 and -4 kPa was determined by applying a crust of hydraulic cement on to the soil surface in the ring infiltrometer and measuring the infiltration rates at unit head gradient at different negative heads with an adjustable Mariotte device (Booltink *et al.*, 1991). Unsaturated conductivities at higher suctions (to

-100 kPa) were determined on 10-14 undisturbed 300 cm³ samples (two samples taken from each infiltrometer sample), using the one-step outflow method (Doering, 1965; Kool *et al.*, 1985). Water retention data at pF 3 and 4.2 were determined by measuring the moisture release in pressure extractors on disturbed samples.

Parameters from the Van Genuchten closed form equations (Van Genuchten, 1980), describing the conductivity and retentivity relations in relation to pressure heads, were derived for each 300 cm³ sample from the water retention data, the measured hydraulic conductivities and the outflow curve, using an optimization program described by Kool and Parker (1987).

Validation: Simulations in Layered Soils

The working hypothesis of this research was, that each thinly stratified soil profile in the studied field could be generalized into a number of functional layers. These functional layers each had a specific set of hydraulic characteristics, allowing simulation of soil water flow at any location where a soil profile description was available. The validation of this hypothesis was based on a comparison of simulations and measurements. The soil moisture regime was simulated with the model LEACHW (Wagenet and Hutson, 1987). Water flow is calculated in LEACHW using a finite difference solution to the soil water flow equation

$$(4) \quad \frac{\partial \theta}{\partial t} = \frac{\partial}{\partial z} (K(\theta) * \frac{\partial H}{\partial z}) - U(z,t)$$

where θ is the volumetric water content (m³/m³); t is the time (days); H is the hydraulic head (10 kPa, defined as $H = h - z$, where h is the soil water matric potential and z is the depth in cm); K = hydraulic conductivity (cm/day) and U is a sink term representing water lost by plant uptake. The relations between K , θ and h that are required were described using the closed form equations proposed by Van Genuchten (1980).

Discretization of the profile, due to the finite difference solution of eq. 4, requires model parameters for each compartment. The Van Genuchten (1980) parameters were obtained by the classification of each compartment into a functional layer using the soil profile description for the site. Three sets of Van Genuchten parameters were available for each functional layer:

- (i) A set based on classification into the Staring database of the texture of the most dominant sublayer;
- (ii) A set based on classification into the Staring database of the texture of a homogenized sample;
- (iii) A set based on measured soil hydraulic characteristics.

In the third set, the average conductivity and retentivity characteristic for each functional layer was obtained by fitting the parameters of the Van Genuchten closed form functions (Van Genuchten, 1980) through a scatter of θ - h and K - h points. These points were obtained from the fitted characteristics from the samples classified in that functional layer.

To test whether the generalization of the soil profile into a vertical sequence of functional layers was applicable, three simulation model input scenarios were carried out. The scenarios differed with respect to the generation of the soil hydraulic characteristics for each functional layer required as model input:

- 1- using only set (i) based on dominant textures;
- 2- using only set (ii) based on homogenized textures;
- 3- using only set (iii) based on measured characteristics.

Simulations were performed on seven plots, located in a field where barley was grown. The boundary inputs are presented in Figure 3. The simulation period was 1 April 1989 to 1 April 1990.

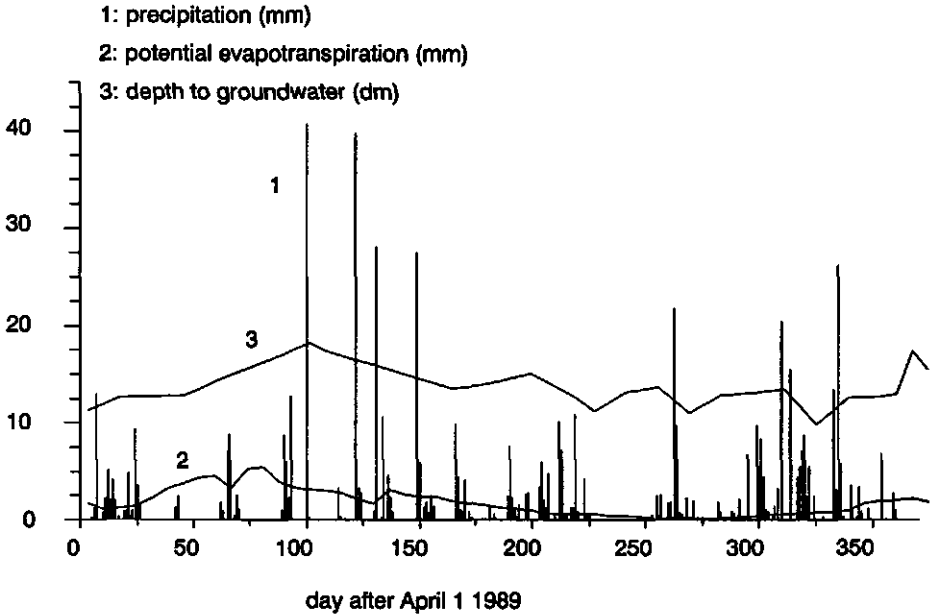


Figure 3 Boundary inputs for simulation of the soil moisture regime. Depth to groundwater in dm, potential evapotranspiration and precipitation in mm.

Simulated soil matric potentials were compared with the time series of measured matric potentials on these plots at depths of 35, 45 and 100 cm. A number of statistical parameters often used to describe quality of simulation results (Loague and Green, 1991) were used to compare measured versus simulated values. These were maximum error (ME), root mean square error (RMSE), coefficient of determination (CD), modelling efficiency (EF) and coefficient of residual mass (CRM).

$$(5a) \quad ME = \text{MAX}_{i=1}^n (\text{ABS}(O_i - S_i))$$

$$(5b) \quad RMSE = \left(\sum_{i=1}^n (S_i - O_i)^2 / n \right)^{1/2} * (100 / \bar{O})$$

$$(5c) \quad CD = \frac{\sum_{i=1}^n (O_i - \bar{O})^2}{\sum_{i=1}^n (S_i - \bar{O})^2}$$

$$(5d) \quad EF = \frac{\sum_{i=1}^n (O_i - \bar{O})^2 - \sum_{i=1}^n (S_i - O_i)^2}{\sum_{i=1}^n (O_i - \bar{O})^2}$$

$$(5e) \quad CRM = \frac{\sum_{i=1}^n O_i - \sum_{i=1}^n S_i}{\sum_{i=1}^n O_i}$$

where O are observed values and S are simulated values. The ME value is the maximum difference between an observed and a simulated value, and indicates the worst case performance of a model. The RMSE value indicates how much the simulations are over- or underestimating measurements, expressed as a percentage of the averaged value of the measurements. The CD statistic, which is not equal to the coefficient of determination used in classical statistics, describes the ratio between the scatter of simulated values and the scatter of measurements. The CD indicates whether the dynamics in measured and simulated values agree. The EF value indicates whether the simulations provide a better estimate of measurements than the average value of the measurements. If the EF is less than 0, the average value of the measurements is a better estimator. The CRM value indicates whether simulations tend to overestimate or to underestimate. A negative CRM value indicates a tendency to underestimate. As all five statistics describe a different aspect of simulation quality, it was decided to select the best performing simulation scenario after comparing all five statistics simultaneously.

The over all best performing simulation input scenario was selected by ranking the scenario's in order of performance for each depth and statistic separately, and taking the average rank as comparative criterion.

RESULTS AND DISCUSSION

Functional Layers

The average values and variability of the functional properties of preliminary and definite functional layers are given in Table 1. The mean value of a functional property in a preliminary functional layer differed significantly from that of other preliminary functional layers in most instances (Table 1). Only the height of upward flux calculated for the plough layer (preliminary functional layer 1) was comparable with that of layer 2. It was concluded, that the 3 preliminary functional layers should be sampled separately.

Calculations of functional properties, using the measured soil hydraulic characteristics, showed significantly different mean values of travel time and height of upward flux in all instances (Table 1). Based on these results, it was concluded, that functional layers 1, 2 and 3 must be distinguished during the soil survey. Definite functional layers are described in Table 2. Generally, the mean values of a functional property for the preliminary and definite version of a functional layer are comparable. The variability, expressed by the coefficient of variation (Table 1), was slightly overestimated during the analysis of the preliminary functional layers. One exception is the mean height of upward flux for preliminary and definite functional layer 1 (the plough layer). The hydraulic characteristics based on texture and those based on measurements lead to clearly different values for this functional property. Soil texture alone probably cannot explain the soil physical behaviour in this plough layer.

Table 1 Results from testing the difference of mean values from functional properties between preliminary (p) functional layers and definite (d) functional layers 1, 2 and 3. Values with asterisk * differ significantly from values for the 2 other functional layers at $\alpha=0.05$ (2-sided). CV is coefficient of variation

functional layer	obs. (n)	Travel time			Height of upward flux		
		μ	$\sigma(n-1)$	CV	μ	$\sigma(n-1)$	CV
		days	days	-	cm	cm	-
p 1	14	81.49*	5.33	0.07	75.43	12.25	0.16
p 2	67	54.89*	14.07	0.26	75.86	21.46	0.28
p 3	67	90.98*	0.38	0.11	47.10*	20.53	0.44
d 1	10	80.33*	5.73	0.07	37.30*	17.68	0.47
d 2	13	65.58*	11.78	0.18	75.04*	18.67	0.25
d 3	14	106.08*	8.64	0.08	54.29*	15.94	0.29

Table 2 Description of functional layers, relation to horizons and some soil characteristics

functional layer and description	horizon	texture when mixed	org. matter	bulk-dens.	Genuchten parameters					
					K-sat	Θ -res	Θ -sat	α	n	γ
1 plow layer	Ap	loam to clay loam	% 2-4	kg/dm ³ 1.44	cm/day 265	cm ³ /cm ³ 0.00	0.44	cm ⁻¹ 0.113	-	-
2 sandy loam layer with clay loam lenses/layers	C1	sandy loam to loam	0-1	1.29	23	0.00	0.44	0.020	1.331	0.959
3 silty clay loam layer with sandy loam lenses	C2	loam, clay loam, silty clay loam	0-1	1.09	21	0.10	0.58	0.012	1.328	6.558

As a result, it can be concluded that both the mean value and variability of the functional properties were well estimated by preliminary functional layers 2 and 3.

Characteristic water retention and hydraulic conductivity curves with confidence zones, based on geometrical averages of 10 to 14 individual curves, are presented in Figure 4.

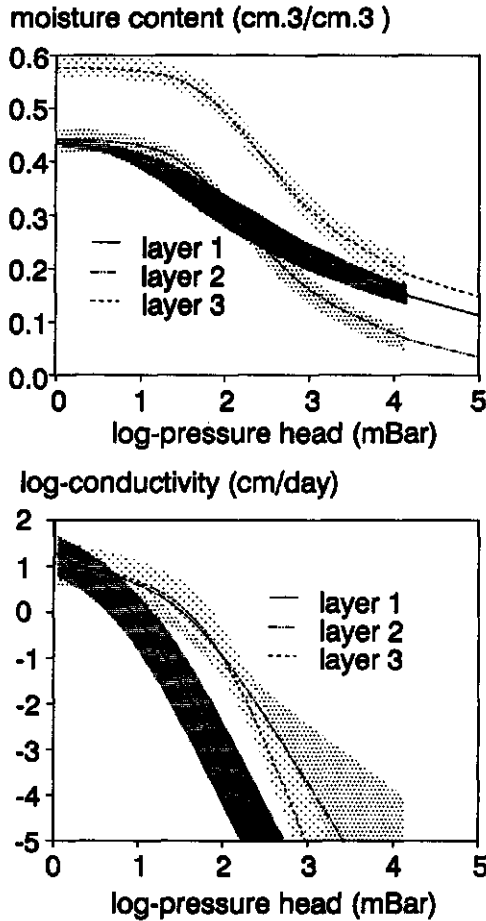


Figure 4 Characteristic water retention and hydraulic conductivity curves and 1 standard deviation zones for functional layers 1 to 3, obtained by geometrically averaging 8 to 14 measured curves.

Simulations

Results of the statistical comparison between observed and simulated soil matric potentials are given in Table 3.

The simulations based on measured soil hydraulic characteristics (scenario 3) were clearly more realistic than simulations based on estimated characteristics (scenarios 1 and 2). In Figure 5, simulations according to the 3 described scenarios are presented for one of the seven plots. Simulations based on scenario 1 and 2 were much dryer during the summer than those based on scenario 3. This is predominantly caused by the stronger capillary upward flux allowed in functional layer 1 by the estimated hydraulic characteristics, relative to the flux allowed by the measured characteristics. This lead to

much higher actual evaporation rates in for scenarios 1 and 2, and thus to a dry simulation of the upper part of the profile.

In addition to these 3 simulation scenarios, a fourth scenario was defined to determine whether the results of scenario 3 could be improved. It was suggested that the functional layer having the most heterogeneous morphology (layer 2, see Fig. 1) would show a more pronounced spatial variability of the soil hydraulic properties between locations. In scenario 4, the plot-specific homogenized texture was used to estimate the hydraulic characteristics for functional layer 2, whereas for functional layers 1 and 3 the set based on measured characteristics was used. The results are presented in Table 3 and Figure 5. Scenario 4 showed a slight improvement relative to scenario 3, considering the 35 cm and 45 cm statistics (Table 3).

Extra simulations were also performed with one profile, taking into account the thin layering of the profile. The compartment size in the model was reduced to 3 mm, and estimated hydraulic characteristics from every thin layer were used. The results are presented in Figure 5 as scenario 5. Measured and simulated matric potentials based on scenario 5 show only very small differences, especially in the topsoil. Simulations with scenario 3 and 4 agree well with this "reference simulation". Scatter plots of simulated and measured matric potentials are given in Figure 6. Simulations based on scenarios 1 and 2 were generally too dry. Simulations based on scenarios 3 and 4 show a more symmetrical distribution around the 1:1 line in Figure 6.

*Table 3 Results of statistical comparison between simulated and measured matric potentials. Best statistics for depth are indicated with asterisk *. N is the number of samples, ME is maximum error, RMSE is root mean square error, CD is coefficient of determination, EF is modelling efficiency and CRM is coefficient of residual mass.*

Depth cm	Input scenario	N	Statistic				CRM	rank
			ME	RMSE	CD	EF		
			range: [0;∞>	[0;∞>	[0;∞>	<-∞;1]	<-∞;∞>	[1;4]
			best : 0	0	1	1	0	1
35	1	108	3.70	1263.74	0.01	-118.48	-3.87	2.8
35	2	108	3.60	1335.82	0.01	-132.50	-4.45	2.6
35	3	108	5.20	87.15	1.76	0.43	0.21	2.2
35	4	108	5.00	91.59	1.59	0.37	0.17	1.8
45	1	98	2.50	877.56	0.02	-47.13	-2.44	3.0
45	2	98	2.80	1133.84	0.01	-79.35	-3.93	4.0
45	3	98	0.40	96.01	1.73	0.42	0.11	1.8
45	4	98	0.30	95.96	1.74	0.43	0.09	1.2
100	1	97	2.62	107.98	1.72	0.42	-0.40	2.6
100	2	97	2.61	114.10	1.54	0.35	-0.47	2.8
100	3	97	3.10	84.83	2.79	0.64	-0.13	2.3
100	4	97	3.10	84.33	2.83	0.65	-0.14	2.3
all 3	1	303	-	-	-	-	-	2.8
all 3	2	303	-	-	-	-	-	3.4
all 3	3	303	-	-	-	-	-	2.0
all 3	4	303	-	-	-	-	-	1.8

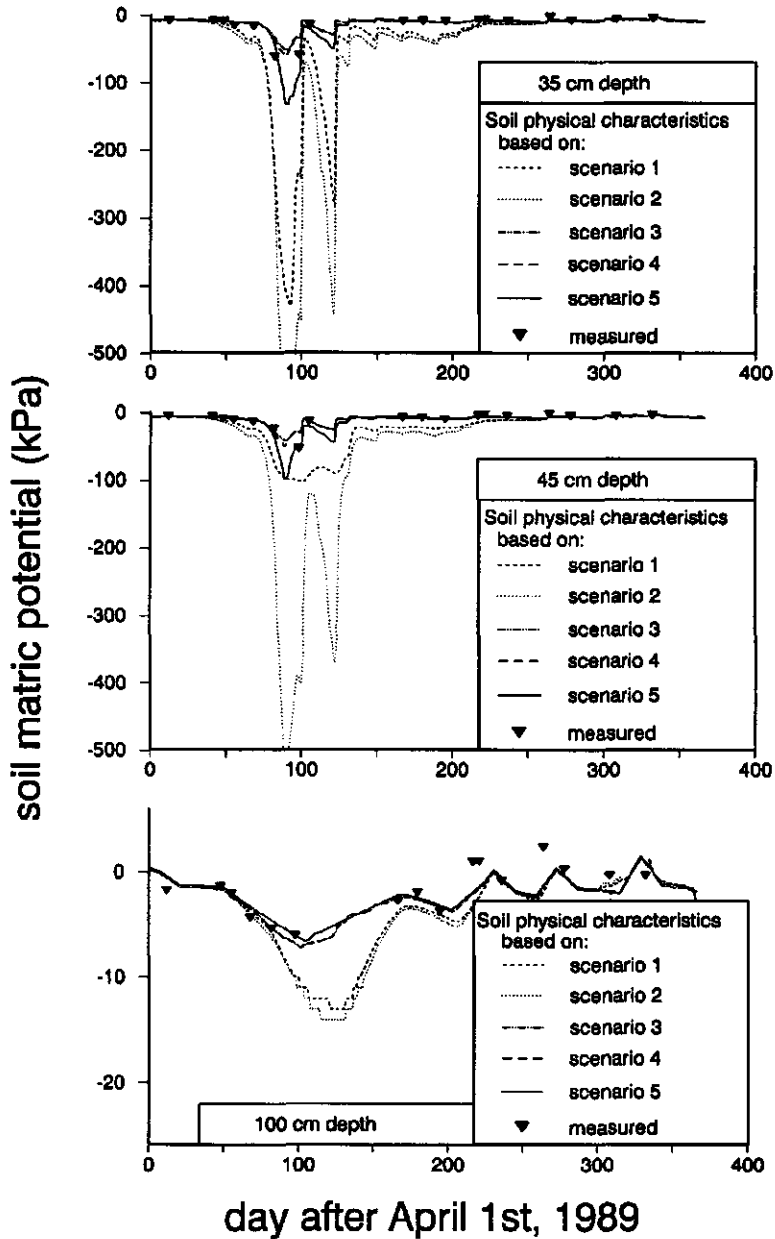


Figure 5 Simulated versus measured soil matric potentials for plot 74 at 35 (a), 45 (b) and 100 cm (c) according to scenario 1 to 5.

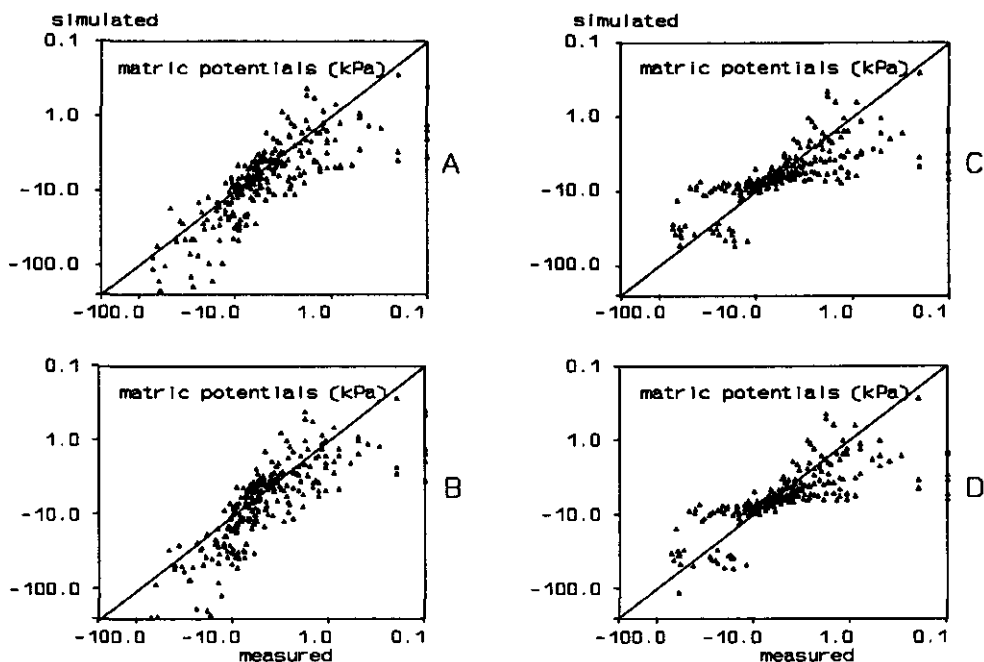


Figure 6 Simulated versus measured soil matric potentials for all 7 plots and 3 depths according to scenario 1 (A) to 4 (D).

CONCLUSIONS

In thinly stratified sedimentary deposits, functional layers were successfully identified that were recognizable in a regular soil survey and which showed significantly different functional properties. Preliminary functional layer definitions in these soils must be based on detailed profile descriptions.

Simulations based on the input of soil hydraulic characteristics for functional layers were realistic when compared with measurements and with a reference simulation for one plot, considering all the thin soil layers separately.

Simulations based on soil hydraulic characteristics that were measured on site were more realistic than those estimated by class pedotransfer functions. For a layer with a strongly varying morphology, slightly better simulation results were obtained when the homogenized texture at each location was classified into a class pedotransfer function to derive the soil hydraulic characteristics.

ACKNOWLEDGEMENTS

The authors are grateful to the EC-project EV4V*0098-NL "Nitrate in soils" for financial support, to P. Peters for measurement of the soil hydraulic characteristics and to Professor Dr J. Bouma for critically reading the manuscript.

REFERENCES

- Booltink, H.W.G., J. Bouma and D. Gimenez. 1991. A suction crust infiltrometer for measuring hydraulic conductivity of unsaturated soil near saturation. *Soil Sci. Soc. Am. J.* 55:566-568.
- Bouma, J. and H.A.J. Van Lanen. 1986. Transfer functions and threshold values: from soil characteristics to land qualities. In: K.J. Beek, P.A. Burrough and D.E. McCormack (Eds.): *Quantified Land Evaluation Procedures*. ITC Publication no. 6, Enschede, pp.106-110.
- Doering, E.J. 1965. Soil-Water diffusivity by the one-step method. *Soil Sci.* 99:322-326.
- Finke, P.A., J. Bouma and A. Stein. 1992. Measuring field variability of disturbed soils for simulation purposes. *Soil Sci. Soc. Am. J.* 56(1): 187-192.
- Kool, J.B., J.C. Parker and M. Th. van Genuchten. 1985. Determining soil hydraulic properties from one step outflow experiments by parameter estimation: I. Theory and numerical experiments. *Soil Sci. Soc. Am. J.* 49:1348-1354.
- Kool, J.B. and J.C. Parker. 1987. Estimating soil hydraulic properties from transient flow experiments: SFTT user's guide. Electric Power Research Institute, Palo Alto, California.
- Loague, K.M. and R.E. Green, 1991. Statistical and graphical methods for evaluating solute transport models. *J. Contaminant Hydr.* 7:51-73.
- Pons, L.J. and M.F. Van Oosten. 1974. (In Dutch) De bodem van Noordholland. Toelichting bij blad 5 van de bodemkaart van Nederland schaal 1:200.000. Dutch soil survey institute, Wageningen.
- Van Genuchten, M. Th. 1980. A closed form equation for predicting the hydraulic conductivity of unsaturated soils. *Soil Sci. Soc. Am. Journal* 44:892-898.
- Vereecken, H., H. Maes, J. Feyen. 1989. Estimating the soil moisture retention characteristic from texture, bulk density and carbon content. *Soil Science* 148 (6):389-403.
- Wagenet, R.J. and J.L. Hutson. 1987. LEACHM: Leaching Estimation And Chemistry Model: A process based model of water and solute movement transformations, plant uptake and chemical reactions in the unsaturated zone. Continuum Vol.2. Water Resources Inst., Cornell Univ. Ithaca, NY.
- Wösten, J.H.M., M.H. Bannink, J.J. de Gruijter and J. Bouma. 1986. A procedure to identify different groups of hydraulic-conductivity and moisture-retention curves for soil horizons. *J. of Hydrol.* 86:133-145.
- Wösten, J.H.M., M.H. Bannink, and J. Beuving. 1987. Water retention and hydraulic conductivity characteristics of top- and sub-soils in the Netherlands: The Staring database. Report 1932, Soil Survey Inst., Wageningen, The Netherlands (in Dutch).
- Wösten, J.H.M. 1987. Description of the water retention and hydraulic conductivity characteristics from the Staring database with analytical functions. Report 2019, Soil Survey Inst., Wageningen, The Netherlands (in Dutch).
- Wösten, J.H.M. and M. Th. Van Genuchten. 1988. Using texture and other soil properties to predict the unsaturated soil hydraulic functions. *Soil Sci. Soc. A. J.* 52:1762-1770.
- Wösten, J.H.M., C.H.J.E. Schuren, J. Bouma and A. Stein. 1990. Functional sensitivity analysis of four methods to generate soil hydraulic functions. *Soil Sci. Soc. A. J.* 54:832-836.

CHAPTER 3

**IMPACT OF SOIL STRUCTURE VARIABILITY ON TRANSPORT PROCESSES
AND CROP YIELDS**

CHAPTER 3.1

**DIFFERENCES IN BARLEY GRAIN YIELDS AS A RESULT OF SOIL
VARIABILITY**

Submitted/in review: *Journal of Agricultural Science*

DIFFERENCES IN BARLEY GRAIN YIELDS AS A RESULT OF SOIL VARIABILITY

P.A. FINKE ¹ AND D. GOENSE ²

¹ Department of Soil Science and Geology, Agricultural University, PO Box 37, 6700 AA Wageningen, The Netherlands

² Department of Agricultural Engineering and Physics, Agricultural University, Wageningen, The Netherlands.

SUMMARY

Field scale variability in the grain yield of barley in 1989 was investigated in 62 field plots in a Dutch Polder area, and compared to soil- and simulation type characteristics. Total grain mass varied between 3409 and 6019 kg/ha, and grain moisture content between 13.1 and 14.7 %. Soil profile descriptions and soil characteristics were used as basic input data for simulations. Soil water flow was simulated at 119 locations with the LEACHM model, for the purpose of quantifying spatial variability in transpiration deficits in the growing season. Both soil- and simulation type characteristics were translated from point values to spatial averages for the harvested fields, using kriging. Kriged characteristics were correlated with yields, and used to construct transfer functions. Simulated transpiration deficits during sensitive crop development phases showed negative correlations with grain yield. Transfer functions explained at maximum 68.2 % of the variance in the yields.

INTRODUCTION

Determination and prediction of crop yields is being researched for economic and scientific reasons. Theoretical studies (Van Keulen & Wolf 1986) suggest that crop yields are determined largely by the potential assimilation rate and may be limited by lack of water and nutrients (Van Diepen *et al.* 1988). Modern agriculture attempts to maximize crop yields by removing the risk of water- and nutrient stress through irrigation and fertilizing.

Usually, fertilizer applications are distributed evenly over a field, the amount applied being based on an average need. It has been established (Neeteson 1989), that the response of yields to plant available nutrients shows small gradients when nutrient levels are nearly optimal. In agricultural practice, it is assumed that a fertilizer application corresponding to the average need should result in a small variability in yields. However, Church *et al.* (1983) and Gales (1983) report a large variability in crop yields on a field scale and a coefficient of variation of 25% was derived from Tits *et al.* (1989). Knowing the factors that cause this variability and, if possible, mapping them, would enable location-specific agricultural measures, like for example focusing irrigation on areas where moisture deficits are most likely to occur and adding fertilizer according to local need. These measures can lead to higher profits per unit area by reducing costs or by increasing yields.

This paper presents a case study linking the spatial variability from soil survey and simulation-type characteristics to the observed variability in crop yields on a field scale.

From comparison, causes of the variability in yields were identified.

MATERIALS AND METHODS

Soils

The study area was located in a polder area in the north-western part of the Netherlands. Before reclamation in 1930, the site was part of a mud-flat landscape of tidal channels separating shoals. One such channel, now filled up, can still be recognized on the soil texture map (Fig. 1).

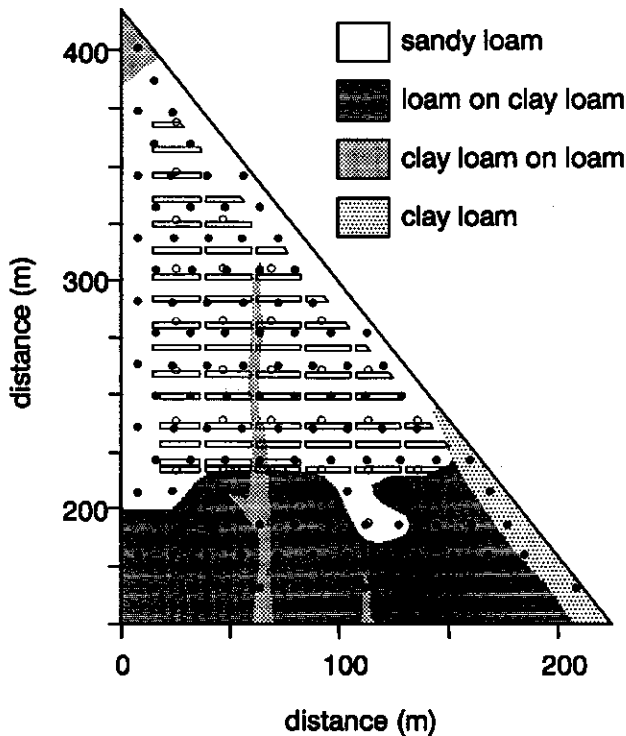


*Figure 1 Soil texture map with sandy loam, loam on clay loam, clay loam on loam and clay loam soils. Soil profile descriptions were sampled at * and mineral N was sampled at o. Rectangles represent harvested field plots.*

The soil material shows a range in texture between sandy loam and silty clay. The soil is strongly layered, varying from place to place and with depth. The variation ranges from a few thin (1 mm - 1 cm) silty clay lenses or layers in a sandy matrix to few thin sandy layers in a silty clay loam matrix. Apart from ripening of the upper profile part, no pedogenesis has occurred since the deposition of the soil material. Soils were classified as

Data Collection

119 Soil profiles were described by augering on a triangular grid at 16 m intervals (Finke, 1991) (Fig. 1). Soil textures were determined for all soil layers in each profile in the laboratory and by field grading, for the 0-40 cm, 40-80 cm and 80-120 cm depths. All soil layers were classified by their texture and organic matter content into one of the units of the Staring series (Wösten 1987), which is a national database for Dutch soils, linking texture class and organic matter content class to soil physical characteristics. Water retention and hydraulic conductivity characteristics derived from this procedure, together with the textures on which they were based, are presented in Figure 2. These characteristics were used in the simulations described later.

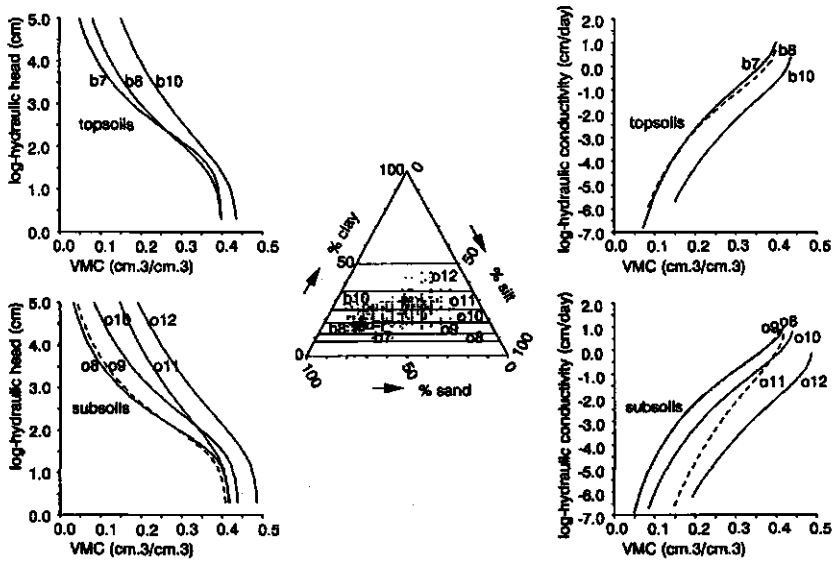


Figure 2 Water retention characteristics (left) and hydraulic conductivity characteristics (right) for topsoils (top, b-codes) and subsoils (bottom, o-codes) from the Staring series. Codes refer to textural classes indicated in the central figure. Courtesy J.H.M. Wösten.

Mineral nitrogen was determined one month before fertilizing and sowing, by analysing soil samples from the layer between the 0 and 60 cm depth at 43 locations on a rectangular grid having a mesh of 22 m (Fig. 1). A 22 m rectangular grid was chosen instead of the 16 m triangular grid to reduce laboratory costs. For barley, the N fertilizer application was calculated using the average mineral N content in the 0 - 60 cm depth. The mineral nitrogen content available to the plant at the start of the growing season was determined for all 43 sampling locations by adding the amount of N in fertilizer and in the soil as mineral N.

Barley yield was measured by harvesting 62 plots ranging in area from 10 to 47 m² (Fig.

1). The width of each plot was 2.2 m, being the cutting width of the combine harvester, the length varied from 4.6 to 21.5 m. Locations were chosen at a minimum distance of 13 m from the edge of the field and a minimum distance of 2 m from fixed tracks used for husbandry practices, thus avoiding yield variations due to edge and husbandry effects. Eight smaller plots at mutual distances smaller than 50 m were harvested also to obtain an estimate of yield variation at short ranges. The smallest area harvested was still large enough to keep mass measurement errors below 1%. Total grain yield was determined on each plot, and subsamples were taken to determine the moisture content of the grains. Measurements of moisture contents and of plot areas were used to correct total grain yield to grain yield at 16% moisture content in kg/ha.

Simulation of Transpiration Deficit

Soil water fluxes and, more specifically, transpiration during the growing season were simulated for the 119 soil profiles described during the soil survey, using the model LEACHM (Wagenet & Hutson 1989). Water flow is calculated in LEACHM using a finite-difference solution to the soil-water flow equation

$$(1) \quad \frac{\partial \theta}{\partial t} = \frac{\partial}{\partial z} K(\theta) \frac{\partial H}{\partial z} - U(z,t)$$

where θ is the volumetric water content (m^3/m^3), t is time (day), H is hydraulic head (kPa, defined as $H = h - z$, where h is soil water matric potential in dm water, equivalent to kPa, and z is depth in dm), K is hydraulic conductivity (cm/day) and U is a sink term representing water lost by transpiration (cm). The functions between K , θ and h that are required, were described using the closed-form equations provided by Van Genuchten (1980). LEACHM divides potential evapotranspiration into potential evaporation and potential transpiration using a crop cover fraction. If actual evaporation falls below potential evaporation, the energy not used for evaporation is assumed to cause a convective air flow that stimulates transpiration. This is simulated in LEACHM by adding the difference between potential and actual evaporation to the transpiration, up to a maximum actual:potential transpiration ratio specified by the user of the model. This may cause the transpiration deficit to become negative when the soil surface can no longer sustain an upward flux equal to the potential evaporation, but the layers in the rooting zone can still supply enough moisture for an increased transpiration.

It is known (Geisler 1980), that the yield of cereals may decrease by stress due to moisture deficits during some sensitive plant development phases. Cereals are considered sensitive to moisture deficits during the vegetative growing phases and the phase of development of inflorescence (Geisler 1980). Moisture deficits during a number of development phases as defined by Feekes (1941) were quantified by the simulated transpiration deficit during that period, being the difference between potential and actual transpiration. A number of development phases were defined in time by dating time of sowing, emergence, florescence and harvest and identifying degree of ripening at harvest. Other development phases were dated using these observations and a decimal code linking crop development stage to fraction of growing season passed (Zadoks *et al.* 1974).

Boundary Conditions and Other Input Data

The upper boundary conditions were satisfied by providing a daily precipitation, corrected for evaporation of intercepted water by a relation which calculates the amount of intercepted rainfall with precipitation and fractional crop cover as dependent variables; a weekly potential evapotranspiration, calculated by correcting evaporation according to Penman (1948) with a crop factor varying during the growing season; and a maximum actual to potential transpiration ratio. It was assumed that precipitation and potential evapotranspiration did not vary within the experimental area, so upper boundary input data were the same for all 119 simulation locations.

The lower boundary condition was satisfied by providing a weekly groundwater depth. Groundwater depths, monitored biweekly on seven locations in an adjacent field, show a strong correlation to surface altitude in the summer. Surface altitude was therefore used to translate the time series of the groundwater depths to the 119 simulation locations. Time series of precipitation, potential evapotranspiration and groundwater depth at a monitoring location are presented in Figure 3.

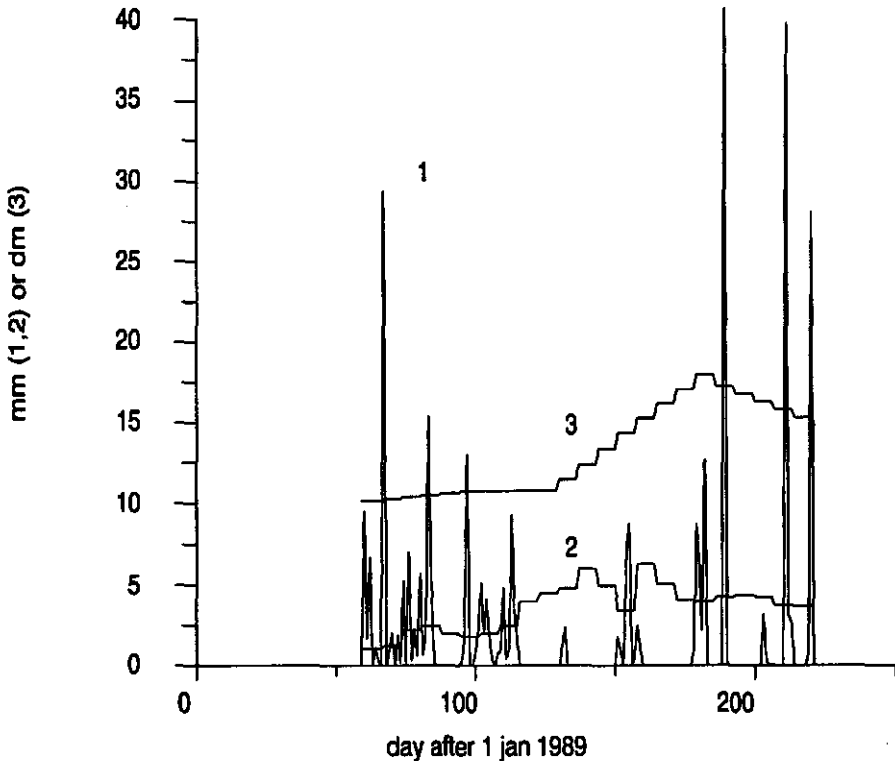


Figure 3 Time series of precipitation events (1, mm) and potential evapotranspiration (2, mm) represented as daily values, and depth to groundwater (3, dm).

Soil hydrological characteristics at 5 cm depth intervals, quantified by the parameters of the analytical functions from Van Genuchten (1980), were obtained by classifying each depth interval into an element of the Staring series (Wösten 1987), using the soil profile descriptions. Simulations started on 1 March 1989 (1 month before sowing) with a soil profile in equilibrium with the initial groundwater depth, and ended on 10 August (day of harvesting). One simulation was carried out at the monitoring location to investigate whether simulation results would be realistic. Simulated and measured matric potentials at 35 cm depth were compared.

Statistical Procedures

Spatial statistics

This study aimed at a comparison between soil- and simulation characteristics on the one hand, and measured yields on the other. However, measured yields are essentially values for an area, and the soil and simulation characteristics are point values. Also, field plots may not contain point observations. To overcome this problem, point values were translated to spatial averages for each of the 62 harvested fields.

To obtain spatial averages, kriging was applied. In this study, kriging will be regarded as a regression procedure (Goldberger 1962; Corsten 1989). In the absence of a trend, assuming that the intrinsic hypothesis holds, the best linear unbiased predictor (BLUP) t of a variable y in an unvisited location can be formulated as (Stein *et al.* 1988; Stein & Corsten 1991):

$$(2) \quad t = \hat{\mu} + g_0' G^{-1} (y - \hat{\mu} 1_n)$$

where $\hat{\mu}$ is a model parameter estimated by $(1' G^{-1} 1)^{-1} 1' G^{-1} y$; g_0 is the n -vector containing the semivariance values between n observations and the prediction point; G is the $n \times n$ matrix containing the semivariance values between the observation points; y is the n -vector containing the observations; and 1_n is the vector of length n containing the elements 1 only.

In this study, a discretized form of block-kriging was used, equivalent to "combining kriging estimates" in the sense of Journel and Huijbregts (1978, p.321). This was preferred to the usual block-kriging (Journel & Huijbregts 1978, p.77), because the fields were unequal in size and were not all rectangular.

The combined kriging estimate T for a field plot was calculated from:

$$(3) \quad T = \frac{1}{M} \sum_{i=1}^M t_i$$

The M prediction locations were situated on a square grid within the field plot. The number of prediction locations ranged from 30 to 36, depending on the shape of the field plot.

Semivariograms of soil- and simulation characteristics were obtained by choosing the best fitted model among a linear model with sill and an exponential model, using a weighted minimal-sum-of-squares criterion between experimental and fitted semivariances. The weighting factor was the number of paired observations used to calculate each point in the experimental semivariogram. The linear semivariogram model with sill is defined

as:

$$(4) \quad \gamma(h) = \begin{cases} C_0(1-\delta(h)) + A * |h| & \text{if } h \leq \text{range} \\ C_0 + A * \text{range} & \text{if } h > \text{range} \end{cases}$$

and the exponential semivariogram model as:

$$(5) \quad \gamma(h) = C_0(1-\delta(h)) + C(1 - \exp\frac{-h}{r})$$

where C_0 is the limit of the semivariogram as h approaches 0 ("nugget variance"); $\delta(h)$ is 1 when $h=0$ and 0 when $h \neq 0$; A is a parameter describing the slope of the linear model, and C is the difference between the nugget and the maximum variance in the exponential model; h is the distance between two locations and r is a distance parameter, that is related to a distance $3*r$ (the "range") at which observations become virtually spatially independent.

Transfer Functions

Measured yields and predicted plot averages (soil- and simulation characteristics) were mutually compared by means of the correlation coefficient. By using multiple linear regression, transfer functions (Bouma & Van Lanen 1986) were constructed that could estimate the yield in 1989 by combinations of soil- and simulation characteristics as independent variables. The quality of the transfer functions was described by the percentage of variance explained. By application of backward elimination, the number of variables used to estimate the yield was reduced until the decrease in the percentage in variance explained became significant. Multiple regression, with and without backward elimination, was performed using SPSS, version 3.32.

RESULTS AND DISCUSSION

Data Collection

Soil Survey and Yield Measurements

The soil survey resulted in the soil map (Fig. 1) and in a database containing soil characteristics at 119 locations. Parameters of fitted variograms of soil characteristics that were used for kriging, are given in Table 1. Grain yields varied between 3409 kg/ha and 6019 kg/ha at 16% moisture content (Fig. 4), where grain moisture contents varied between 13.1 and 14.7%. The mean yield was 4622 kg/ha with a coefficient of variation of 9.2 %. The difference in crop yields between the harvested fields that had smallest areas, which were located close to each other (small values of x - and y -coordinates in Fig. 4) indicate that a considerable variability existed at short distances.

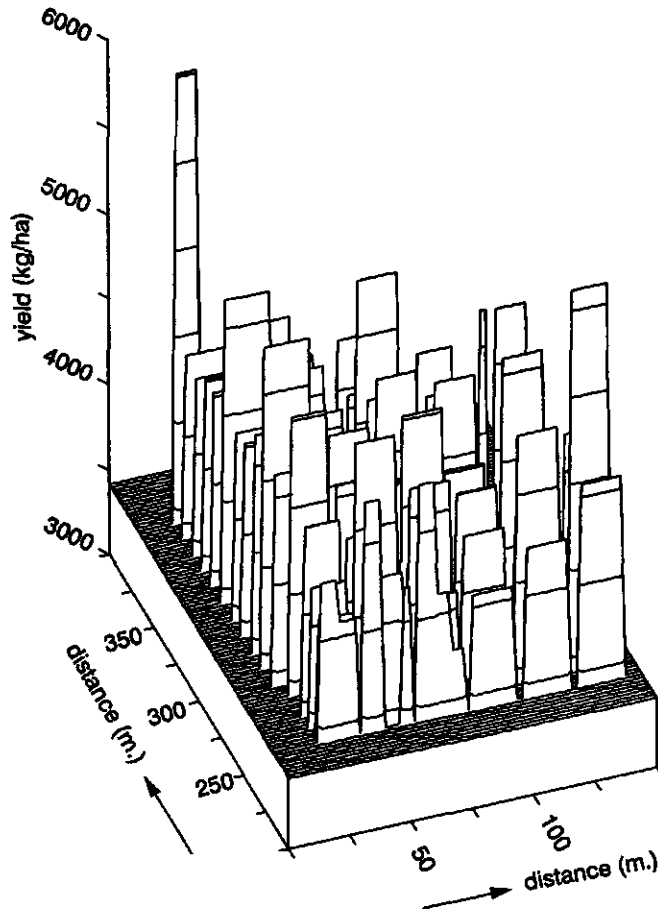


Figure 4 Measured barley grain yields on field plots.

Simulations

A comparison between simulated and observed soil matric potentials at an adjacent site showed a realistic simulation (Fig. 5). During a rewetting phase in the growing season (near day 153), simulated matric potentials were slightly more negative than observed values. This may be explained by hysteresis. Because the differences were small, we thought that simulations with LEACHM at the 119 locations would yield realistic results also. These simulations resulted in a database of simulated transpiration deficits during several crop development stages at 119 locations. Parameters of fitted variograms of simulation characteristics are given in Table 1.

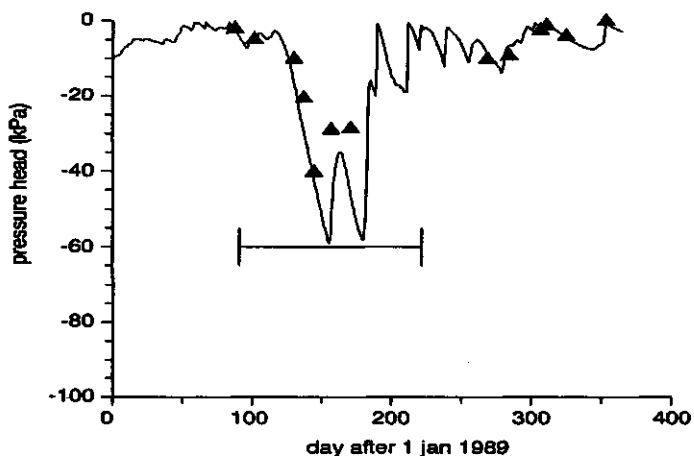


Figure 5 Simulated (solid line) and measured (triangles) soil matric potentials in the rooting zone (35 cm) during 1989 in an adjacent field. Horizontal line indicates growing season.

Table 1 Variogram models fitted to experimental data. TDF_{xxx} is transpiration deficit at Feekes stage *xxx*. CC=Clay Content (%); SC=Sand Content (%); 1=layer 0-40 cm; 2=layer 40-80 cm; 3=layer 80-120 cm.

Variable	Variogram model	----- Variogram parameters -----					R ²
		C0	A	C	r	range	
					m	m	
CC1	exponential	1.57	14.1	-	21.2	-	0.97
SC1	exponential	21.6	85.9	-	79.0	-	0.95
CC2	exponential	5.12	10.4	-	33.3	-	0.80
SC2	exponential	17.0	48.8	-	64.0	-	0.88
CC3	linear/sill	0.0	-	0.38	-	155.0	0.96
SC3	linear/sill	0.0	-	1.45	-	93.1	0.97
TDF4	linear/sill	0.000939	-	0.00000105	-	45.0	0.06
TDF6	linear/sill	0.000836	-	0.00000021	-	113.0	0.01
TDF7	linear/sill	0.000075	-	0.00000016	-	57.7	0.04
TDF8	linear/sill	0.000077	-	0.00001669	-	33.2	0.82
TDF9	linear/sill	0.001963	-	0.00001819	-	36.0	0.47
TDF10	linear/sill	0.002253	-	0.00000422	-	138.0	0.22
TDF10.1	pure nugget	0.001135	-	-	-	-	0
TDF10.2	exponential	0.0	0.00168	-	9.2	-	0.51
TDF10.3	linear/sill	0.001223	-	0.00005877	-	22.8	0.30
TDF10.4	linear/sill	0.001423	-	0.00001490	-	34.9	0.64
TDF10.5	linear/sill	0.001550	-	0.00002114	-	29.8	0.46
TDF11.1	exponential	0.025130	0.00871	-	50.0	-	0.25
TDF11.2	linear/sill	0.025403	-	0.00004235	-	30.7	0.61
TDF11.3	exponential	0.030200	0.01561	-	45.0	-	0.52
mineral N	pure nugget	26.22	-	-	-	-	0

Cumulative transpiration deficits, derived after kriging the 119 point-values to the 62 harvested areas, are presented in Figure 6. Cumulative transpiration deficits were negative between day 140 and 160. Negative deficits occur because the upper soil compartment in the simulated soil profile starts to desiccate. The vertical bars in Figure 6 show that variation is small when the transpiration deficit increases (after crop development stage 10.5). During crop development phases 7 to 10.5, transpiration deficits are small, and variation is larger. Figure 7 gives a map of the simulated cumulative transpiration deficit at harvest date. At harvest, transpiration deficits are largest in the sandy loam soil unit (Fig. 1), and smallest in the clay loam soil unit. The filled up tidal channel (Fig. 1) can be recognized in Fig. 7 by the lower transpiration deficits.

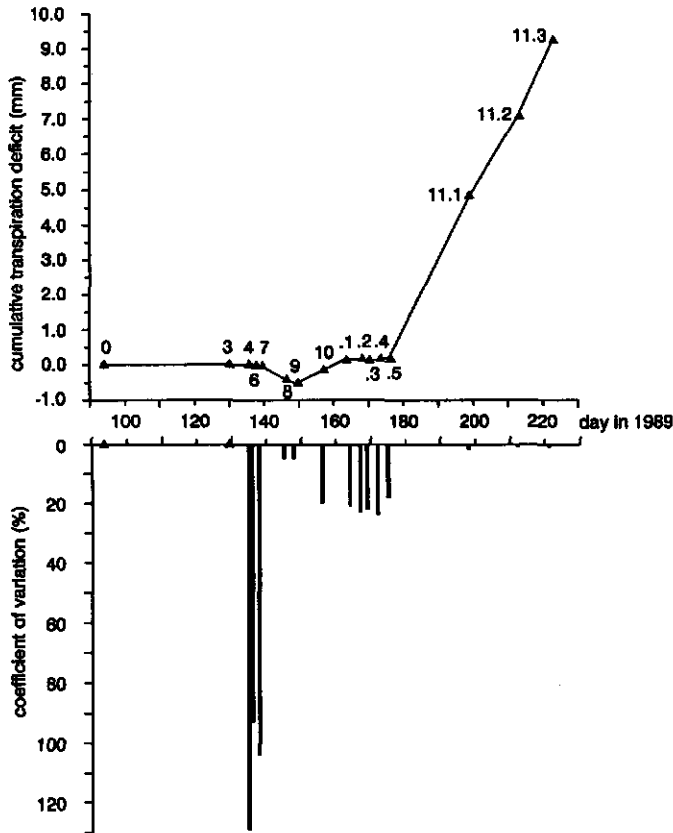


Figure 6 Spatial averages and variability of cumulative transpiration deficits on 62 harvested field plots at several crop development phases according to Feekes. vertical bars indicate the coefficient of variation (CV). Number 11.3 is development stage at harvest.

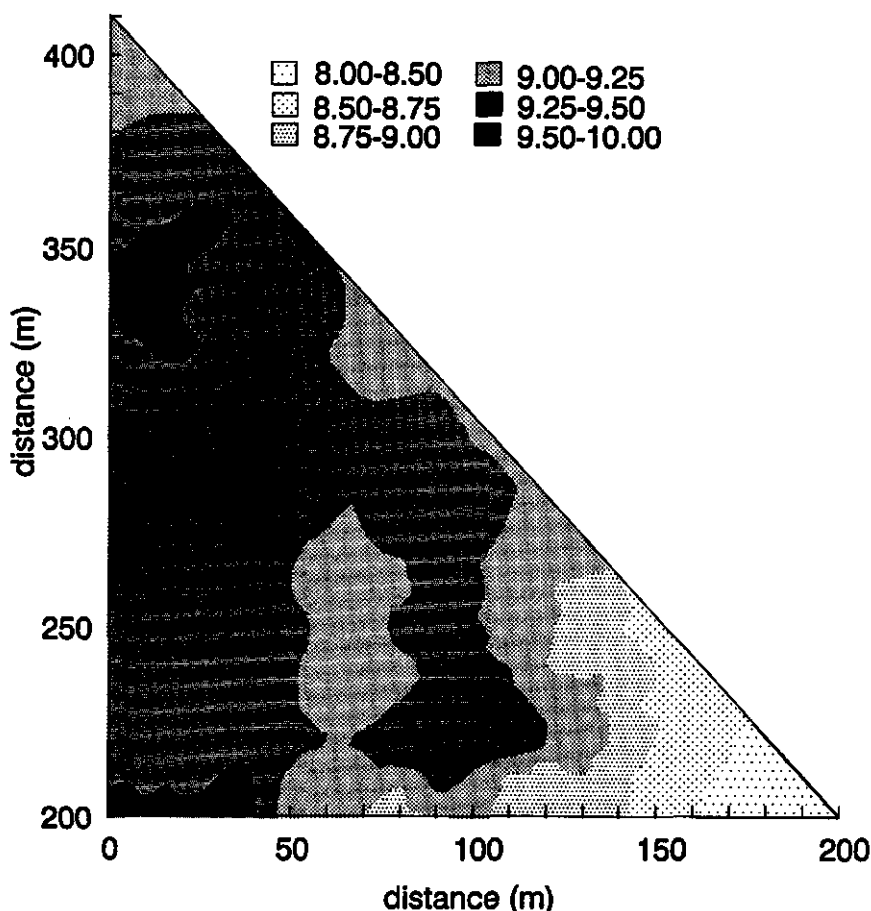


Figure 7 Kriged map of cumulative transpiration deficit (mm) at date of harvest.

Correlating Soil- and Simulation Characteristics to Crop Yields

Soil Characteristics

Correlation coefficients of kriged soil characteristics with grain yields are given in Table 2. Soil texture at depths between 80 and 120 cm showed the strongest correlation with grain yields. Large sand contents in this layer are associated with large yields, and large clay contents with small yields. Clayey texture in this layer possibly limits the upward movement of water, which may cause moisture stress in the rooting zone when evapotranspiration demand is large.

After fertilizing, mineral nitrogen contents in the 0 to 60 cm layer showed a negative correlation with grain yields. This was unexpected, since a positive correlation would seem more logical. However, a negative correlation may be explained if drought occurs. At

locations with more available nitrogen, plants may initially grow faster. In dry periods, the greater Leaf Area Index of a bigger plant induces a greater potential transpiration, which may lead to a transpiration deficit and to stressed growth.

Table 2 Correlations of kriged soil characteristics with barley grain yields on 62 harvested fields.

soil characteristic (% or kg/ha)	layer depth (cm)	barley grain mass yield (at 16% moisture)	moisture content grains
clay content	0- 40	0.11	0.44
sand content	0- 40	-0.17	-0.18
clay content	40- 80	-0.22	0.39
sand content	40- 80	-0.07	-0.22
clay content	80-120	-0.38	0.27
sand content	80-120	0.36	-0.16
mineral N	0-60	-0.32	0.14

Simulation Characteristics

Correlations between kriged simulated transpiration deficits and grain yields are given in Table 3. Transpiration deficits during crop development stages 9, 10.1 and 10.4 show the strongest (negative) correlations with grain yields, indicating that a positive transpiration deficit during these periods is associated with small yields. Correlations between transpiration deficits during the ripening phases (11.1 to 11.4) and grain yields are low. The barley crop appears to be more sensitive to moisture deficits during its vegetative growth and the development of inflorescence than during the ripening phase. This is in agreement with the views from crop science (Geisler 1980). For the positive correlation between transpiration deficits during the florescence and grain yields, no explanation can be given.

Transfer Functions

Measured grain yields were compared to yields estimated by multiple linear regression using soil- and simulation characteristics as explanatory variables (Table 4). Comparisons were made using the percentage of variance explained as the criterion. A pedotransfer function, based on all soil characteristics considered in this study, explained 34.2 % of the variance in crop yields. Backward regression yielded a pedotransfer function, based on clay and sand contents in the 0 - 40 cm layer, and clay contents in the 40-80 cm and 80-120 cm layers that still explained 33.1 % of the crop yield variation. Comparable percentages of variance explained were obtained by regression functions based on simulated transpiration deficits. A combination of both soil- and simulation characteristics into one transfer function gave a substantial rise in the percentage of variance explained to 68.2 %. This indicates, that simulation of the transpiration deficit considerably increased the degree to which the variability could be explained. The effect of the variability of mineral nitrogen contents on Leaf Area Indexes, and thus on variability of potential transpiration, cannot be described by the simulation model used. This effect might have added substantially to the percentage of variance explained.

Table 3 Correlations of kriged transpiration deficits during several crop development stages with barley grain yields on 62 harvested fields. Grains are supposed to be present after growth stage 10.5 (n.r.=not relevant).

crop development stage (Feekes)	description	barley grain mass yield (at 16% moisture)	moisture content grains
4,5		-0.18	n.r.
6		0.01	n.r.
7	stem growth	-0.19	n.r.
8		0.09	n.r.
9		-0.37	n.r.
10		0.04	n.r.
10.1	development	-0.27	n.r.
10.2	of	0.07	n.r.
10.3	inflorescence	0.15	n.r.
10.4		-0.42	n.r.
10.5	florescence	0.26	n.r.
11.1		-0.08	-0.19
11.2	ripening	-0.18	-0.16
11.3/4		-0.12	-0.14

CONCLUSIONS AND RECOMMENDATIONS

Field scale variability of barley grain yield could be explained partly by pedotransfer functions based on soil texture and initial mineral nitrogen content. Another considerable part of the variability could be explained by transfer functions based on simulated transpiration deficits during sensitive plant development phases. This indicates that the spatial variability of transpiration is a major cause of field-scale variability in yields.

This knowledge may be implemented in a procedure leading to a soil quality map which shows areas of relative drought hazard, based on a map of transpiration deficits in a dry growing season as presented in Fig. 7. This would give the farmer a tool to prevent local drought through selected irrigation, and thus of raising average and total yield at minimal costs.

Variability of mineral nitrogen showed a strong correlation to grain yields, indicating that incorporation of nutrient fluxes in simulation models may pay off when yield variability is being predicted.

Table 4 Results of multiple regression analysis. *m.r.* = multiple regression; *b.e.* = backward elimination; *CC*=Clay Content (%); *SC*=Sand Content (%); *MNC*=Mineral Nitrogen Content (kg N/ha); *TDF_{xx}*=Transpiration Deficit at Feekes stage *xx.x*; 1=layer 0-40 cm; 2=layer 40-80 cm; 3=layer 80-120 cm.

Method	----- Independent variables used for regression -----		Percent of variance explained
	type	name	
m.r.	soil	CC1, CC2, CC3, SC1, SC2, SC3, MNC	34.2
b.e.	soil	CC1, SC1, CC2, CC3	33.1
m.r.	simulation	TDF4/5 TO TDF11.4	43.1
b.e.	simulation	TDF9, TDF10.4, TDF11.1, TDF11.2	31.6
m.r.	soil&simulation	CC1, CC2, CC3, SC1, SC2, SC3, MNC, TDF4/5 TO TDF11.4	68.2
b.e.	soil&simulation	SC1, CC3, SC3, TDF4/5, TDF6, TDF7, TDF9, TDF10, TDF10.2, TDF10.3, TDF10.4, TDF10.5, TDF11.1, TDF11.3	65.4

		name	coefficient	standard error
b.e.	soil	CC1	44.6	31.54
		SC1	-16.9	23.92
		CC2	79.0	41.55
		CC3	-110.7	26.36
b.e.	simulation	-	4842.1	2106.43
		TDF9	-6986.8	2092.98
		TDF10.4	-11144.2	3064.65
		TDF11.1	-1148.1	1089.19
		TDF11.2	4967.2	2330.14
b.e.	soil&simulation	-	-2739.9	5085.66
		SC1	-225.3	41.06
		CC3	80.9	37.63
		SC3	-161.8	40.25
		TDF4/5	36540.6	13496.28
		TDF6	33369.5	12806.23
		TDF7	72947.3	22279.45
		TDF9	-15353.4	3480.26
		TDF10	-8727.5	4061.06
		TDF10.2	-11908.9	3686.77
		TDF10.3	-19499.8	5486.05
		TDF10.4	-24653.4	6782.80
		TDF10.5	-6822.9	5479.79
TDF11.2	13051.3	3595.76		
TDF11.3	4518.2	2980.81		
-	14967.7	12107.94		

ACKNOWLEDGEMENT

The authors are grateful to EC-project EV-4V-0098 for funding this study, to A. Stein for helpful comments and to L. Spoelstra and D. Schipper for technical assistance.

REFERENCES

- Bouma, J. & Van Lanen, H.A.J. (1986). Extension functions and threshold values: from soil characteristics to land qualities. In *Quantified Land Evaluation Procedures* (Eds K.J. Beek, P.A. Burrough & D.E. McCormack), pp.106-110. Enschede: ITC.
- Church, B.M. & Austin, R.B. (1983). Variability of wheat yields in England and Wales. *Journal of Agricultural Science, Cambridge*. 100, 201-204.
- Corsten, L.C.A. (1989). Interpolation and optimal linear prediction. *Statistica Neerlandica* 43, 69-84.
- Feekes, W. (1941). De tarwe en haar milieu. Verslag van de technische Tarwe Commissie Groningen. (In Dutch)
- Finke, P.A. (1991). Soil survey to obtain basic simulation data for a heterogeneous field with stratified marine soils. In *EUR 13501 - Soil and Groundwater Research Report II: Nitrate in soils*. Luxemburg: Office for Official Publications of the European Communities, pp. 26-41.
- Gales, K. (1983). Yield variation of wheat and barley in Britain in relation to crop growth and soil conditions -a review. *Journal of the Science of Food and Agriculture* 34, 1085-1104.
- Geisler, G. (1980). *Pflanzenbau*. Berlin: Verlag Paul Parey.
- Goldberger, A.S. (1962). Best linear unbiased prediction in the generalized linear model. *Journal of American Statistic Association* 57, 369-375.
- Journel, A.G., & Huijbregts, C.J. (1978). *Mining Geostatistics*. New York: Academic Press.
- Neeteson, J.J. (1989). Assessment of fertilizer nitrogen requirement of potatoes and sugar beet. PhD Thesis, Agricultural University, Wageningen.
- Penman, H.L. (1948). Natural evaporation from open water, bare soil and grass. *Proceedings of the Royal Society of London Series A* 193, 120-146.
- Soil Survey Staff (1975). *Soil Taxonomy: A basic system of soil classification for making and interpreting soil surveys*. USDA-SCS Agricultural Handbook 436 Washington DC: US Government Printing Office.
- Stein, A. & Corsten, L.C.A. (1991). Universal kriging and cokriging as a regression procedure. *Biometrics* 47, 575-587.
- Stein, A., Bouma, J., Van Dooremolen, J. & Bregt, A.K. (1988). Cokriging point data on moisture deficit. *Soil Science Society of America Journal* 52, 1418-1423.
- Tits, M., Delcourt, H., Vervaeke, F., Vansichen, R. & De Baerdemaeker, J. (1989). Grain yield maps and related field characteristics. *Proc. 11th Int. Congr. Agric. Eng., Dublin*, 4-8 Sept. 1989 1, 2791-2796.
- Van Diepen, C.A., Rappoldt, C., Wolf, J. & Van Keulen, H.(1988). *CWFS Crop Growth Simulation Model WOFOST documentation version 4.1*. Staff working paper SOW-88-01, Centre for World Food Studies, Amsterdam/Wageningen.
- Van Genuchten, M. Th. (1980). A closed form equation for predicting the hydraulic conductivity of unsaturated soils. *Soil Science Society of America Journal* 44, 892-898.
- Van Keulen, H. & Wolf, J. (eds.) (1986). *Modelling of agricultural production: weather, soils and crops*. Simulation monographs. Wageningen: Pudoc.
- Wagenet, R.J. & Hutson, J.L. (1989). Leaching Estimation And Chemistry Model: A

process based model of water and solute movement transformations, plant uptake and chemical reactions in the unsaturated zone. Continuum Vol. 2. Water Resources Institute, Cornell University Ithaca, New York.

- Wösten, J.H.M. (1987). Description of water retention and hydraulic conductivity characteristics from the Staring series with analytical functions. Internal report no. 2019, Dutch Soil Survey Centre, Wageningen. (In Dutch).
- Wösten, J.H.M., Bannink, M.H., De Gruijter, J.J. & Bouma, J.(1986). A procedure to identify different groups of hydraulic-conductivity and moisture-retention curves for soil horizons. *Journal of Hydrology*. 86, 133-145.
- Zadoks, J.C., Chang, T.T. & Konzak, C.F. (1974). A decimal code for the growth stages of cereals. *Weed Research* 14, 415-421.

CHAPTER 3.2

INTEGRATION OF REMOTE SENSING DATA IN THE SIMULATION OF SPATIALLY VARIABLE YIELD OF POTATOES

In press: *Soil Technology* (1992)

INTEGRATION OF REMOTE SENSING DATA IN THE SIMULATION OF SPATIALLY VARIABLE YIELD OF POTATOES

P.A. FINKE

Department of Soil Science and Geology, P.O. Box 37, 6700 AA Wageningen, The Netherlands

ABSTRACT

Field scale variation of final potato tuber yields was measured on 36 plots of 4.5*4.5 sq. meters. The average yield was 9014 kg dry matter/ha, and the coefficient of variation was 10.4%. A model was developed that simulates tuber dry matter production as a function of radiation and of water- and nitrogen availability. Water flow and Nitrogen fate were simulated satisfactorily. The model was sensitive to changes of the Leaf Area Index (LAI) during the growing season.

If LAI, measured by a remote sensing technique at 5 dates and 76 locations, was used for input to the model, 39.2% of the variance of measured final yields could be explained by the simulated final yields. Significantly different average yields were measured and simulated between two soil units present in the field. Simulations proved, that the spatial variation in final dry matter yields was largely caused by variability of moisture availability.

Integration of remote sensed LAI into a model allows the identification of stress factors during the growing season, and their spatial coordinates, which can be used for location-specific land management.

INTRODUCTION

Several studies have been published on field-scale variability of crop yields (Church *et al.*, 1983; Gales, 1983) and on possible causes. Bresler and Dagan (1988a, 1988b) and Dagan and Bresler (1988) used a deterministic simulation model to identify soil- and plant related factors to which yield variability is sensitive. It was concluded (Dagan and Bresler, 1988) that crop yield was sensitive to parameters describing the water retention and hydraulic conductivity characteristics. Furthermore, they identified the potential transpiration as a sensitive parameter. In the present study, it is attempted to explain field-scale yield variability by simulation of the combined effects of variability of soil physical characteristics and variability of potential transpiration. The spatial variation of the potential transpiration can be estimated by spatial measurements of the leaf area index.

Applications of remote sensing in evaluating spatially variable soil and crop properties or soil cover properties are abundant. High correlations between measured yields and infrared reflectance are reported in literature (Aase *et al.*, 1984, Van der Heijden *et al.*, 1989). In the near infrared region (700-1300 nm) of the electro-magnetic spectrum, reflectance can be considered as a function of the total amount of leaves present, and consequently of the Leaf Area Index (LAI). As long as leaves do not turn yellow, accumulated biomass can be considered proportional to the LAI.

Remote sensing may efficiently be used to estimate final yield levels and yield variability. However, it does not explain the reasons why local peaks and depressions in

yield develop. A combination of regularly measuring the LAI and simulating crop growth may reveal these reasons, and may provide a tool to remove stress factors during the growing season.

This paper presents a study where space and time series of remote sensing data were integrated in a simulation model describing potato growth as a function of radiation, LAI, water availability and nitrogen availability during the growing season. The contribution to the simulation quality of the LAI-space and time series obtained by remote sensing, was evaluated by comparison to simulations using a relation between soil coverage fraction and the LAI from literature.

MATERIALS AND METHODS

Study Area

The study area, a 2.5 ha part of an agricultural field of about 7 ha, is located in the Wieringermeer polder in the North-Western part of the Netherlands. Since reclamation in 1930, the area has been in agricultural use. Soils are thinly stratified, and were classified as fine-loamy, calcareous, mesic Typic Udifluvents (Soil Survey Staff, 1975). A strong variability in texture in both lateral and vertical directions was encountered during a detailed soil survey (Finke, 1991), during which 402 profile descriptions were collected in the 7 ha field. A map of the soil texture is presented in Fig. 1.

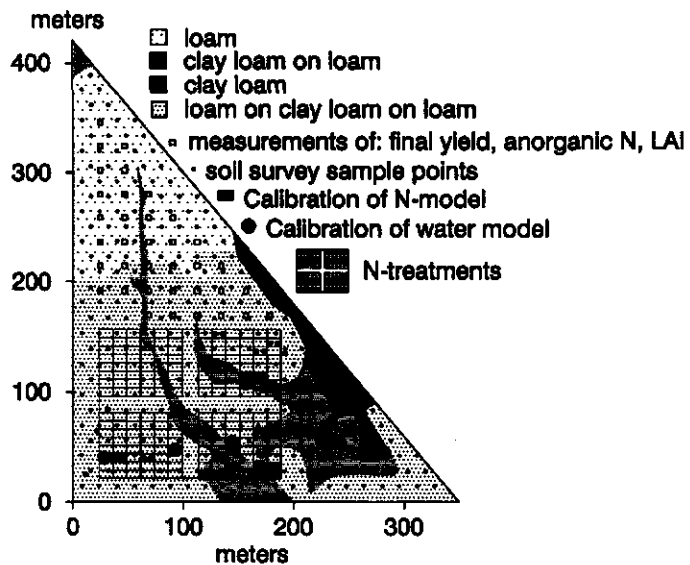


Figure 1 Soil texture map of the study area on which sampling and simulation locations are indicated.

Soil physical characteristics were measured on 7 locations and in twofold for functional

soil layers, which are layers that are easily recognizable in a soil survey, and show significantly different hydraulic behaviour. Functional layers were defined using a methodology presented elsewhere (Finke *et al.*, 1992; Finke and Bosma, in press). Functional layers are used to generate simulation model input data (more specifically, soil physical characteristics) from soil profile descriptions. Spatial variation of the thickness, depth of occurrence and type of functional layers, which is inventoried during the soil survey, allows the location-specific estimation of soil physical characteristics.

Field Measurements

During a 3 year period, including the growing season of 1990, soil matric potentials at several depths and depth to groundwater were monitored biweekly on 7 locations. Of the 7 time series thus obtained, 5 were used in this study (Fig. 1). Meteorological data, like precipitation, potential evapotranspiration, relative air humidity and global radiation were measured daily at the farm (1 km distance).

Before fertilizing, anorganic nitrogen content was measured in a layer between 0 and 60 cm depth on 43 locations. These 43 locations were located on a square grid having a mesh of 22 meters (Fig. 1). Near 38 of these grid locations, paired observations were made of reflections in near-infrared and red wavelengths, using a multi-spectral radiometer. The distance between the paired observations was 1 meter. Purpose of the grid sampling with replicates at one meter was, to determine the scale at which spatial variation occurs. At these locations, also soil coverages were estimated by point counting 100 grid points. Observations were made at several dates in the growing season: June 15 and 26, July 4, 17 and 27. Each remote sensing observation covered a ground area bordered by a circle having a diameter of 1 meter, each soil coverage point count covered a square of 1 sq. meter. At June 26 and August 13, additional LAI-measurements were made on 16 locations, whereafter corresponding areas of 1 sq. meter were harvested to determine the LAI in the laboratory.

At the end of the growing season, potato tuber yields were determined on 36 experimental plots of 4.5*4.5 sq. meters, each plot covering the area of 2 time series of LAI-measurements and of 1 anorganic N measurement. To test whether 2 major soil units present in the field had different yields, a t-test on difference of means was used.

Remote Sensing Methodology

When estimating the LAI, it is necessary to estimate first the soil coverage fraction to correct for reflection for bare soil. In the visible part of the electromagnetic spectrum, roughly 80% of incoming radiation is absorbed and about 10% is reflected by each plant leaf layer. In practice, the reflection of the upper leaf layer determines the total reflection of the crop in these wavelengths. Since reflections of bare soil and plants contrast strongly, reflection percentages in the visible spectrum can be used to estimate the soil coverage fraction. In near infrared wavelengths (700-1300 nm), reflectance and transmittance of a green leaf are both about 50%, and absorption is of little magnitude (Colwell, 1983). Since transmittance is relatively high, also green leaves under the top leaves contribute significantly to the total reflectance. Reflection percentages in the near infrared spectrum can therefore be used to determine the LAI.

Clevers (1986) developed a reflection model that expresses measured reflection as the combined reflections of plant and soil:

$$(1) \quad r = r_v * B + r_s * (1 - B)$$

where r = total measured reflection (%); r_v = reflection (%) of the vegetation; r_s = reflection (%) of the soil, and B is the apparent soil cover fraction (dimensionless). A corrected reflection is calculated by subtracting the contribution of the soil from the measured reflection:

$$(2) \quad r' = r - r_s * (1 - B)$$

where r' = the corrected reflection percentage. For many soils (Clevers, 1986) the ratio between infrared and red reflection is constant, and independent of the moisture content of the soil, so

$$(3) \quad \frac{r'_{ir}}{r'_{r}} = C$$

By combination of equations 2 (for r'_{ir} and r'_r) and 3, one obtains:

$$(4) \quad r'_{ir} - C * r'_r = r_{ir} - C * r_r$$

Since r'_{ir} can be expected to be much greater than r'_r , and C was found to be close to unity, equation 4 can be simplified by removing the $C * r'_r$ term.

A relation between the LAI and r'_{ir} was given by Clevers (1986):

$$(5) \quad LAI = -\frac{1}{\alpha} * \ln\left(1 - \frac{r'_{ir}}{r_{\infty,ir}}\right)$$

where α is a combination of extinction- and dispersion-coefficients, regarded as a fitting parameter, and $r_{\infty,ir}$ is the asymptotic value of the corrected infrared reflection at very large LAI. The empirical parameters α and $r_{\infty,ir}$ were derived by fitting equation 5 to experimental data consisting of measurements of the LAI and corresponding infrared- and red- reflections. Fitting was done using the NLIN (non-linear regression) subroutine from the SAS-package release 5, SAS Institute Inc..

Reflection measurements were made using an hand-held multi-spectral radiometer (CROPSCAN, Inc.) attached to a portable microcomputer (Tandy 102 Radio Shack TRS 80). Wavelengths used were 670 nm (red) and 870 nm (near infrared).

Translating Measured Data to Equal Space Scales

One purpose of this study was to compare simulated versus measured final crop yields. Measured yields are the result of sampling a plot of 4.5*4.5 sq. meters. Other measurements such as soil profile descriptions and anorganic nitrogen content are essentially point values, whereas LAI-measurements refer to a smaller area of 0.79 sq. meters. To overcome this scale problem, all variables that would serve as input to the simulation model, were translated to a spatial average for each harvested field of 4.5*4.5 sq. meters.

To obtain a spatial average within a harvested field, a large number of kriging interpolations to points within the relevant area were made, and these interpolations were averaged. This kriging method is known as "combining kriging estimates" (Journel and Huijbregts, 1978 p.321). It was assumed that taking the spatial average following this method would cause no bias in simulation results, so the response of the simulation model to variability of input parameters within each harvested field was assumed linear.

Simulation of Water Flow, Nitrogen Fate and Crop Growth

Simulation of water flow, Nitrogen transformations and uptake of water and of nitrogen compounds by plants was simulated by the LEACHN-model (Hutson and Wagenet, 1991). This model was extended to simulate crop growth.

Water flow is simulated by a numerical solution of the Richards equation:

$$(6) \quad \frac{\partial \theta}{\partial t} = \frac{\partial}{\partial z} \left[K(\theta) \frac{\partial H}{\partial z} \right] - A(z,t)$$

where θ is the volumetric water content (m^3/m^3), $K(\theta)$ is the hydraulic conductivity function dependent on θ (mm/day), $\partial H/\partial z$ is the hydraulic gradient (mm/mm), A represents water extraction by roots, z is depth (mm) and t is time (days). For the functions between K , θ and the matric potential h that are required, the closed form equations of Van Genuchten were used (Van Genuchten, 1980). The lower boundary condition was satisfied by providing a weekly groundwater depth, translated from a monitoring plot in the same field by surface altitude. The upper boundary condition was provided by daily potential evapotranspiration and precipitation data. Plant uptake of water is a function of the potential transpiration and moisture availability in the rootzone. Daily potential transpiration was calculated as follows, according to Belmans *et al.* (1983):

$$(7) \quad T_p = ET_p * [1 - \exp(-0.6I)]$$

where T_p is potential transpiration (cm/day), ET_p is potential evapotranspiration (cm/day, input in the model) and I is the Leaf Area Index (m^2/m^2 soil).

Nitrogen cycling is described in LEACHN according to the concepts and equations of Johnsson *et al.* (1987). Nitrogen cycling pathways are given in Fig. 2. Three organic pools of Nitrogen, characterized as a quickly degrading manure and litter pool and a relatively stable humus pool are distinguished in the model. Also a urea pool and a mineral ammonia and nitrate pool are identified. Mineralization processes, nitrification and denitrification are described by first order rate constants. Volatilization is defined as a first order process in the surface layer. Rate constants are adjusted for temperature and water content effects (Johnsson *et al.*, 1987). For the temperature effect, a Q_{10} -type response is assumed. In LEACHN, ammonium, nitrate and urea can be partially sorbed onto soil surfaces through a linear sorption isotherm:

$$(8) \quad S = K_d * c$$

where c is chemical concentration in the liquid phase (mg/dm^3), s is chemical concentration in the sorbed phase (mg/kg dry soil) and K_d is the distribution coefficient (dm^3/kg). Chemical transport is simulated by a numerical solution to the convection-

dispersion equation (Wagenet, 1983):

$$(9) \quad \frac{\partial(\theta c)}{\partial t} + \frac{\partial(\rho s)}{\partial t} = \frac{\partial}{\partial z} [\theta D(\theta, q) \frac{\partial c}{\partial z} - qc] - U(z, t) \pm \phi(z, t)$$

where ρ is soil bulk density (kg/dm^3), $d(\theta, q)$ is the effective dispersion coefficient (mm^2/day), q is water flux density (mm/day), ϕ is a source/sink term ($\text{mg}/\text{dm}^3, \text{day}$) representing gains/losses through transformation and $U(z, t)$ is plant uptake of nitrogen ($\text{mg}/\text{dm}^3, \text{day}$). The plant uptake of nitrogen is determined by the transpiration flux and the concentration in the compartments of the rootzone.

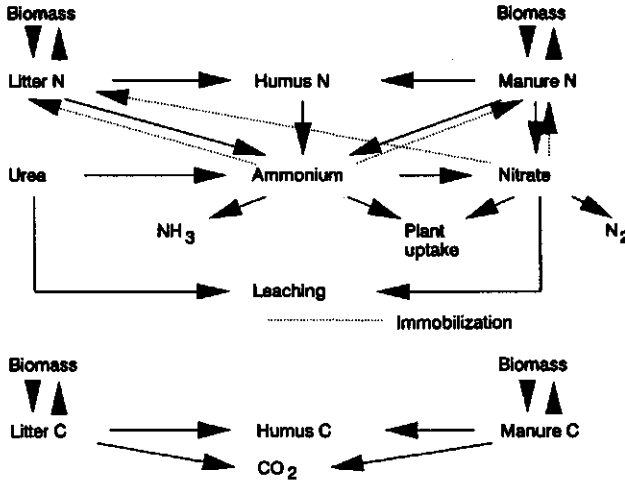


Figure 2 Transformation and fate pathways of nitrogen and carbon species, which can be simulated with LEACHN (adapted from Johnsson *et al.* 1987).

Crop growth, stressed only by limiting water availability, is modelled according to a method described by Feddes *et al.* (1988). A theoretically possible maximum growth rate of dry matter, suffering no water- or nutrient stress, can be expressed as:

$$(10) \quad q_m = c * [P_{st} * (1 - e^{-vI}) - \chi_m]$$

where q_m is theoretically possible maximum dry matter growth rate ($\text{kg}/\text{ha}, \text{day}$), c is conversion factor from sugars to starch, P_{st} is the photosynthetic rate ($\text{kg}/\text{ha}, \text{day}$) of a standard canopy with a leaf area index of 5, depending on radiation and geographical latitude, v is solar radiation extinction factor, I is leaf area index (m^2/m^2 soil) and χ_m is maintenance respiration (CH_2O in $\text{kg}/\text{ha}, \text{day}$). The water stressed dry matter growth rate as a result of the actual transpiration rate is calculated according to Feddes *et al.* (1988):

$$(11) \quad q_w = 0.5 * [W \frac{T}{\Delta e} + \sqrt{(q_m + W \frac{T}{\Delta e})^2 - 4q_m W \frac{T}{\Delta e} (1 - \xi)}]$$

where q_w is water stressed dry matter growth rate (kg/ha.day), W is maximum water use efficiency (kg.mbar/ha.mm), T is actual transpiration (mm/day), Δe is the average vapour pressure deficit of the air (mbar) and ξ is a mathematical parameter.

Furthermore, growth rate stressed by a limiting nitrogen availability is simulated by multiplication of the water stressed growth rate q_w by a stress factor S_n , calculated from (Greenwood *et al.*, 1985; Neeteson *et al.*, 1987):

$$(12) S_n = \min\left[1, \frac{P_w - P_0}{P_M - P_0}\right]$$

where S_n is the stress factor for the current day, P_w is the actual %N in total dry matter, P_0 is the %N in total dry matter when growth ceases (increasing from 0% at the start of crop growth to 0.8% at plant maturity) and P_M is the minimum %N in total dry matter to have the maximum growth rate. P_M is defined as (Greenwood *et al.*, 1985):

$$(13) P_M = 1.35 * [1 + 3 * \exp(-0.26 * W)]$$

where W is the total weight of dry matter (kg.10³/ha).

Model Calibration and Evaluation of Model Performance

The model was calibrated in three successive phases. Generally, calibration was done for a number of plots simultaneously, by adjusting the calibration parameter for all plots in the same way. Simulation- and measurement-time series were compared statistically and graphically. It was assumed, that the calibration parameter did not show spatial variation.

First, the water flow model was calibrated. For the time period between April 1 and September 3 in 1990, simulated and measured soil matric potentials at 35, 45 and 75 cm depth were compared at 5 locations. Tuning of the model was done through varying the thickness of the rooting zone.

Second, the nitrogen model was calibrated. Since no time series of N measurements were available from the 1990 growing season, the nitrogen model was calibrated on data from the hydrological year between April 1, 1989 and April 1, 1990. Simulations and measurements of soil mineral N (0-100 cm depth) were compared for 8 locations. These locations received various amounts of manure, corresponding to N-additions between 0 and 300 kg N/ha, and received an anorganic fertilizer gift of 35 kg N/ha. On some plots a catch crop was grown. Tuning of the model was done by adjusting the Q_{10} -factor, the nitrification rate factor and the distribution coefficient K_a of ammonia.

Third, the potato-growth model was calibrated by comparing measured and simulated final dry matter yields in 1990 on 8 locations. Tuning was done by adjusting the maximum water use efficiency W . The potato-growth model was tuned twice: once when LAI-values estimated by remote sensing measurements were input to the model, and once when no LAI measurements were available.

To evaluate model performance when using or disregarding remote sensing information, the calibrated model was run on 36 locations where harvests were done. The quality of simulated final dry matter yields of potato tubers was established by direct comparison to measurements and by calculating the percentage of variance of measured final yields that could be explained by the simulations.

RESULTS AND INTERPRETATION

Potato Yield, Anorganic Nitrogen and Remote Sensing Measurements

Measured final potato tuber yields varied between 6195 and 11155 kg dry matter/ha. The average yield amounted to 9014 kg dry matter/ha, and the coefficient of variation was 10.4%. Yields in the loam soil unit (Fig. 1) were significantly lower than yields in the loam soil unit with a clay loam layer (Table 1).

Table 1 Results of test that average yields in two soil units differ. Unit A = loamy textured soils; unit C = loamy textured soils with a clay loam layer below the plow layer; n.r. = not relevant; N = nitrogen availability; n = number of yields in smallest soil unit.

Yields	Stress factor	--- Average yield ---		n	Significance
		Unit A	Unit C		
		kg/ha	kg/ha	-	
measured	n.r.	8555	9527	17	> 0.99
simulated	water	8827	9913	17	> 0.99
simulated	water, N	8510	9880	17	> 0.99

The average amount of anorganic nitrogen in the layer from 0 to 60 cm before fertilizing was 315 kg N/ha, with a coefficient of variation of 32%. These high levels are probably due to the strong mineralization in the relatively warm winter of 1989-1990. Before planting, an additional gift of 115 kg N was given as anorganic fertilizer.

Space and time series of the LAI could be estimated from remote sensing measurements after the parameters from equation 5 were fitted. The quality of estimated LAI-values relative to measurements was good ($R^2=88.8\%$), and is presented in figure 3.

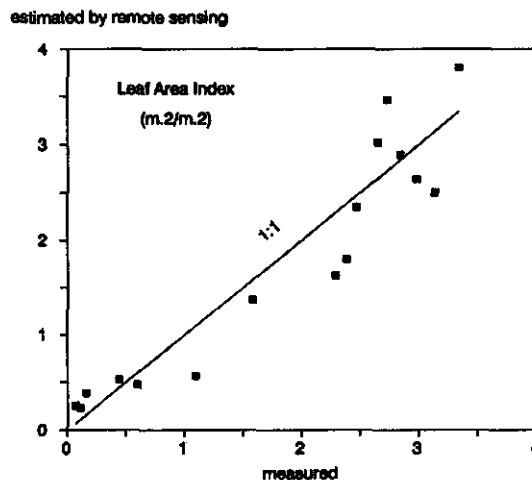


Figure 3 Comparison of the LAI estimated by remote sensing and directly measured LAI.

Spatial structure of the LAI at 5 dates in the growing season is expressed by the variograms of fig 4. In all cases, spatial structure could be modelled adequately by simple linear or gaussian semivariogram models. Spatial variability of the LAI decreases after plants have reached maturity in the last week of June, as appears from the lower values of semi-variances after the June 26 measurements.

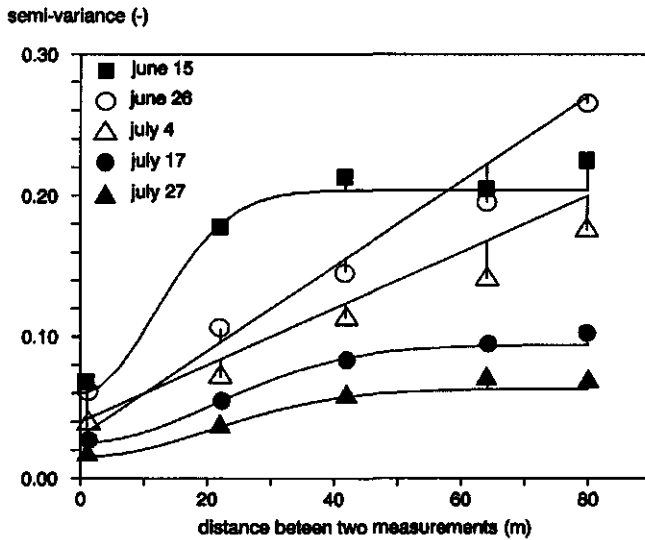


Figure 4 Variograms of the LAI at 5 dates.

Measured final yields and LAI-estimations by remote sensing, kriged to the harvested fields, are moderately to strongly correlated, as appears from table 2. The LAI on 4 July showed the strongest correlation. After this date, correlations decrease, presumably because leaves start turning yellow, and biomass production goes predominantly to tubers.

Table 2 Correlation coefficients between LAI-values estimated by remote sensing and measured final yields.

Variable	Correlation	Significance
LAI June 15	0.555	> 0.999
LAI June 26	0.610	> 0.999
LAI July 4	0.727	> 0.999
LAI July 17	0.554	> 0.999
LAI July 27	0.514	> 0.99

Simulations

The calibration of the water flow model resulted in good simulations of soil matric potentials relative to measurements ($R^2=73.7\%$), as indicated in figure 5. Only at wet matric potentials between 0 and approximately 3 kPa, simulations are somewhat drier than measurements. Simulated matric potentials agreed best to measurements when the depth of

the rooting zone at root maturity was 65 cm, which corresponded well with field observations done in an adjacent field.

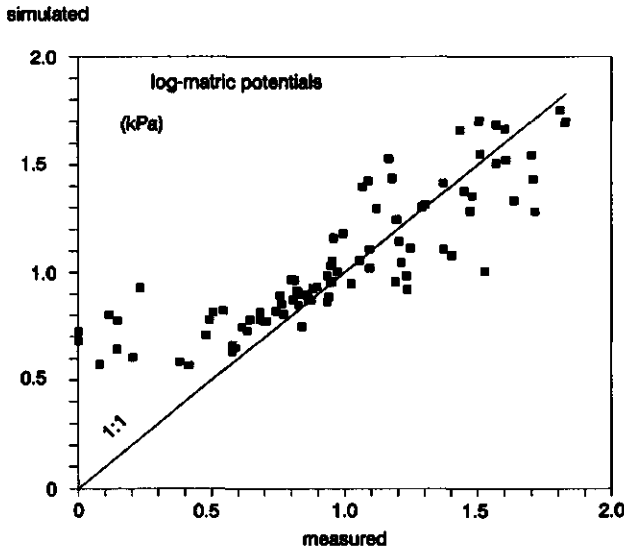


Figure 5 Calibration results of the water submodel.

The calibration of the nitrogen model resulted in reasonably good predictions ($R^2=70.5\%$) of the total anorganic nitrogen content of the upper profile meter (fig. 6).

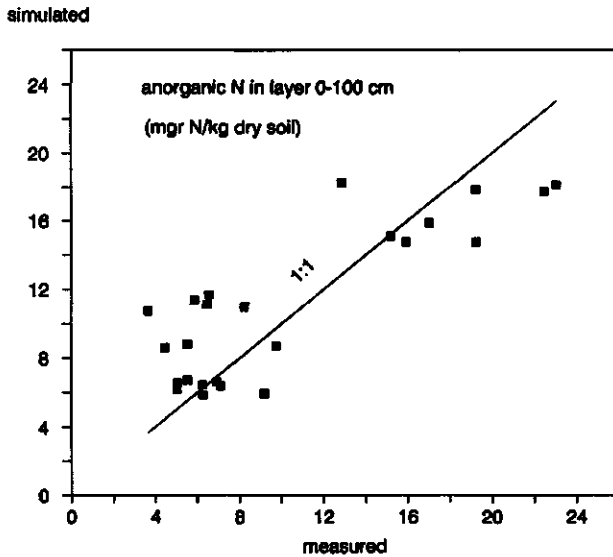


Figure 6 Calibration results of the nitrogen submodel with respect to anorganic nitrogen over the upper profile meter.

Simulations on 36 harvested plots, using the remote sensing data to obtain LAI-space and

time series, are presented in figure 7. Simulated yields in the loam soil unit (Fig. 1) were significantly lower than yields in the soil unit with a clay loam layer (Table 1). Simulations of potato tuber final dry matter yields could explain 36.2 % of the variance of measured yields (table 3). Simulations on the same 36 plots, considering only the effect of moisture stress on crop growth, could explain 39.2%.

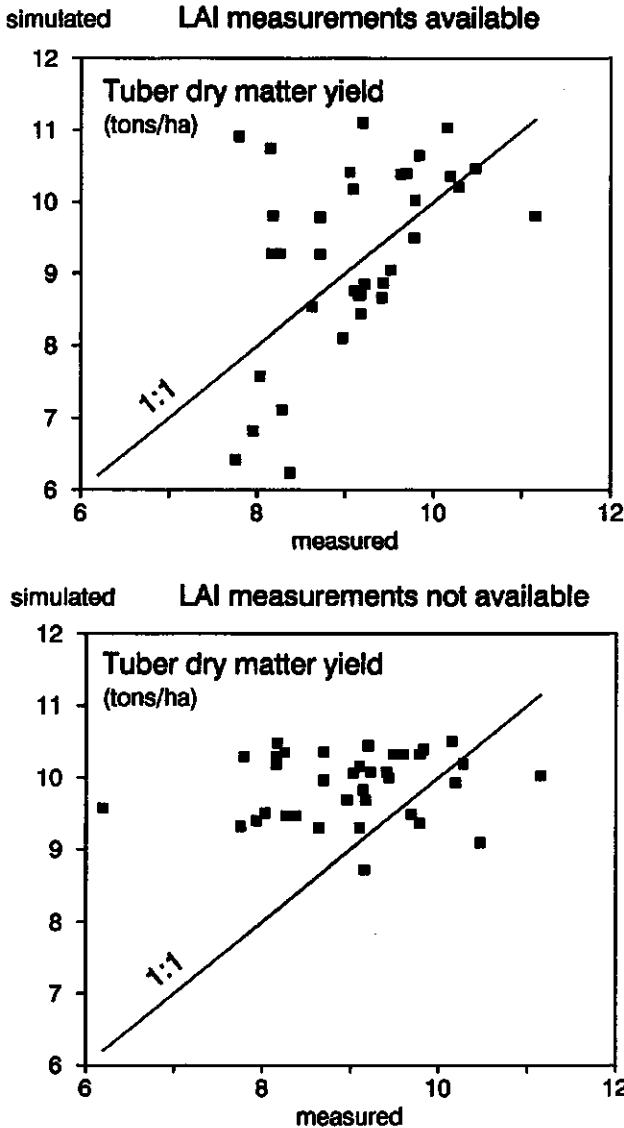


Figure 7 Simulation results of the potato-crop growth model, with and without incorporation of remote sensing measurements of the LAI.

Table 3 Comparison of simulated to measured tuber dry matter yields in 1990.

Type of stress	LAI measured by remote sensing	Correlation coefficient	Percentage of variance explained
water	yes	0.63	39.2
water, nitrogen	yes	0.60	36.2
water, nitrogen	no	0.14	1.9

Simulations incorporating the effects of both water- and nitrogen stress performed slightly worse than simulations only regarding water stress. This may be due to the high spatial variability at short distances of anorganic nitrogen present in the 0-60 cm soil layer at the beginning of the growing season. This resulted in relatively inaccurate kriging predictions for the 4.5*4.5 sq. meters fields of initial amounts of nitrogen present. Another reason is probably, that the distribution of anorganic nitrogen over depth was assumed constant, which may not have been the case on all locations.

It was concluded, that moisture availability was probably the most important source of variation in potato tuber yields in 1990. This was not unexpected, since anorganic nitrogen levels in the beginning of the growing season were sufficiently high to meet crop demand. Knowledge about spatial patterns of moisture availability can be used for soil management practices. In figure 8, a map is given in which the week is indicated when the transpiration deficit exceeds 2mm. A farmer could use a map such as this one to determine the area for irrigation.

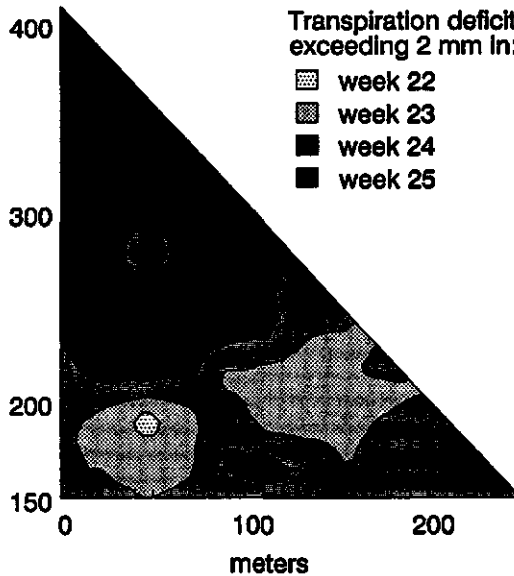


Figure 8 Kriged map showing the week in which the transpiration deficit exceeds 2 mm.

In one other series of 36 simulations, the LAI-space and time series were estimated by a relation from literature between soil coverage fraction and LAI, where soil coverage was monitored in the field. Simulations and measurements of dry matter tuber yields are compared in figure 7. Simulation results are not correlated to measurements (1.9% of variance explained by simulations). It was concluded, that direct incorporation of remote sensed LAI into the model considerably increased the extent to which measured final yield variability could be explained.

CONCLUSIONS

Three conclusions can be drawn from this study:

- (1) Integration of remote sensing data into simulation modelling can explain a considerable part of spatial variability of final crop yields on field scale. It allows the determination of the causes of developing yield depressions and their spatial coordinates.
- (2) Field scale variability of final crop yield could for a considerable part be explained by variability of moisture availability during the growing season.
- (3) Two major soil units found in the study area had significantly different final yields, both when yields were measured as when yields were simulated.

Furthermore, it can be concluded that, when variability of crop production is to be simulated on a field scale, a correct estimation of the variability of the potential and actual transpiration is essential. Potential transpiration strongly depends on the Leaf Area Index, which can be estimated accurately using remote sensing techniques. Actual transpiration is also a function of soil hydraulic properties, which indicates, that knowledge about these properties and their spatial variation is needed.

ACKNOWLEDGEMENTS

Assistance of Ir. I. Janssen and Drs. G.F. Epema with remote sensing measurements is gratefully acknowledged. Also thanks are due to EC-project EV-4V-0098 for funding this study.

REFERENCES

- Aase, J.K., Siddoway, F.H. and Millard, J.P., 1984. Spring wheat leaf phytomass and yield estimates from airborne scanner and hand-held radiometer measurements. *Int. J. Rem. Sens.* 5:771-781.
- Belmans C., Wesseling, J.G. and Feddes, R.A., 1983. Simulation model of the water balance of a cropped soil: SWATRE. *Journal of Hydrology* 63 (3/4):271-286.
- Bresler, E. and G. Dagan. 1988a. Variability of an irrigated crop and its causes. 1. Statement of the problem and methodology. *Water Res. Research* 24(3): 381-387.
- Bresler, E. and G. Dagan. 1988b. Variability of an irrigated crop and its causes. 2. Input data and illustration of results. *Water Res. Research* 24(3): 389-394.
- Church, B.M. & Austin, R.B. (1983). Variability of wheat yields in England and Wales. *Journal of Agricultural Science, Cambridge*. 100, 201-204.

- Clevers, J.G.P.W., 1986. Application of remote sensing to agricultural field trials. Thesis. Agricultural University Wageningen Papers 86-4. 227 pp.
- Colwell, R.N. (Ed.), 1983. Manual of remote sensing, 2nd edition. American Society of Photogrammetry, Fall Church, Virginia.
- Corsten, L.C.A., 1989. Interpolation and optimal linear prediction. *Statistica Neerlandica* 43:69-84.
- Dagan, G. and E. Bresler. 1988. Variability of an irrigated crop and its causes. 3. Numerical simulation and field results. *Water Res. Research* 24(3): 395-401.
- Feddes, R.A., de Graaf, M., Bouma, J. and van Loon, C.D., 1988. Simulation of water use and production of potatoes as affected by soil compaction. *Potato research* 31 (1988) 225-239.
- Finke, P.A., 1991. Soil survey to obtain basic simulation data for a heterogeneous field with stratified marine soils. Soil and groundwater research report II "Nitrate in soils" EUR 13501 EN. Directorate-General for Science, Research and Development, Commission of the European Communities. pp. 26-41.
- Finke, P.A. and Bosma, W.J.P. (In Press). Obtaining basic simulation data for a heterogeneous field with stratified marine soils. *Hydrological processes*.
- Finke, P.A., J. Bouma and A. Stein. 1992. Measuring field variability of disturbed soils for simulation purposes. *Soil Sci. Soc. Am. J.* 56(1): 187-192.
- Gales, K. (1983). Yield variation of wheat and barley in Britain in relation to crop growth and soil conditions -a review. *Journal of the Science of Food and Agriculture* 34, 1085-1104.
- Goldberger, A.S., 1962. Best linear unbiased prediction in the generalized linear model. *Jou. Am. Stat. Ass.* 57:369-375.
- Greenwood, D.J., Neeteson, J.J. and Draycott, A., 1985. Response of potatoes of N fertilizer: Quantitative relations for components of growth. *Plant and Soil* 85: 163-183.
- Hutson, J.L. and Wagenet, R.J., 1991. Simulating nitrogen dynamics in soils using a deterministic model. *Soil use and management* 7(2), 74-78.
- Johnsson, H., Bergstrom, L., Jansson, P.-E. and Paustian, K., 1987. Simulated nitrogen dynamics and losses in a layered agricultural soil. *Agriculture, Ecosystems and Environment* 18, 333-356
- Journel, A.G. and Huijbregts, Ch.J., 1978. *Mining geostatistics*. Academic press, London.
- Neeteson, J.J., Greenwood, D.J. and Draycott, A., 1987. A dynamic model to predict yield and optimum nitrogen fertilizer application rate for potatoes. *Proceedings* 262. The Fertiliser Society, London, 31 pp.
- Soil Survey Staff., 1975. *Soil Taxonomy: A basic system of soil classification for making and interpreting soil surveys*. USDA-SCS Agric. Handb. 436. U.S. Gov. Print. Office, Washington DC.
- Stein, A., Bouma, J., van Dooremolen, J. and Bregt, A.K., 1988. Cokriging point data on moisture deficit. *Soil Sci. Soc. Am. J.* 52:1418-1423.
- Stein, A. and Corsten, L.C.A., 1991. Universal kriging and cokriging as a regression procedure. *Biometrics* 47:575-587.
- Van der Heijden, G.W.A.M., Clevers, J.G.P.W. and Brinkhorst-van der Swan, D.L.C., 1989. Evaluation of the suitability of arable fields for field trials by means of remote sensing. *Euphytica* 41: 199-205.
- Van Genuchten, M. Th., 1980. A closed form equation for predicting the hydraulic conductivity of unsaturated soils. *Soil Sci. Soc. Am. Journal* 44:892-898.

Wagenet, R.J., 1983. Principles of salt movement in soils. In: Chemical mobility and reactivity in soil systems (eds. D.W. Nelson *et al.*). Special publication 11, American Society of Agronomy, Madison, Wisconsin pp. 123-140.

CHAPTER 3.3

FIELD SCALE VARIABILITY OF SOIL STRUCTURE AND ITS IMPACT ON CROP GROWTH AND NITRATE LEACHING IN THE ANALYSIS OF FERTILIZING SCENARIOS

Presentation at: *1992 Conference of Working Group MV of the ISSS:
Operational Methods to Characterize Soil Behavior in Space and Time.*

July 26-29, 1992, Cornell University, N.Y., U.S.A.

To appear in *Geoderma*

FIELD SCALE VARIABILITY OF SOIL STRUCTURE AND ITS IMPACT ON CROP GROWTH AND NITRATE LEACHING IN THE ANALYSIS OF FERTILIZING SCENARIOS

P.A. Finke

Department of Soil Science and Geology, PO.Box 37, 6700 AA Wageningen, The Netherlands

ABSTRACT

Soil structure variability was inventoried on a field scale, and translated to basic input data for a solute transport and crop production simulation model. After validation of the model, it was used to simulate the spatially varying effect of slurry application and N-fertilizing scenarios by multiple point-simulations. Feasibility of scenarios was determined by comparing nitrate leaching concentrations with current and pursued threshold levels. Disjunctive kriging was used to estimate and map the probability that these threshold levels were exceeded.

Emphasis was given to the effect of soil-specific slurry application rates and N-fertilizer levels on leaching probabilities and crop yields. Soil specific N-treatments increased field yields, because crop response to N, both in slurry and in fertilizer, was soil dependent. Also leaching response to N-treatment was soil dependent.

INTRODUCTION

Currently, legislation is being developed in the Netherlands to restrict inputs into the environment of polluting substances. Agriculture has been identified as a possible source of (e.g.) biocides, nitrates and ammonia. In order to make effective laws, possible effects of protective measures have to be evaluated by scenario analyses. In agricultural practice, management takes place on a field scale at farm level, and since the management can be influenced by legislation, scenario analyses should be carried out on the same field scale. Management scenarios can be analyzed by using simulation models. Input data should reflect field variability. This enables the evaluation of not only the average result of implementing a measure, but also its field scale variability. Knowledge about this variability allows the effect of an implemented measure to be expressed in terms of a probability distribution. Such a distribution can be used to estimate the probability that the effect of a measure is violating a statutory threshold value. Spatial variability of a variable can be translated into probability density functions by using the spatial prediction method Disjunctive Kriging.

This paper describes two scenario-analyses that were made to optimize the addition of organic manure and of anorganic fertilizer on a field scale with respect to nitrogen losses to atmosphere and groundwater. Special emphasis was given to the effect these additions would have on crop production. Both scenarios that were analyzed explicitly used soil structure variability to generate the dynamic soil physical characteristics water retention and hydraulic conductivity, and the static characteristics bulk density, texture and organic matter content. These characteristics were necessary to describe field scale variability of water flow and Nitrogen fate by using a simulation model.

MATERIALS AND METHODS

Spatial Variability of Soil Structure

The area under study is an agricultural field in the Wieringermeer polder in the north-western part of the Netherlands. Soils were classified as fine-loamy, calcareous, mesic Typic Udifluvents (Soil Survey Staff, 1975) and show a highly variable soil structure. Soil structure variability was caused by the complex sedimentation history of the area, which was part of a mud-flat landscape of tidal channels separating shoals before it was reclaimed.

A problem encountered when the behaviour of these stratified soils is to be simulated, is how to discretize the soil profile. Obviously, the thin layers visible in a vertical section (Fig. 1) cannot be analyzed separately for the determination of soil physical characteristics, and cannot be recognized from auger-cores in a soil survey. However, vertical successions of these thin layers can be recognized by their over-all structure and can be analyzed. A study was dedicated to whether these generalised layers could serve as functional layers.

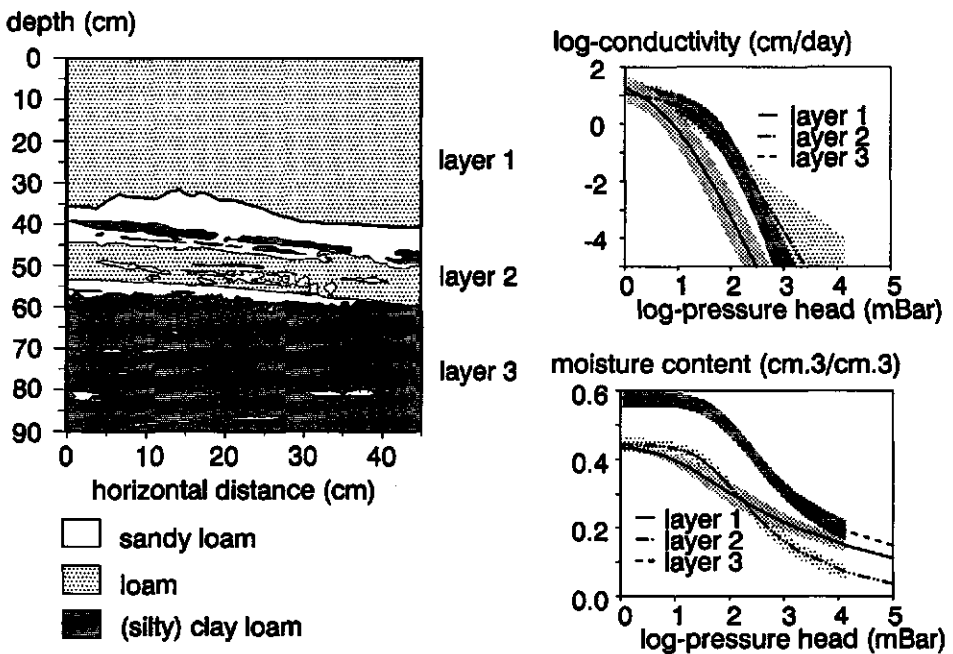


Figure 1 Vertical section showing thinly stratified soil profile and its generalization into three functional layers.

A functional layer is a layer that has functional hydrological properties significantly

different from those of other functional layers, and has a low internal variability (Wösten *et al.*, 1990; Finke *et al.*, 1992). Functional properties used were (Wösten *et al.*, 1986):

- (1) the *travel time* during a period of steady infiltration and
- (2) the *maximal height above the water table* at which a defined upward flux can be maintained.

For the study area, Finke and Bosma (1993) concluded, that soil profiles could successfully be generalized into a vertical sequence of three different functional layers, which were easily recognizable in a regular soil survey. The properties of different functional layers proved to be significantly different, and using the functional layers to generate input for a simulation model on a number of test plots resulted in accurate simulations.

The problem of inventorying spatial variability of soil structure was thus reduced to mapping the thickness and depth of functional layers. A two-phase soil survey was made. In the first phase, a nested sampling scheme was followed (Webster, 1977) during which 93 profile descriptions were collected with the purpose to quantify variability at both short and longer ranges relative to the field scale. Based on variogram analysis and interpretation of aerial photographs it was decided to sample a triangular grid with a mesh of 16 meters in the second phase of the soil survey (Finke, 1991). The resulting 402 profile descriptions that were collected, were used to produce a soil map (fig. 2), and were translated into as many location-specific inputfiles for computersimulations.

Model Description

To perform the scenario analyses, an existing model (LEACHM, Hutson and Wagenet, 1991) was extended with a potato crop growth submodel. The model simulates water flow, nitrogen transformations and - transport and potato crop growth. Water flow is calculated using a finite-difference solution to the Richard's equation:

$$(1) \quad \frac{\partial \Theta}{\partial t} = \left(\frac{\partial}{\partial z} \right) \left[K(\theta) \frac{\partial H}{\partial z} \right] - U(z,t)$$

where Θ is the volumetric water content (m^3/m^3), t is time (day), H is hydraulic head (100.Pa), defined as $H=h-z$, where h is the soil matric potential and z is the depth in cm, K is hydraulic conductivity (cm/day) and U is a sink term representing water lost by transpiration (cm). Daily potential transpiration was calculated by (Belmans *et al.*, 1983):

$$(2) \quad T_p = ET_p * [1 - \exp(-0.6I)]$$

where T_p is potential transpiration (cm/day), ET_p is potential evapotranspiration (cm/day) and I is the leaf area index (m^2/m^2). The functions between K , Θ and h that are required, were described using the closed form equations by Van Genuchten (1980).

The performance of the water flow submodel, using functional layers to generate the hydraulic characteristics, was tested by comparison of measured and simulated matric potentials on five plots at three depths (Finke and Bosma, 1993; Finke, 1992).

Nitrogen cycling is described according to the concepts and equations of Johnsson *et al.* (1987). Three organic nitrogen pools, characterized as a quickly degrading manure and litter pool and a relatively stable humus pool, are distinguished in the model. Also a urea pool and mineral ammonia and nitrate pools are identified. Mineralization processes,

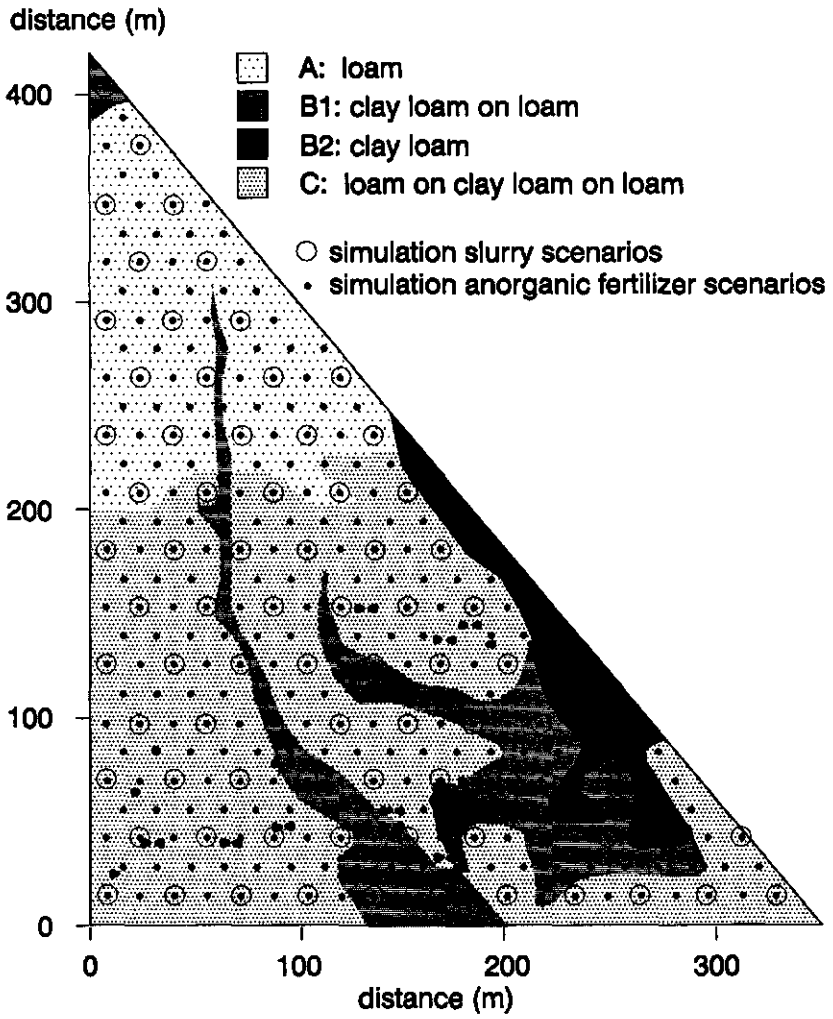


Figure 2 Soil map and simulation locations in scenario analyses.

volatilization, nitrification and denitrification are described by first order rate constants, volatilization occurring only from the surface layer. Rate constants are adjusted for temperature and water content effects (Johnsson *et al.*, 1987). Ammonium, nitrate and urea can be partially sorbed onto soil surfaces through a linear sorption isotherm. Chemical transport is simulated by a numerical solution to the convection-dispersion equation (Wagenet, 1983):

$$(3) \quad \frac{\partial(\theta c)}{\partial t} + \frac{\partial(\rho S)}{\partial t} = \frac{\partial}{\partial z} [\theta D(\theta, q) \frac{\partial c}{\partial z} - qc] - U(z, t) + \phi(z, t)$$

where c is chemical concentration in the liquid phase (mg/dm^3), s is chemical concentration in the sorbed phase (mg/kg dry soil), ρ is soil bulk density (kg/dm^3), $d(\theta, q)$ is the effective dispersion coefficient (mm^2/day), q is water flux density (mm/day), ϕ is a source/sink term ($\text{mg}/\text{dm}^3, \text{day}$) representing gains/losses through transformation and $u(z, t)$ is plant uptake of nitrogen ($\text{mg}/\text{dm}^3, \text{day}$). The plant uptake of nitrogen is determined by the transpiration flux and concentrations in the compartments of the rooted zone. For a extensive description of LEACHN, reference is made to Hutson and Wagenet (1991).

The performance of the nitrogen submodel was tested by comparing measured and simulated mineral nitrogen of the upper profile meter on 8 plots receiving various fertilizer and organic manure treatments (Finke, 1992).

Potato crop biomass production is schematized in Fig. 3.

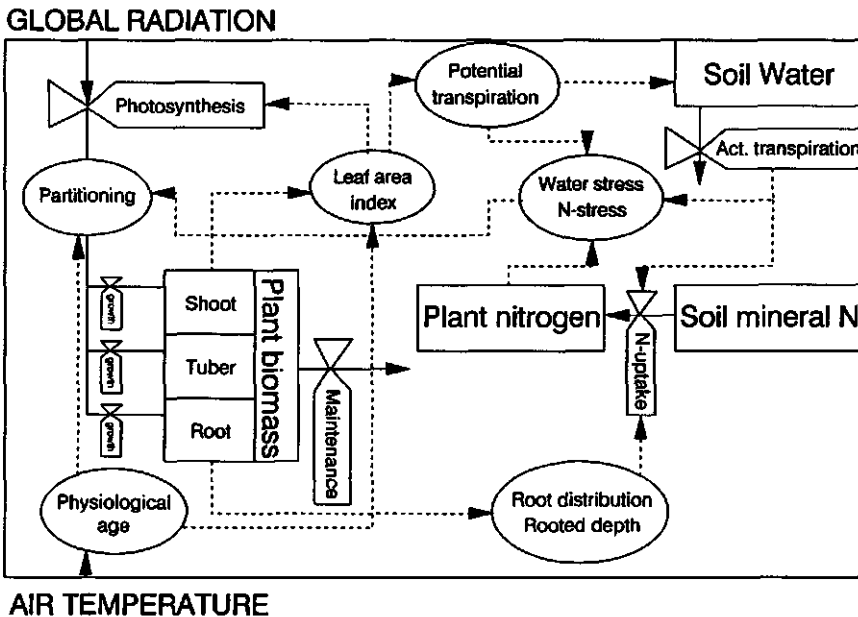


Figure 3 Processes simulated in the potato growth submodel. Boxes indicate pools, valves indicate processes, ellipses indicate auxiliary variables or processes, solid lines indicate mass or energy transport and dashed lines indicate information flows.

The water stressed dry matter growth rate as a result of the actual transpiration rate is calculated according to Feddes *et al.* (1988):

$$(4) \quad q_w = 0.5 * [W \frac{T}{\Delta e} + \sqrt{(q_m + W \frac{T}{\Delta e})^2 - 4q_m W \frac{T}{\Delta e} (1 - \xi)}]$$

In this equation, q_m is the maximum dry matter growth rate (depending upon latitude, global radiation, the leaf area index and the maintenance respiration), q_w is water stressed dry matter growth rate (kg/ha,day), W is maximum water use efficiency (kg.mbar/ha,mm), T is actual transpiration (mm/day), Δe is the average vapour pressure deficit of the air (mbar) and ξ is a mathematical parameter.

Furthermore, growth rate stressed by a limiting nitrogen availability is simulated by multiplication of the water stressed growth rate q_w by a stress factor S_n , calculated from (Greenwood *et al.*, 1985; Neeteson *et al.*, 1987):

$$(5) \quad S_n = \min[1, \frac{P_w - P_0}{P_M - P_0}]$$

where S_n is the stress factor for the current day, P_w is the actual %N in total dry matter, P_0 is the %N in total dry matter when growth ceases and P_M is the minimum %N in total dry matter to have the maximum growth rate.

The plant physiological age, characterized by the temperaturesum since the day of emergence, is used to partition the biomass increase to shoots, tubers and roots. Occurrence of stress due to limited nitrogen and/or water availability will cause the partitioning to be changed in favour of root growth and disfavour of shoot- and tuber biomass growth. The leaf area index (LAI) is considered to be a linear function of the shoot biomass until a certain temperaturesum is reached, whereafter the LAI becomes a monotonously decreasing function of the temperaturesum and the shoot biomass according to:

$$(6) \quad I = \begin{cases} a * B_T & \text{if } \sum_{\text{day-emergence}}^{\text{current}} T_{\text{day}} < b \\ a * B_T * (1 - \frac{\sum_{\text{day-emergence}}^{\text{current}} T_{\text{day}} - b}{\sum_{\text{day-emergence}}^{\text{current}} T_{\text{day}} - b + c}) & \text{if } \sum_{\text{day-emergence}}^{\text{current}} T_{\text{day}} \geq b \end{cases}$$

where a is coefficient (ha/kg), b is critical temperaturesum ($^{\circ}\text{C}$), T is average temperature for the current day ($^{\circ}\text{C}$) and c is a constant ($^{\circ}\text{C}$).

The performance of the potato crop growth model was tested by comparison of measured (through remote sensing) and simulated leaf area indexes, and by comparison of measured versus simulated final tuber yields.

Fertilizer Scenarios

In conventional agriculture in the Netherlands, nitrogen fertilizer additions are high. In areas with factory-farming, organic manure applications are reported to cause leaching of nitrates to the groundwater. Legislation is being implemented to minimize leaching hazards. In order to evaluate the effects on nitrate leaching of different levels of manure application and of anorganic fertilizer, two scenario analyses were made.

The first scenario analysis was made to optimize organic manure additions with respect to ammonia volatilization, nitrate leaching and potato tuber yield levels. The simulation period comprised a period of 17 months, from April 1 1989 to September 1 1990. In this period 3 crops were grown: Spring Barley, followed by a catchcrop (Ryegrass) in the same year and by Potatoes in the next spring. A surface application of chicken slurry was compared with an incorporation in the upper 15 cm. The application date was set the day after the harvest in August of the Barley crop. Both simulations focused on a representative profile for each one of the four soil types present in the field. The best type of application, leading to the smallest loss of N by volatilization and leaching, was thereafter optimized by stepwise adjusting the amount of applied manure until a critical leaching concentration (at 80 cm depth) would not be exceeded over the year following the application. Each optimization step comprised a series of 82 simulations, spatially distributed following a triangular grid with a mesh of 32 m. (Fig. 1).

The second scenario evaluated 6 variants of anorganic fertilizer application. The variants were based on the fertilizer advice obtained from:

$$(7) \quad N_{adv} = N_{opt} - a * N_{min}$$

in which N_{adv} is the advice, N_{opt} is the optimal amount of nitrogen in the rootable zone before planting (evaluated from national trials), a is a crop-dependent factor and N_{min} is the amount of anorganic nitrogen present in the rootable zone before fertilizing. Variants 1 to 5 comprised modifications of the real N_{adv} by factors of 0.25, 0.50, 1.00, 1.50 and 2.00 respectively, and variant 6 modified N_{opt} by a factor of 2 (Table 1).

Table 1 Description of scenarios analyzed. *B* and *P* are regular Dutch fertilizer advice levels for barley and potatoes respectively, where $B=110-N$ and $P=285-1.1N$. *b*, *c* and *p* are actual fertilizer gifts for barley, catchcrop and potatoes. *N* is the amount of mineral nitrogen (kg/ha) in layer 0-60 cm before planting.

Scenario	Variant	No. simulations	Amount given (kg N/ha)		
Chicken Slurry	1: Surface appl.	4	300		
	2: incorp.0-15 cm	4	300		
	3: optimization	82	250-500		
Anorganic N	0: initializing run	402	b=B	c=60	p=P
	1: advice - 75%	402	b=0.25B	c=15	p=0.25P
	2: advice - 50%	402	b=0.50B	c=30	p=0.50P
	3: conform advice	402	b=B	c=60	p=P
	4: advice + 50%	402	b=1.50B	c=90	p=1.50P
	5: advice +100%	402	b=2.00B	c=120	p=2.00P
	6: optimal N +100%	402	b=220-N	c=120	p=570-1.1N

Nitrate leaching concentrations in the hydrological year between April 1 1989 and April 1 1990 were simulated. These loadings were compared with the current (50 mgr nitrate/dm³) and with the pursued (25 mgr nitrate/dm³) critical concentration levels in leaching water in the Netherlands. Potato dry matter yields were simulated to evaluate the effect of changed fertilizing levels on crop production.

Simulations started with 2 years of fertilizing according to the current advice (variant 0 in Table 1), with initial nitrogen amounts corresponding to the level observed in the field. Thereafter, variants 1 to 6 were simulated, each with a initial nitrogen amount that would be present after two years of standard fertilization. This was done to avoid lagged effects of the current high fertilizer levels on low input scenarios. A period of 17 months was next simulated, assuming the same cropping sequence as in the slurry scenarios. All variants were simulated on 402 locations (Fig. 1).

After simulating the effect of varying fertilizer levels, also the effect of varying the spatial resolution of application was investigated. For variants 0-3, three methods were compared, different in the way fertilizing advices are obtained, using eq. 7:

- (1) the advice is based on *point-specific* N-status;
- (2) the advice is based on the average N-status for the *soil unit*;
- (3) the advice is based on the *field-average* N-status.

Method (3) is the method followed in traditional agricultural practice, method (2) uses available soil survey information and method (1) reflects the maximal attainable spatial precision.

Inputs into the simulation model that varied according to spatial variability observed in the field, were:

- (1) Thickness and texture of each functional layer: by location;
- (2) Hydraulic characteristics, bulkdensity and organic matter content: by functional layer;
- (3) Depth of groundwater in time: translated from a monitoring series from the same field to other locations by surface topography.

Inputs into the simulation model that were supposed not to vary over the field were:

- (1) Initial nitrogen amounts and depth distribution
- (2) Precipitation, air temperature and potential evapotranspiration;
- (3) Nitrogen transformation rate constants (though correction for temperature and water content may cause variability in actual rate factors).

Disjunctive Kriging

The simulated scenarios aimed at minimizing the risk that nitrate loadings into the groundwater would exceed a critical value of 50 mgr nitrate/dm³. It is intuitively clear, that when this risk is to be estimated at locations where no value is known, it will depend on values obtained in the neighbourhood and on the variability. In areas where leaching amounts are large, the risk of a leaching that is too high is greater. In areas where leaching is highly variable, uncertainty leads also to a greater estimated risk. This risk can be evaluated by estimating the probability that the 50 mgr nitrate/dm³ level is exceeded.

Estimating a probability requires the distribution of the variable "nitrate loading" to be known. Because loadings are concentrations, a skew distribution can be expected, since negative concentrations cannot occur. This may require, that the actual distribution be transformed to a standard normal distribution before probabilities based on the observed data can be calculated. The spatial prediction procedure Disjunctive Kriging (DK) aims at

obtaining an estimator of the conditional probability that a measured variable exceeds a cutoff level at an unvisited location, irrespective of its distribution (Yates *et al.*, 1986; Webster and Oliver, 1989). The probability is conditional, because:

(i) the spatial correlation structure of the variable is taken into account; (ii) the probability is conditioned on a set of observations.

In the application of DK, three assumptions are made:

(i) The original observations $Z(x)$ must be second order stationary; (ii) A function exists that transforms arbitrarily distributed $Z(x)$ to normally distributed $Y(x)$ and that is invertible. This assumption has been proven to be always correct (Kim *et al.*, 1977); (iii) The function produced by the transform ($Y(x)$) has a bivariate normal distribution for each pair of locations.

In DK, a function is sought that is invertible, and that can transform values from whatever distribution to a standard normal distribution. Such a function can be approximated by composing each observation from a number (K) of Hermite polynomials with the appropriate coefficients. The prediction of the variable $Z(x_0)$ on an unvisited point x_0 is thus expanded to a linear combination of predictions in x_0 for each one of K Hermite polynomials:

$$(8) \quad Z_{DK}^*(x_0) = \sum_{k=0}^K C_k H_k^*[Y(x_0)]$$

in which the coefficients C_k were obtained from the observations by Hermite integration (Abramowitz and Stegun, 1965); and $H_k[Y(x_0)]$, the value for the k th Hermite polynomial of the normalized variable Y on location x_0 , is estimated by weighing Hermite polynomials from the same order at n neighbouring observation points by:

$$(9) \quad H_k^*[Y(x_0)] = \sum_{i=1}^n b_{ik} H_k[Y(x_i)]$$

where the weights b_{ik} are determined by solving the system

$$(10) \quad (\rho_{ij})^k = \sum_{i=1}^n b_{ik} (\rho_{ij})^k \quad j=1,2,\dots,n$$

in which ρ_{ij} is the autocorrelation between observations i and j .

A predictor of the conditional probability of exceeding a cutoff level is evaluated by defining an indicatorfunction Θ :

$$(11) \quad \Theta_{y_c} = \begin{cases} 1 & \text{if } Y \geq y_c \\ 0 & \text{if } Y < y_c \end{cases}$$

where y_c is the normalized cutoff level (relating to the actual cutoff level z_c) and Y is the normalized variable (relating to Z). The conditional probability of $Z(x_0)$ exceeding z_c is estimated by the conditional expectation of the indicatorfunction $\Theta_{y_c}(Y)$ in location x_0 . Hereto $\Theta_{y_c}(Y(x_0))$ is expanded to a series of Hermite polynomials, so that the conditional probability is estimated by the sum of the predictions of the Hermite polynomials describing $\Theta_{y_c}(Y(x_0))$:

$$(12) P^*(x_0) = 1 - G(y_c) + g(y_c) \sum_{k=1}^K H_{k-1}(y_c) H_k^*(Y(x_0)) / k!$$

in which H_{k-1} is known; and $H_k^*(Y(x_0))$ was estimated during the disjunctive prediction procedure; and $G(y_c)$ is the cumulative standard normal probability density for y_c ; and $g(y_c)$ is the standard normal probability density for y_c .

For a detailed description of the DK procedure, reference is made to Yates *et al.* (1986).

RESULTS AND DISCUSSION

Model performance

A comparison between simulated and measured characteristics is given in figs 4a-d. Simulated soil matric potentials agreed well with measurements (R^2 of 0.74) when the soil matrix was unsaturated. Near saturation, simulations deviate from measurements, but differences are small. Simulated anorganic nitrogen contents in the upper meter were simulated reasonably well ($R^2=0.71$), when deviations from measurements (tens of kg N/ha) are compared to fertilizer levels (hundreds of kg N/ha).

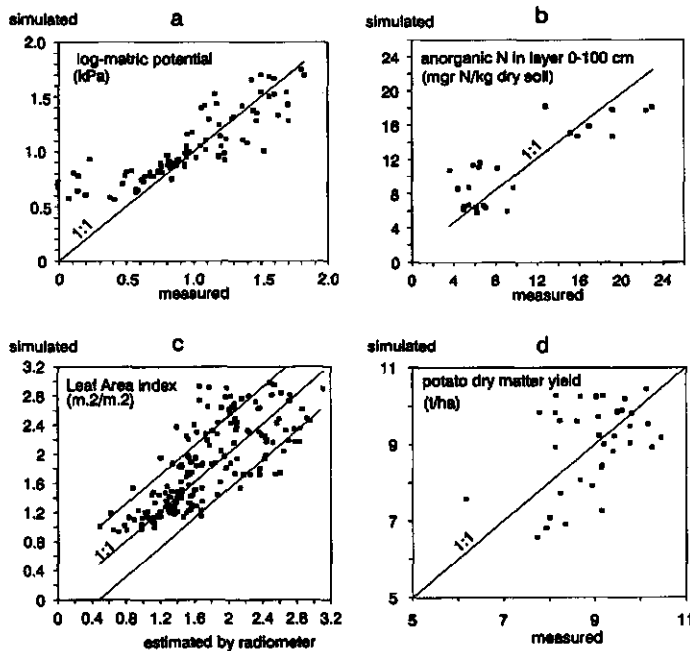


Figure 4 Simulated and measured characteristics of the water submodel (a), the nitrogen submodel (b) and the potato production submodel for leaf area indexes (c) and final potato yields (d). Two lines parallel to the 1:1 line in (c) indicate one standard deviation confidence zones of the LAI estimated by remote sensing.

Simulated leaf area indexes are generally simulated well ($R^2=0.58$), since most simulated values are found within the 1σ confidence zone associated with the remote sensing estimates (fig. 4c). Simulated final potato yields are compared to measurements in fig 4d. The relatively small R^2 (0.18) is probably caused by variability in the depth distribution of anorganic N at the start of the growing season, which was unknown and therefore assumed homogeneous (Finke, 1992).

Slurry scenarios

Simulation results at four soil profiles, each representative for one soil unit, are given in table 2. In all soil units, a positive response of crop production and plant nitrogen uptake occurred when slurry was incorporated into the upper 15 cm in the soil. In case of surface application, nitrate leaching was slightly lower, but this was more than compensated for by the far higher ammonia volatilization. Both crop production and total nitrogen losses to the environment were more favourable in case of incorporation. For these reasons, further scenario analyses considered slurry applications to be incorporated into the soil.

Table 2 Simulated nitrogen losses (17 months) and dry matter tuber yields in four characteristic soil profiles for surface application (s) and incorporation (i) of 300 kg N/ha slurry. Soil unit codes refer to figure 2.

Soil unit	NH ₃ -volat.		NO ₃ -leaching		Plant uptake		Yield	
	kg N/ha s	kg N/ha i	kg N/ha s	kg N/ha i	kg N/ha s	kg N/ha i	t/ha s	t/ha i
A	193.3	151.6	9.1	10.3	697.7	701.2	11.3	12.0
B1	193.6	151.9	6.7	7.4	657.2	679.4	10.4	12.0
B2	192.6	150.9	6.9	8.0	646.1	664.4	8.7	9.5
C	194.0	152.5	7.3	8.0	672.5	696.4	10.8	12.3

Simulated effects on nitrate leaching of slurry additions of 500, 400, 300 and 250 kg N/ha are presented as leaching probability maps in figure 5. The criterion that "nowhere in the field the probability of exceeding the cutoff-leaching concentration may be greater than 5%" was met with a slurry addition equalling 250 kg N/ha. The important role of the catchcrop in minimizing nitrate leaching concentrations is obvious from the leaching probability map at 300 kg N/ha slurry addition when no catchcrop is grown (fig. 5e). Comparing leaching probability maps with the soil map, shows that soil units A en C (Fig. 2) are more sensitive to nitrate leaching than soil units B1 and B2. This result was used to determine soil specific slurry application rates. If the slurry gift would be 300 kg N/ha for soil A, 400 kg N/ha for soils B1 and B2, and 250 for soil C, the leaching criterion would still be met, but 21% more slurry could be applied to the whole field, and the crop yield for the whole field would increase by 4% (Table 3).

Simulated potato yield response to the various slurry gifts and its spatial variation is presented in figure 6. Slurry additions higher than 250 kg N/ha still showed a positive effect on potato yields, but the differences are not large. The photosynthetic maximum was not reached by far, indicating that something else than nitrogen deficiency depressed crop yields. This cause has been identified as moisture stress (Finke, 1992), and explained why the variability in crop yields (fig. 6) was not decreasing when slurry-N additions increased.

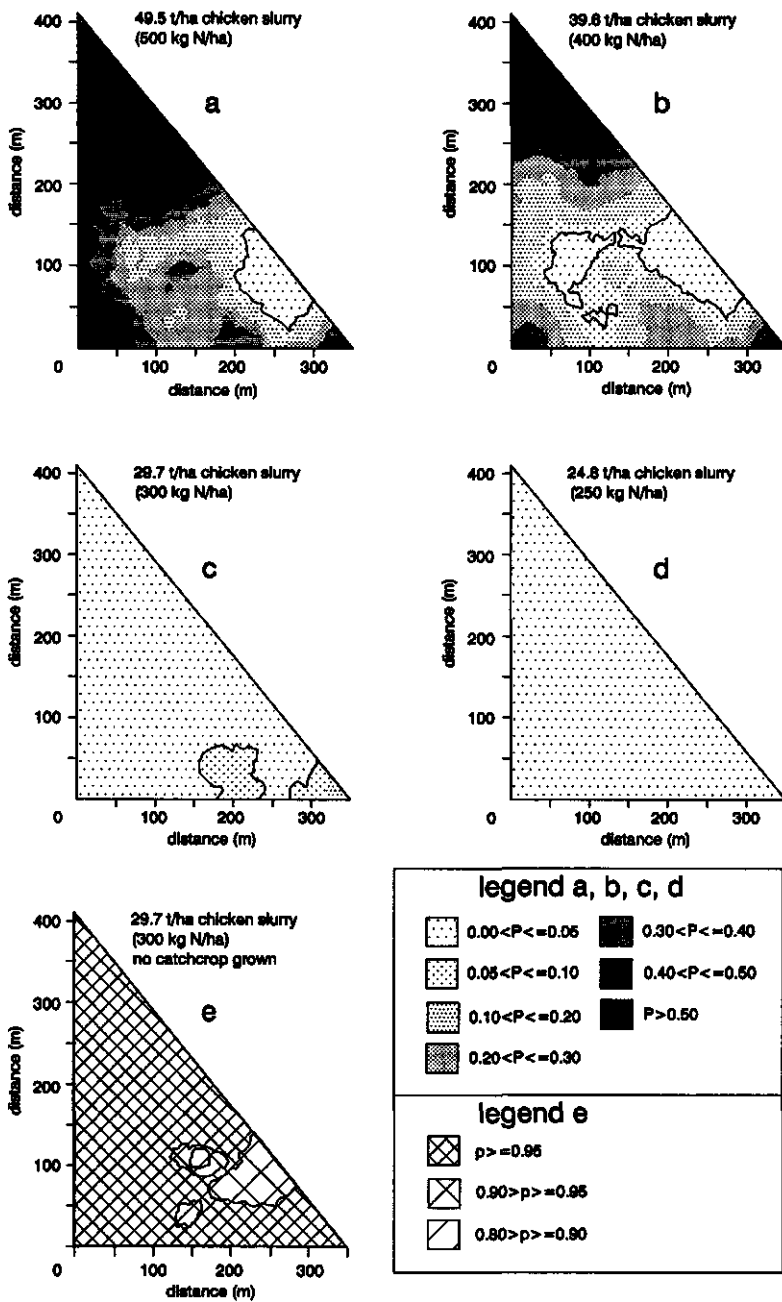


Figure 5 Maps of the probability (P) that leaching exceeds 50 mg NO₃-N/dm³ at slurry applications from 500-250 kg N/ha when a catchcrop is grown (a to d) or not grown (e).

Different soil units showed a different response to slurry-N (fig. 6). When no catchcrop would be grown, not only would leaching drastically increase, but also crop yields would be significantly less (Fig. 6).

Table 3 Comparison of field specific and soil specific maximum amounts of slurry not leading to exceedance of the leaching criterium. Soil codes refer to figure 2.

Soil Area unit	%	Application of slurry			
		soil specific		field specific	
		level	yield	level	yield
		t slurry/ha	t dm/ha	t slurry/ha	t dm/ha
A	23	29.7	9.4	24.8	9.1
B1	19	39.6	9.5	24.8	8.4
B2	8	39.6	7.3	24.8	6.3
C	50	24.8	9.2	24.8	9.2
		tonnage	tonnage	tonnage	tonnage
Field		215.1	65.7	177.9	63.1

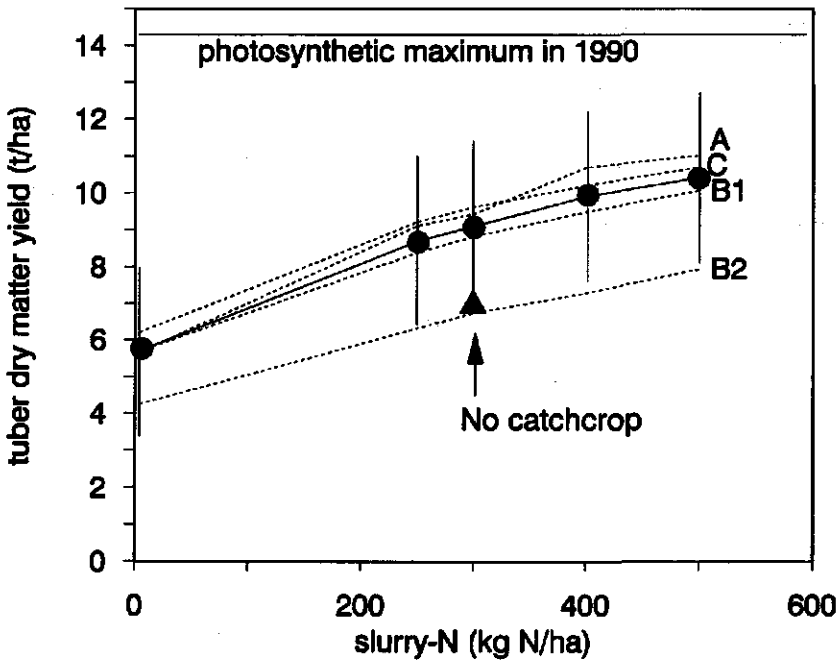


Figure 6 Simulated average and soil specific crop response in 1990 to slurry additions in 1989. A, B1, B2 and C refer to soil units (see Figure 2); solid line connects average crop-response and zones of 1 standard deviation, dotted lines connect soil-specific responses; solid circles represent average yields; closed triangle represents average yield for scenario without a catchcrop.

Anorganic nitrogen fertilizer scenarios

Simulated nitrate leaching concentrations did not exceed the criterion based on the current threshold concentration of 50 mgrs nitrate-N/dm³. However, the pursued threshold concentration of 25 mgrs nitrate-N/dm³ was exceeded in case of scenario variants 0 en 6 (Table 4).

Table 4 Percentage of the area not satisfying quality criteria based on the probability that a leaching concentration greater than 25 mgr nitrate-N/dm³ is exceeded. Variants refer to Table 1.

Variant	----- Probability greater than -----				
	0.50	0.25	0.10	0.05	0.025
	%	%	%	%	%
0	66.8	94.1	99.0	99.5	99.8
1	0	0	0	0	0
2	0	0	0	0	0
3	0	0	0	0	0
4	0	0	0	0	0
5	0	0	0	0	0
6	0	0	0	1.4	15.5

Variants 0 and 3 were identical in terms of the way the fertilizer level was calculated (see Table 1). The strong difference in probability of leaching between variants 0 and 3 must therefore be attributed to a lagged effect of high fertilizer levels in the past, which created a pool of (organically bound) nitrogen that was emptied largely during the simulation period of variant 0. The high input scenario variant 6 resulted in exceedance of the threshold probability of 5% in part of the field, which indicates that this scenario will not reduce leaching to the pursued level. Scenario variants 1 to 5 would not violate the threshold probability during the simulation period.

In Figure 7, the average and soil-specific response of potato yield to the fertilizing scenario is presented. Scenario variant 0 resulted in clearly higher average yields than variant 3, because more anorganic nitrogen is mineralized during the growing season. The vertical bars in Fig. 7 indicate, that crop yield becomes more variable when fertilizer gifts are higher. This must be attributed to the increasing importance of water-availability as a factor that is stressing crop growth. Soil units B2 and, to a lesser extend, B1 show a clearly weaker response to N availability, because capillary rise in these soils is limited by a thick clay loam layer, causing the actual transpiration to be lower than the potential transpiration.

In case of scenario variant 6, the pursued leaching concentration of 25 mgr/dm³ was exceeded only in soil unit C. Soil unit specific fertilizing according to scenario variant 5 for soil C and according to variant 6 for units A, B1 and B2 would satisfy the leaching criterion. This would result in a field yield of 77.0 ton dry matter whereas field-specific fertilizing according to scenario variant 5 would produce 70.7 ton dry matter. Soil specific fertilizing would thus increase field yields by 9%.

A comparison of some simulation results of point-specific, soil unit specific and field-specific fertilizing for variants 0 to 3 (Table 1) is made in Table 5.

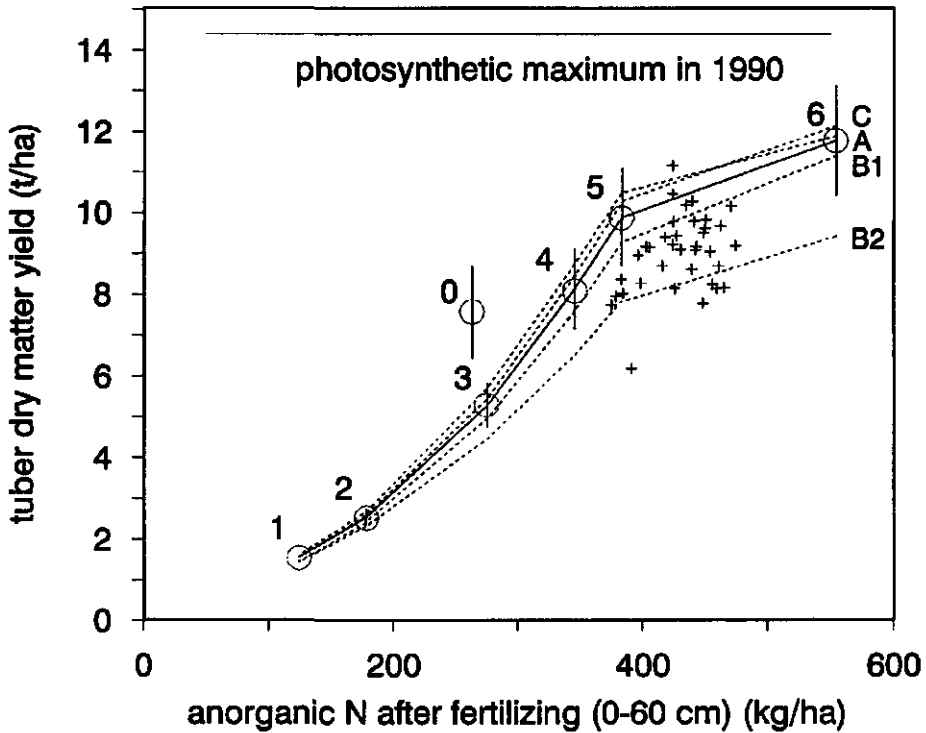


Figure 7 Simulated average and soil specific crop response in 1990 to fertilizer levels. A, B1, B2 and C refer to soil units (see Figure 2); 0 to 6 refer to fertilizer scenarios (see Table 1); solid line connects average crop-response and zones of 1 standard deviation, dotted lines connect soil-specific responses; + represent field measurements in 1990.

Differences between treatments are small or absent. The variability of yields would decrease when fertilization would change from field-specific to soil-specific only when fertilizer levels are low (variants 1 and 2). Further differences between soil- and field-specific fertilizing are negligible. The residual amount of anorganic nitrogen after 17 months is consequently more variable for field-specific fertilizer applications than for point-specific applications. This indicates that, on the long run, plot-specific fertilizing may produce a less variable nitrogen status than field-specific fertilizing.

As a result, it is concluded that fertilizing by soil instead of fertilizing by field would not have a significant effect on crop yields when it pursues a homogeneous nitrogen distribution over the field. When fertilizer levels are obtained from soil specific response characteristics (Fig. 7), soil specific fertilizing may result in raising average yields.

Table 5 Variability (coefficients of variation) of simulated yields, nitrate leaching concentrations and residual anorganic nitrogen after 17 months for plot-specific, soil-specific and field-specific fertilizing. Variants refer to Table 1.

Variant	Variable	Spatial resolution of application		
		plot CV	soil CV	field CV
		%	%	%
0	yield	14.97	14.84	14.80
1		6.41	6.43	6.47
2		7.58	7.55	7.62
3		10.28	9.87	9.88
0	leaching concs	20.65	20.65	20.65
1		68.90	68.90	68.90
2		59.61	59.61	59.61
3		38.63	38.63	38.63
0	residual N	6.36	6.47	6.49
1		3.58	3.63	3.63
2		3.95	4.02	4.02
3		5.37	5.50	5.51

CONCLUSIONS

1. Scenario analyses by simulation modelling form an operational tool to evaluate the effect of fertilizer management. When simulation model parameters reflect soil spatial variability, variability of simulation results can be used to map the probability that critical levels are exceeded. A promising tool to determine these probabilities is the method of Disjunctive Kriging.
2. Both leaching response and crop yield response to the slurry application level differ by soil unit. Soil specific optimal slurry treatments (optimal in the sense that leaching criterion is not exceeded) results in higher total applications and higher yields than field specific optimal treatments.
3. Soil specific nitrogen fertilizer advices did not result in different leaching or crop yields when compared to field- or point-specific advices. Soil specific crop response curves show that the response to anorganic nitrogen differs by soil type.
4. Spatial variability of yields increased when nitrogen levels increased. This is caused by an increasing variability of the transpiration deficit due to differences in foliar growth as governed by water availability.

ACKNOWLEDGEMENT

Financial support by EC-project EV4V*0098-NL "Nitrate in Soils" is gratefully acknowledged. Thanks are due to J. Bouma for critically reading the manuscript.

REFERENCES

- Abramowitz, M. and A. Stegun. 1965. Handbook of mathematical functions. Dover, New York.
- Belmans C., Wesseling, J.G. and Feddes, R.A., 1983. Simulation model of the water balance of a cropped soil: SWATRE. *Journal of Hydrology* 63 (3/4):271-286.
- Feddes, R.A., de Graaf, M., Bouma, J. and van Loon, C.D., 1988. Simulation of water use and production of potatoes as affected by soil compaction. *Potato research* 31 (1988) 225-239.
- Finke, P.A. 1991. Soil Survey to obtain basic simulation data for a heterogeneous field with stratified marine soils. In: Nitrate in Soils. Commission of the European Communities Soil and Groundwater Research Report II (EUR 13501 EN). Luxemburg.
- Finke, P.A., J. Bouma and A. Stein. 1992. Measuring field variability of disturbed soils for simulation purposes. In: *Soil Sci. Soc. Am. J.*:187-192.
- Finke P.A. and W.F.P. Bosma, 1993. Obtaining basic simulation data for a heterogeneous field with stratified marine soils. In: *Hydrological Processes* 7(2): (in press).
- Finke, P.A. (1992) Integration of remote sensing data in the simulation of spatially variable yield of potatoes. (in press)
- Greenwood, D.J., Neeteson, J.J. and Draycott, A., 1985. Response of potatoes of N fertilizer: Quantitative relations for components of growth. *Plant and Soil* 85: 163-183.
- Hutson, J.L. and Wagenet, R.J., 1991. Simulating nitrogen dynamics in soils using a deterministic model. *Soil use and management* 7(2), 74-78.
- Johnsson, H., Bergstrom, L., Jansson, P.-E. and Paustian, K., 1987. Simulated nitrogen dynamics and losses in a layered agricultural soil. *Agriculture, Ecosystems and Environment* 18, 333-356.
- Kim, Y.C., D.E. Myers, and H.P. Knudsen. 1977. Advanced geostatistics in ore reserve estimation and mine planning practitioner's guide. Report to the U.S. Energy Research and Development Administration, subcontract No. 76-003-E, Phase II.
- Neeteson, J.J., Greenwood, D.J. and Draycott, A., 1987. A dynamic model to predict yield and optimum nitrogen fertilizer application rate for potatoes. *Proceedings* 262. The Fertiliser Society, London, 31 pp.
- Soil Survey Staff, 1975. *Soil Taxonomy: A basic system of soil classification for making and interpreting soil surveys*. USDA-SCS Agric. Handb. 436. U.S. Gov. Print. Office, Washington DC.
- Van Genuchten, M. Th., 1980. A closed form equation for predicting the hydraulic conductivity of unsaturated soils. *Soil Sci. Soc. Am. Journal* 44:892-898.
- Wagenet, R.J., 1983. Principles of salt movement in soils. In: *Chemical mobility and reactivity in soil systems* (eds. D.W. Nelson *et al.*). Special publication 11, American Society of Agronomy, Madison, Wisconsin pp. 123-140.
- Webster, R. 1977. *Quantitative and numerical methods in soil classification and survey*. Clarendon Press, Oxford.
- Webster, R. and M.A. Oliver. 1989. Optimal interpolation and isarithmic mapping of soil properties. VI. Disjunctive kriging and mapping the conditional probability. *Journal Soil Sci.* 40: 497-512.
- Wösten, J.H.M., M.H. Bannink, J.J. de Gruijter and J. Bouma. 1986. A procedure to identify different groups of hydraulic-conductivity and moisture-retention curves for

- soil horizons. *J. of Hydrology* 86: 133-145.
- Wösten, J.H.M., C.H.E.J. Schuren, J. Bouma and A. Stein. 1990. Functional sensitivity analysis of four methods to generate soil hydraulic functions. *Soil Sci. Soc. Am. J.* 54: 832-836.
- Yates, S.R., A.W. Warrick and D.E. Myers. 1986. Disjunctive kriging 1. Overview of estimation and conditional probability. *Water Resources Research* 22/5: 615-621.

CHAPTER 3.4

APPLICATION OF DISJUNCTIVE COKRIGING TO OPTIMIZE FERTILIZER ADDITIONS ON A FIELD SCALE

Presentation at: *Conference of the Working Group on Pedometrics of the ISSS:
Developments in Spatial Statistics for Soil Science.
September 1-3 1992, Wageningen, The Netherlands.*
To appear in *Geoderma*

APPLICATION OF DISJUNCTIVE COKRIGING TO OPTIMIZE FERTILIZER ADDITIONS ON A FIELD SCALE

P.A. FINKE AND A. STEIN¹

¹ *Department of Soil Science and Geology, Agricultural University, P.O.Box 37, 6700 AA Wageningen, The Netherlands.*

ABSTRACT

To evaluate the effect of various levels of fertilizer applications, 6 fertilizing scenarios were analyzed by computer simulations using a process-based simulation model. In order to reduce the total cost of making these calculations, the number of simulations was reduced without much loss of accuracy of predicted values by applying Disjunctive CoKriging (DCK) to expand a minimum data set. Previously obtained simulation results served as covariable. DCK resulted in a reduction of 80% of the original number of simulation calculations. This number was sufficient to reach a prediction quality in 50 test points satisfying two criteria based on the sample variance. When the conditional probability of exceeding a threshold value is to be mapped, an expanded data set is of limited use because some variance is lost in the expansion process.

INTRODUCTION

Agricultural practices are aiming at maximizing production by satisfying prerequisites for optimal plant growth and minimal stress. Examples of such practices are fertilizing and application of biocides. Unfortunately, some of these applications are reported to cause environmental problems due to leaching (Anderson *et al.*, 1985, Commission of the European Communities, 1991). Leaching of fertilizer can occur when plants are not efficiently taking up the nutrients or when the demand is smaller than the nutrient status plus the application. Also soil physical properties strongly influence the occurrence and magnitude of leaching. Leaching may show a strong spatial variation when nutrient status or soil physical properties are variable (Dagan and Bresler, 1983).

Minimization of leaching and maximization of production are possibly conflicting goals, because a uniform fertilizer application level that will maximize production on the location with the worst nutrient status, may cause leaching on locations with a better nutrient status. A possible alternative is location-specific or soil-specific fertilizing instead of the usual field-specific fertilizing (Robert, 1988).

In this study, the spatially varying impact of different scenarios of fertilizer applications is estimated by simulating water and solute transport on a large number of discrete points in an agricultural field. Note that throughout the text the word *simulation* is used to indicate the application of a process-based computer model which calculates the movement of water and nutrients in the unsaturated zone.

When scenarios are to be compared, results are usually interpreted by comparing the mean value to some threshold value (Commission of the European Communities, 1991). In this study, the field average leaching concentration would have to be compared to the current threshold value of 50 mg NO₃/dm³ or the pursued threshold value of 25 mg

NO_3/dm^3 . A value of $49 \text{ mg}/\text{dm}^3$ would be acceptable whereas a value of $51 \text{ mg}/\text{dm}^3$ would not. This is not realistic, because uncertainties caused by model inaccuracies and spatial variation of the property obscure the sensible use of absolute values. Hence, in this study a leaching criterion was formulated as: "Nowhere in the field the probability may be greater than 5% that a leaching concentration of $25 \text{ mg NO}_3/\text{dm}^3$ is exceeded". One may notice that this criterion is based on a probabilistic approach.

When scenario results are expressed as probabilities of exceeding a threshold value it allows the use of spatial variation of the property for decision making. However, it requires intensive sampling and the calculation of a great number of simulations to be able to take the spatial variation

into account. The use of existing spatial information, for instance soil characteristics sampled previously, may help to reduce the simulation effort.

One main purpose of this study is to obtain field scale maps of the probability that the nitrate loading into the groundwater exceeds a threshold value of $25 \text{ mg nitrate}/\text{dm}^3$. In order to obtain these, Disjunctive Kriging and Disjunctive CoKriging were used (Matheron, 1976; Yates *et al.*, 1986; Yates, 1986, Webster and Oliver, 1989). To minimize the number of simulations, data from a previous simulation served as a covariable.

SIMULATION MODEL AND FERTILIZING SCENARIOS

Fertilizing scenarios were compared by simulation of the impact of each scenario on nitrate leaching and crop production in 402 soil profiles that were described in a field soil survey. To allow a realistic simulation of the spatially varying impact of a fertilizing scenario, model input variables showing spatial variation were sampled thoroughly. Location-specific soil physical characteristics (bulk density and the water retention and hydraulic conductivity functions) were generated for each location and depth using the available soil profile descriptions. The procedure followed is described in detail by Finke and Bosma (1993). Additionally, the texture and organic matter content were input to the model.

The model LEACHN (Wagenet and Hutson, 1989; Hutson and Wagenet, 1991) was used for the simulation of water flow and Nitrogen fate. In order to simulate crop production, the LEACHN model was extended with a validated crop growth submodel (Finke, 1992).

The fertilizing scenarios that were analyzed related to the current method to obtain the fertilizer level in the Netherlands. The advised fertilizer level is determined by the equation:

$$(1) \quad N_{adv} = N_{opt} - a + N_{min}$$

where N_{adv} is the advised nitrogen gift ($\text{kg N}/\text{ha}$); and N_{opt} is the crop-specific optimum ($\text{kg N}/\text{ha}$) as determined in national trials; a is a crop specific factor and N_{min} is the amount of anorganic nitrogen present in the rootable layer ($\text{kg N}/\text{ha}$). To investigate the impact of modifications of fertilizer additions on crop production and nitrate leaching, 6 scenarios were defined (Table 1). Before simulating each scenario, a 2-year period was simulated on all 402 locations (scenario S-0 in Table 1). This was done to avoid lagged nitrate leaching caused by the current high fertilizing levels which built up a pool of potentially leachable nitrogen.

Table 1 Description of fertilizer scenarios. N_{adv} and N_{opt} are current advice and optimal levels in kg N/ha (see equation 1).

Scenario	Modification relative to current situation	Number of simulations
S-0	none	402
S-1	$N_{adv} * 0.25$	optimized
S-2	$N_{adv} * 0.50$	optimized
S-3	none	optimized
S-4	$N_{adv} * 1.50$	optimized
S-5	$N_{adv} * 2.00$	optimized
S-6	$N_{opt} * 2.00$	optimized

These lagged effects would obscure the effect of especially the low-input scenarios S-1 and S-2, in which only a fraction of the advised level would be applied. In scenario S-3 the application would equal the advice and in scenarios S-4 and S-5 the actual fertilizer gift would be 50% or 100% more than the advice. Scenario S-6 comprises an increase by 100% of the pursued level of anorganic nitrogen (N_{opt}). This scenario is most likely to cause over-fertilization, because the amount of anorganic nitrogen in the soil is kept systematically much higher than the crops theoretically need. Scenarios S-4 and S-5 also give more nitrogen than needed, but these scenarios are self-corrective: When the advice N_{adv} is small because N_{min} levels are near N_{opt} , which will happen when high fertilizer gifts were given in the past, also the modification will be small.

Scenario S-1 to S-6 comprised a simulation period of 17 months, from April 1, 1989 to September 1, 1990. In this period three crops were grown: Spring Barley, a catchcrop (Ryegrass) and Potatoes. The variable of interest in this study was the simulated nitrate concentration in the leaching water at 80 cm depth during the hydrological year from April 1, 1989 to April 1, 1990. Since the processes simulated in scenario S-0 to S-6 are the same, and vary only in magnitude, it was expected that simulation outcomes of different scenarios would be highly correlated.

SPATIAL STATISTICS

Disjunctive Kriging and Cokriging

One main purpose of this study is to obtain field scale maps of the probability that nitrate loadings into the groundwater exceed a threshold value of 25 mg nitrate/dm³. The spatial prediction procedure Disjunctive Kriging (DK) aims at obtaining an estimator of this (conditional) probability at an unvisited location, taking its distribution into account (Matheron, 1976; Yates *et al.*, 1986; Webster and Oliver, 1989). This requires the distribution of this variable to be known or to be estimated from available data. Because nitrate loadings are concentrations, a skew distribution can occur, since negative concentrations do not exist. Also, distributions may be not unimodal, because different soil types may show a different sensitivity to nitrogen leaching. This may require a transformation of the observed distribution into the standard normal distribution before probabilities at unvisited locations can be calculated. When Disjunctive Cokriging (DCK) is applied,

observations on a covariable are used as well (Yates, 1986). In DK and DCK the probability is conditioned on both the spatial distribution of the variable(s) and on a set of n observations, and hence is a conditional probability. It is assumed that the observations are obtained from second order stationary random fields. For such fields, it is well-known that there always exists a function that transforms any observed distribution into the normal distribution (Kim *et al.*, 1977).

Let n observations $z(x_{1i})$, $i = 1, \dots, n$, from the field $Z(x)$ be available on the predictand and m observations $v(x_{2j})$, $j = 1, \dots, m$ on a covariable. Let $\rho_{i0,\alpha}$ be the autocorrelation between the prediction location x_0 and the i^{th} observation location of the α^{th} variable ($\alpha = 1, 2$), and $\rho_{\alpha\beta,ij}$ the autocrosscorrelation between the i^{th} and the j^{th} observation locations of variable α and β ($\alpha, \beta = 1, 2$). In DK and in DCK 5 steps are distinguished to obtain both a prediction and the conditional expectation of exceeding a cutoff value in an unvisited location x_0 .

1. For the two variables, the observations are transformed into standard-normal distributed values. This is usually achieved for each variable by putting the observations in ascending order, followed by setting the cumulative probability $Q[Z(x_{1i}) \leq x]$ equal to $(i-0.5)/n$, where i is the number of observations less than or equal to x . By inverting the cumulative standard normal distribution for values thus obtained, transformed observations $y(x_{1i})$ equivalent to $z(x_{1i})$ are found, which follow the standard normal distribution. Similarly for the second variable, observations $u(x_{2j})$ equivalent to $v(x_{2j})$ are found, also following the standard normal distribution.
2. Based on the observed distributions of the observations on the two variables, assumed to be valid throughout the study area, the sequences of Hermite polynomials $\sum C_k H_k[Y]$ and $\sum D_k H_k[U]$ with coefficients C_k and D_k (see Appendix), are determined for the predictand and the covariable, respectively, upto a degree K that with sufficient precision represents the observed distributions. Values of Hermite polynomials $H_k[y(x_{1i})]$ and $H_k[u(x_{2j})]$ are determined in the observation locations.
3. In order to carry out a DK-prediction at an unvisited location x_0 , K predictors at this location, each associated with one Hermite polynomial, are determined by weighing the values of the Hermite polynomial at the n observation points:

$$(2) \quad H_k^*[Y(x_0)] = \sum_{i=1}^n b_{ik} H_k[Y(x_{1i})]$$

The weights b_{ik} are determined by solving the linear disjunctive Kriging system:

$$(3) \quad \rho_k = R_k b_k$$

in which ρ_k is a vector with elements $\rho_{i0,1}^k$, and R_k is a matrix with elements $\rho_{ij,11}^k$. In the case of two variables, K predicted values each associated with one Hermite polynomial are determined by weighing the values of the Hermite polynomials at the $n+m$ neighbouring observation points:

$$(4) \quad H_k^*[Y(x_0)] = \sum_{i=1}^n b_{ik} H_k[Y(x_{1i})] + \sum_{j=1}^m a_{jk} H_k[U(x_{2j})]$$

The weights b_{ik} and a_{jk} are determined by solving the linear disjunctive Cokriging

system:

$$(5) \quad \begin{pmatrix} \rho_{1,k} \\ \rho_{2,k} \end{pmatrix} = \begin{pmatrix} R_{11,k} & R_{12,k} \\ R_{21,k} & R_{22,k} \end{pmatrix} \begin{pmatrix} b_k \\ a_k \end{pmatrix}$$

in which $\rho_{\alpha,k}$ are vectors with elements $\rho_{10,\alpha}^k$, and the $R_{\alpha\beta,k}$ are matrices with elements $\rho_{\alpha\beta,ij}^k$.

4. The DK and the DCK predictors are obtained by adding the predictions of the K individual Hermite polynomials at x_0 :

$$(6) \quad Z_{DK}^*(x_0) = \sum_{k=0}^K C_k H_k^*[Y(x_0)]$$

using the coefficients C_k obtained previously. The prediction error variance for DK and DCK are then given by:

$$(7) \quad \begin{aligned} \sigma_{DK}^2 &= \sum_{k=1}^K k! * C_k^2 * [1 - b'_k \rho_k] \\ \sigma_{DCK}^2 &= \sum_{k=1}^K k! * C_k^2 * \left[1 - (b'_k \ a'_k) \begin{pmatrix} \rho_{k,1} \\ \rho_{k,2} \end{pmatrix} \right] \end{aligned}$$

respectively. Extension of these equations towards more than 1 covariable is straightforward.

5. The conditional probability P that the predicted leaching concentration at location x_0 exceeds a critical threshold (the cutoff value y_c) is estimated:

$$(8) \quad P_{y_c}^*(x_0) = 1 - \Phi(y_c) + \phi(y_c) \sum_{k=1}^K \frac{H_{k-1}[y_c] H_k^*[Y(x_0)]}{k!}$$

where $\phi(\cdot)$ is the standard normal density function and $\Phi(\cdot)$ the standard normal distribution function (see Appendix).

Optimizing the Number of Simulations

The maximum number of possible simulation points was 402. Simulations on all locations would result in a very high computing effort (11.2 CPU-days on a 486-25MHz machine). We tried therefore to minimize the number of simulations and use these simulation results to complete the data set to $n=402$. Since values of a presumably highly correlated covariable were known on all 402 locations, Disjunctive CoKriging was used in the minimization procedure.

A testset of 50 randomly selected locations was chosen. Scenario S-0 was used to define two quality criteria. The 402 results were split in the testset (50 samples) and a set of predictand values (352 samples). Interpolated values of nitrate leaching concentrations were obtained by Disjunctive Kriging to the 50 test points, and the Mean Variance of Prediction Error (MVPE) and the Mean Square Error of Prediction (MSEP) were

calculated. Both the MVPE and the MSEP were expressed as a fraction of the sample variance at $n=352$, and these fractions were defined as quality criteria for MVPE and MSEP. Relative instead of absolute criteria were set, because leaching values and variance levels of scenarios S-1 to S-6 were expected to be different. An absolute criterium based on scenario S-0 could easily be satisfied by a scenario with a lower mean leaching concentration or variance level (the lower input scenarios), whereas it could be impossible to satisfy by a scenario with higher mean or variance levels.

For each scenario, a minimal data set was defined, consisting of 38 simulations, located on a triangular grid with a base distance of 48 m. to cover the entire field. On the 50 test points simulations were done as well. Exponential and Spherical variogram models were fitted to experimental semivariances by a weighted least squares method. Crossvalidation, using Ordinary Kriging, was done to choose the best performing model (McBratney and Webster, 1986). Disjunctive CoKriging (DCK) predictions were carried out on the 50 test points, always using the nearest 12 observations on the predictand and 16 on the covariable. The MVPE and MSEP were calculated, expressed as a fraction of the sample variance, and compared to the criteria described above. If not both the MVPE and MSEP criteria were satisfied, the data set was expanded by performing 10 more simulations, randomly chosen from the remainder of available locations. Variograms were fitted and validated anew, and the test was repeated. If both criteria were satisfied, it was concluded, that the data set could be expanded to $n=402$ accurately by DCK, using the available simulations and the values of the covariable.

RESULTS AND DISCUSSION

Interpolation Quality

Figure 1 shows the variogram and distribution of simulation scenario S-0. An exponential variogram model with parameters Nugget=0.8, Sill=1.538 and $r=99.5$ was chosen to fit the data best after crossvalidation. Hermite polynomials of 5 terms could accurately reproduce the sample distribution, as the lines in the probability graph pass through the sample values. The critical nitrate leaching concentration of $25 \text{ mg NO}_3/\text{dm}^3$ is exceeded in more than 60% of the simulated cases.

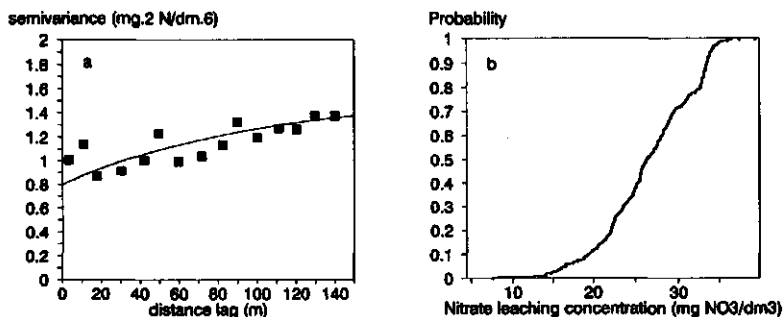


Figure 1 Sample and fitted model variograms (a) and sample and hermite transform distributions (b) of scenario S-0. Points indicate sample values, lines indicate model estimates.

In figure 2, variograms and crossvariograms are given for scenarios S-1 to S-6, based on the minimal data set of 38 samples. In all cases, exponential variograms better fitted the data than spherical variograms. As expected, nitrate leaching concentrations obtained with these scenarios were highly correlated to those obtained with scenario S-0 (Table 2).

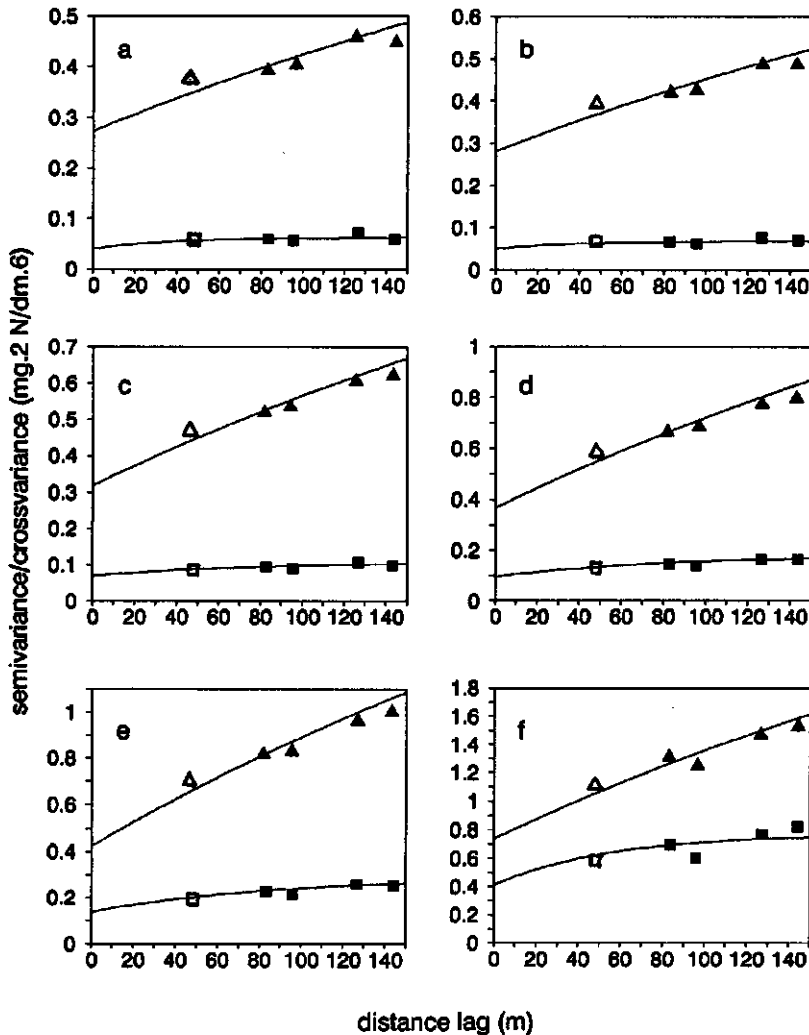


Figure 2 Sample variograms (squares) and crossvariograms (triangles) with scenario S-0 and fitted models for the minimum data set ($n=38$). Open markers indicate 30-50 pairs, closed markers indicate more than 50 pairs. Graphs a to f indicate scenarios S-1 to S-6 respectively.

Table 2 Correlations between scenarios S-1 to S-6 and S-0 for datasizes of 38 to 80 observations. *n.d.* is not determined.

Data size	Scenario					
	S-1	S-2	S-3	S-4	S-5	S-6
38	0.93	0.93	0.96	0.98	0.98	0.85
50	0.90	0.91	0.95	0.97	0.98	0.84
60	0.90	0.92	0.95	0.97	0.98	0.83
70	0.90	0.91	0.95	0.97	0.97	0.82
80	n.d.	n.d.	n.d.	n.d.	0.97	0.80

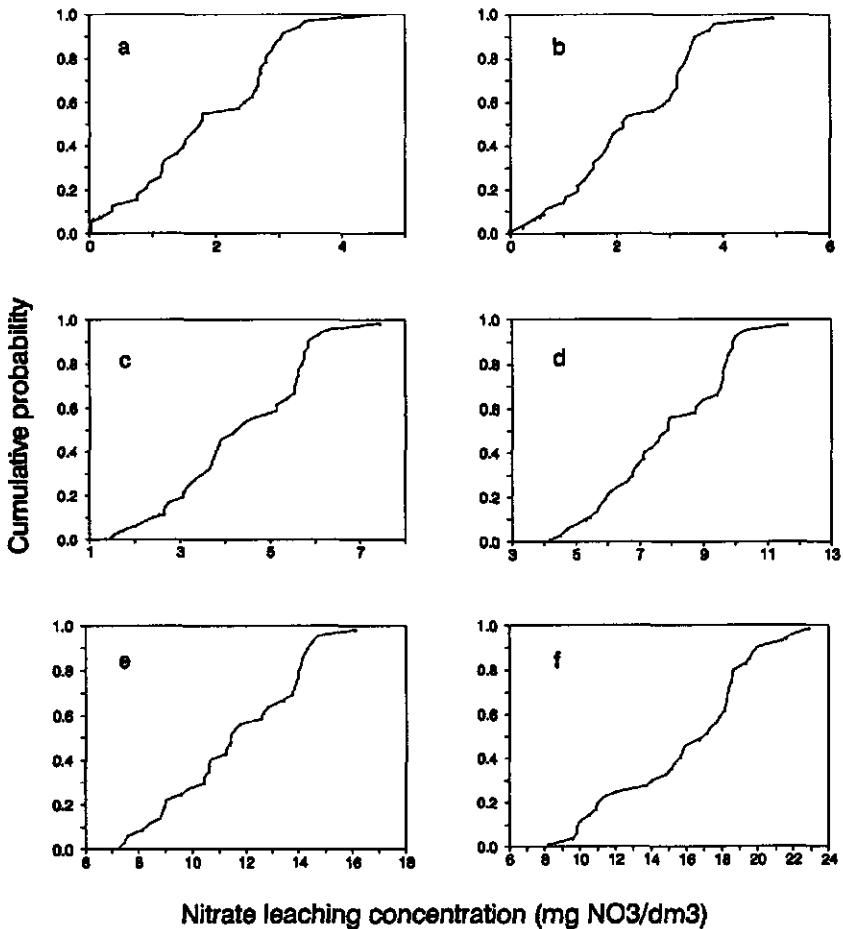


Figure 3 Sample distributions (dots) and Hermite transform distributions (closed lines) for a sample size *n* of 38. Graphs a to f indicate scenarios S-1 to S-6 respectively.

Sample distributions and reconstructed distributions based on 5-term Hermite polynomials are given in Figure 3. Sample distributions could be reconstructed well from normalized data by 5-term Hermite polynomials. The sample distributions of scenario S-3 (fig. 3c) and S-0 (fig. 1) clearly differ. The higher leaching concentrations from S-0 indicate the lagged effect of a history of over-fertilization.

Interpolation of S-0 values to 50 test points yielded a MVPE value of 0.980 and a MSEP value of 0.541, where the sample variance was 1.588. By taking the ratios MVPE/variance and MSPE/variance, quality criteria were defined as:

1. MVPE: $0.617 \cdot \text{sample variance}$, and
2. MSEP: $0.341 \cdot \text{sample variance}$.

A comparison of interpolated values to the MVPE and MSEP criteria is made in Figure 4. For scenario S-1, S-2, S-3 and S-4, 70 simulations were sufficient to satisfy both criteria, a reduction of 80% relative to the 352 simulations of scenario S-0 (testset not counted). Scenario S-5 and S-6 needed 10 more simulations.

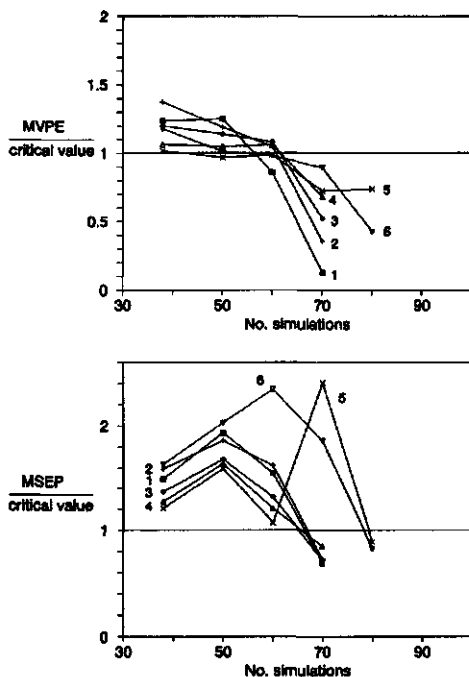


Figure 4 Quality of interpolations by DCK to 50 test points. Critical values are defined in text.

MVPE-values relative to the critical value of $0.617 \cdot \text{sample variance}$ show a tendency of steady decrease when the number of simulations increases. Relative MSEP-values tend to fluctuate in case of scenarios S-5 and S-6. This is partially caused by the smaller critical value ($0.341 \cdot \sigma_{n-1}^2$), which makes the value on the Y-scale more sensitive to variations in the sample variance. Partially it may also be caused by inaccuracy of the (cross-)

variogram models.

Conditional Probability

From the sample distributions of scenarios S-1 to S-6 (Fig. 3) it is clear that only for S-6 the leaching criterion may be locally violated, because the tail of the distribution approaches the 25 mg NO₃/dm³ threshold. Whether this is identified by Disjunctive Kriging depends both on the tail of the distribution and on the prediction value. A larger data set results in a wider distribution, because when data are generated by DCK, some variance is lost. For S-6, this difference in shape is crucial, because it determines whether or not the tail of the distribution exceeds the threshold value of 25 mg NO₃/dm³. It was therefore decided to do simulations on all available locations (n=402) for this specific scenario.

In figure 5, the cumulative probability density graphs are given of scenario S-6, based on the complete data set (n=402) and the smaller data set expanded by DCK to n=402. The expanded data set evidently exhibits a narrower distribution, indicating that reduction of the number of simulations by DCK is not advisable when probabilities of exceedance are to be estimated.

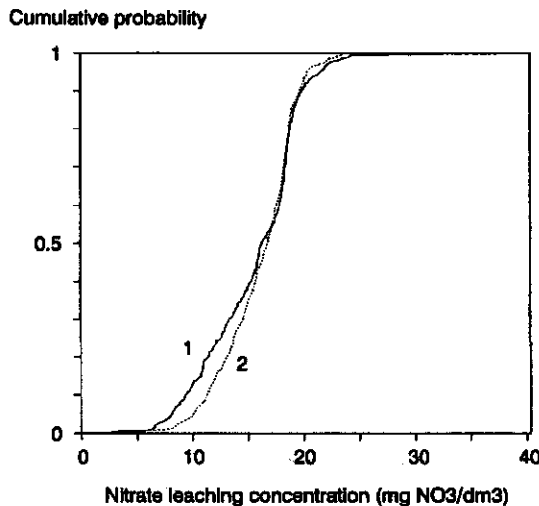


Figure 5 Cumulative probability graphs of scenario S-6 nitrate leaching concentrations based on 402 simulations (1) and on 80 simulations expanded to 402 by DCK (2).

A map of the conditional probability of exceeding the threshold leaching concentration of 25 mg NO₃/dm³ at fertilizer levels corresponding to scenario S-0 and S-6 is given in Fig. 6. Scenario S-0 results in leaching concentrations clearly exceeding the criterion. The leaching criterion is scarcely exceeded in case of scenario S-6. In 1.4% of the field area the probability of exceeding the threshold level is higher than 5%, implicating the area where the scenario is rejected. A map of scenario S-6 (not shown), whereby the data set was expanded to 402 simulations by DCK first, did not show any areas where the leaching criterion was exceeded, because of the loss of variance associated with this method.

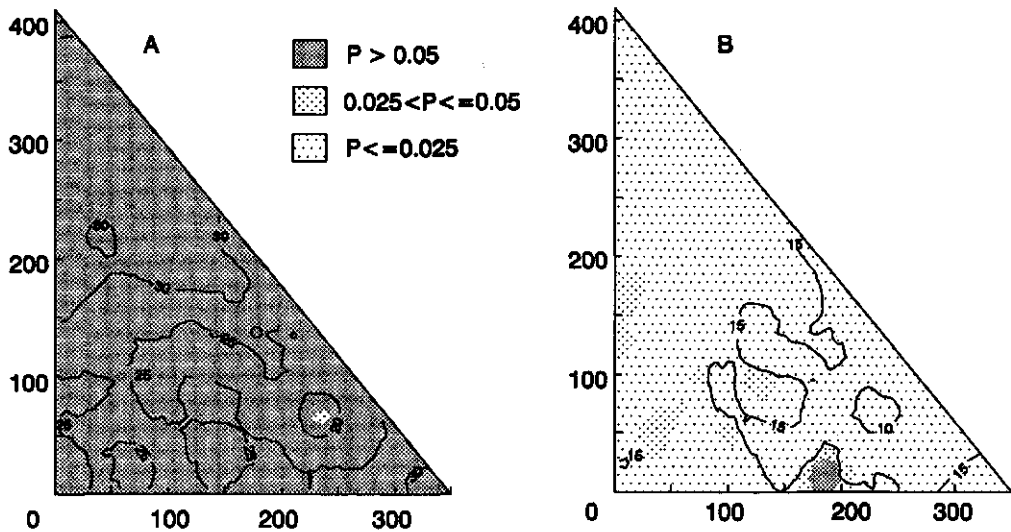


Figure 6 Maps of simulated Nitrate leaching concentrations (isolines) and of the probability (P) of exceeding a $25 \text{ mg NO}_3/\text{dm}^3$ cutoff level (gray levels). A and B denote scenarios S-0 and S-6 respectively.

As a result, it was concluded that pursued nitrate leaching concentrations of $25 \text{ mg NO}_3/\text{dm}^3$ will be violated with high probability for one hydrological year after lowering fertilizer gifts because of lagged leaching as a result of a history of over-fertilization (scenario S-0). In the first hydrological year, fertilizing according to scenario S-6 will lead to a locally too high probability that the pursued level is exceeded. All other scenarios are safe in terms of nitrate leaching on the short term. This implies that scenario S-5 would be the most attractive to implement, because it will give the highest crop yields.

CONCLUSIONS

1. Disjunctive CoKriging with a highly correlated covariable greatly reduced the number of simulations in a scenario analysis without loss of prediction quality in terms of MSE and MVPE.
2. When the cutoff-value is in the tail of the distribution, it is important to estimate the distribution function correctly. It is then better to take many samples of the predictand than to use a covariable to expand the data set, because variance is lost in this process.

ACKNOWLEDGEMENT

This research was partly carried out during a stay of the second author at the University of Arizona, with a grant of the Netherlands Integrated Soil Research Programme. Financial support by EC-project EV4V*0098-NL "Nitrate in Soils" is gratefully acknowledged.

APPENDIX Hermite polynomials and conditional probability

Hermite polynomials

Hermite polynomials $H_k(y)$ of order k are defined as:

$$(A1) \quad H_k(y) = (-1)^k e^{\frac{y^2}{2}} \frac{d^k}{dy^k} \left(e^{-\frac{y^2}{2}} \right)$$

It is easily seen that $H_0(y)=1$ and $H_1(y)=y$. A simple relation exists between $H_{k+1}(y)$, $H_k(y)$ and $H_{k-1}(y)$ for $k \geq 2$: $H_{k+1}(y) = yH_k(y) - kH_{k-1}(y)$. Hermite polynomials are orthogonal with respect to the weighting function $\exp(-y^2/2)$ on the interval $[-\infty, \infty]$, that is:

$$(A2) \quad \frac{\int_{-\infty}^{\infty} H_i(y)H_j(y)e^{-\frac{y^2}{2}} dy}{i! \sqrt{2\pi}} = \delta_{ij}$$

with $\delta_{ij}=0$ when $i \neq j$ and $\delta_{ij}=1$ when $i=j$.

Many functions can be approximated by a finite series of Hermite polynomials:

$$(A3) \quad f(x) = \sum_{k=0}^{\infty} C_k H_k(x)$$

where fitting the coefficients C_k is based upon the orthogonality relationship (A2). It may be done efficiently by means of Hermite integration (Abramowitz and Stegun, 1965).

Conditional probability

An estimator of the conditional probability that a variable at a location x_0 exceeds a cutoff level z_c is based on the indicator function $\Theta_{y_c}(Y) = 1$ if $Y \geq y_c$ and $\Theta_{y_c}(Y) = 0$ if $Y < y_c$, where y_c is the transformed cutoff level related to the actual cutoff level z_c and Y is the transformed variable related to Z . The conditional expectation of Θ_{y_c} in the unvisited location x_0 is given by:

$$(A4) \quad E [\Theta_{y_c}(Y(x_0)) \mid Y(x_i)] = P [\Theta_{y_c}(Y(x_0))=1 \mid Y(x_i)]$$

since Θ_{y_c} is either 1 or 0. The conditional probability of $Z(x_0)$ exceeding z_c is thus estimated by the conditional expectation of the indicator function $\Theta_{y_c}(Y)$ in location x_0 . Now, $\Theta_{y_c}(Y(x_0))$ can be estimated when it is expanded in Hermite polynomials (Yates *et*

al., 1986) as:

$$(A5) \quad \Theta_{y_c}(Y(x_0)) = \sum_{k=0}^K \vartheta_k H_k(Y(x_0))$$

where the Hermite coefficients ϑ_k for order k are determined using the orthogonality relations (A2): $\vartheta_0 = 1 - \Phi(y_c)$, and $\vartheta_k = \phi(y_c) H_{k-1}(y_c) / k!$, where $\Phi(\cdot)$ is the cumulative standard normal probability distribution and $\phi(\cdot)$ its probability density function.

Combination of (A4) with the DK or the DCK predictor gives the conditional probability that $Y(x_0) \leq y_c$, estimated by the sum of the predictions of the Hermite polynomials that describe $\Theta_{y_c}(Y(x_0))$:

$$(A6) \quad P^*(x_0) = 1 - G(y_c) + g(y_c) \sum_{k=1}^K H_{k-1}(y_c) H_k^*(Y(x_0)) / k!$$

REFERENCES

- Abramowitz, M. and A. Stegun. 1965. Handbook of mathematical functions. Dover, New York.
- Anderson, G.D., J.J. Opaluch and W.M. Sullivan. 1985. Nonpoint agricultural pollution: pesticide contamination of groundwater supplies. Am. J. of Agric. Econom. 67/5: 1238-1243.
- Commission of the European Communities. 1991. Soil and groundwater research report II "Nitrate in Soils". CEC, Luxembourg.
- Dagan, G. and E. Bresler. 1983. Unsaturated flow in spatially variable fields. 1. Derivation of models of infiltration and redistribution. Water Res. Research 19: 413-420.
- Finke P.A. and W.F.P. Bosma, 1993. Obtaining basic simulation data for a heterogeneous field with stratified marine soils. In: Hydrological Processes 7(2): (in press).
- Finke, P.A. 1992. Field scale variability of soil structure and its impact on crop growth and nitrate leaching in the analysis of fertilizing scenarios. 1992 Conference of working group MV of the International Society of Soil Science: Operational methods to characterize soil behaviour in space and time.
- Hutson, J.L. and Wagenet, R.J., 1991. Simulating nitrogen dynamics in soils using a deterministic model. Soil use and management 7(2): 74-78.
- Johnsson, H., Bergstrom, L., Jansson, P.-E. and Paustian, K., 1987. Simulated nitrogen dynamics and losses in a layered agricultural soil. Agriculture, Ecosystems and Environment 18, 333-356.
- Kim, Y.C., D.E. Myers, and H.P. Knudsen. 1977. Advanced geostatistics in ore reserve estimation and mine planning practioner's guide. Report to the U.S. Energy Research and Development Administration, subcontract No. 76-003-E, Phase II.
- Matheron, G. 1976. A simple substitute for conditional expectation: the disjunctive kriging. In M. Guarascio *et al.* (ed.) Advanced geostatistics in the mining industry. NATO Advanced study institute series, Reidel, Dordrecht.
- McBratney, A.B. and R. Webster. 1986. Choosing functions for semivariograms and fitting them to sampling estimates. J. Soil Sci. 37: 617-639.
- Robert, P.C. 1988. Land evaluation at farm level using soil survey information systems.

- In: Land Qualities in Space and time. Proceedings of a symposium organized by the International Society of Soil Science (ISSS) Wageningen, The Netherlands, 22-26 August 1988: 299-311.
- Wagenet, R.J. and J.L. Hutson. 1989. Leaching Estimation And Chemistry Model: A process-based model of water and solute movement, transformations, plant uptake and chemical reactions in the unsaturated zone. Continuum Water Resources Institute, Cornell University, NY.
- Webster, R. and M.A. Oliver. 1989. Optimal interpolation and isarithmic mapping of soil properties. VI. Disjunctive Kriging and mapping the conditional probability. *Journal Soil Sci.* 40: 497-512.
- Yates, S.R., A.W. Warrick and D.E. Myers. 1986. Disjunctive Kriging 1. Overview of estimation and conditional probability. *Water Resources Research* 22/5: 615-621.
- Yates, S.R., 1986. Disjunctive Kriging 3. Disjunctive Cokriging. *Water Resources Research* 22/5: 1371-1376.

SAMENVATTING

In dit proefschrift wordt de invloed behandeld van bodemvariabiliteit op de variabiliteit van gesimuleerde landkwaliteiten op veldschaal. In hoofdstuk twee en drie worden procedures behandeld die werden gevolgd om deze invloed te kunnen vaststellen. In totaal zijn in dit proefschrift zeven manuscripten opgenomen, die alle bij internationale, gejureerde tijdschriften zijn ingediend dan wel reeds zijn verschenen.

Hoofdstuk twee besteedt aandacht aan methoden die zijn gehanteerd om de ruimtelijke variabiliteit te bemonsteren en aan het beschrijven van aan de bodemstructuur gerelateerde bodemkarakteristieken. In een manuscript wordt een nieuwe methode beschreven om betrouwbaarheidsintervallen te verbinden aan de resultaten van punttellingen aan slijpblaten in het geval dat de waarnemingen ruimtelijk zijn gecorreleerd. Betrouwbaarheidsintervallen zoals die worden bepaald met behulp van de traditionele methode, waarbij alle waarnemingen onafhankelijk worden verondersteld, zijn aanzienlijk smaller dan wanneer de ruimtelijke afhankelijkheidsstructuur bij de bepaling wordt betrokken.

Twee andere manuscripten in hoofdstuk twee beschrijven een methode om profielbeschrijvingen te vertalen in bodemfysische invoergegevens voor computermodellen die het transport van opgeloste stoffen in de bodem simuleren. Hiertoe wordt het begrip functionele laag toegepast. Een functionele laag is een combinatie van lagen of horizonten in de bodem die, voor wat betreft hun stromingsgedrag, vergelijkbaar zijn. Deze benadering is getest en geaccepteerd voor verstoorde en fijn-gelaagde bodems nadat functionele eigenschappen met betrekking tot de waterstroming onder goed gedefinieerde hydrologische condities waren berekend. Nadat de functionele lagen zijn gedefinieerd, kan de ruimtelijk variërende bodemfysische invoer worden verkregen door het uitkarteren of bemonsteren van het type, de dikte en de aanvangsdiepte van de functionele lagen. Een van de manuscripten in hoofdstuk twee gaat in op de vraag hoe deze gegevens het meest efficiënt kunnen worden verzameld, lettend op de kwaliteit van interpolaties en op het aantal benodigde waarnemingen. Hiertoe worden een geostatistische methode en een methode voortkomend uit de klassieke steekproeftheorie als alternatieven vergeleken.

Hoofdstuk drie behandelt de invloed van de bodemvariabiliteit op variabiliteit van gewasopbrengsten en nitraatuitspoeling. In een manuscript wordt een empirische studie beschreven, waarin de variabiliteit van de gerstoogst wordt gecorreleerd met de variabiliteit van bodemeigenschappen en gesimuleerde transpiratietekorten. Regressiefuncties gebaseerd op gesimuleerde transpiratietekorten alleen konden 43% van de gerstoogstvariabiliteit verklaren. Dit suggereerde dat de variabiliteit van de transpiratie een belangrijke oorzaak van oogstvariabiliteit zou zijn. Deze hypothese werd getest in een andere studie. Metingen van de gewasreflectie voor infrarood straling werden gebruikt om het bladoppervlak te schatten op een groot aantal locaties en vijf tijdstippen. Deze gegevens werden vervolgens gebruikt om de potentiële transpiratie van het gewas locatie-specifiek te schatten. Door de aldus verkregen bladoppervlaktes in te brengen in een gewasgroeimodel werden locatie-specifieke oogstopbrengsten gesimuleerd, welke werden vergeleken met metingen. Er bleek op deze manier 39% van de oogstvariabiliteit te kunnen worden verklaard. Er werd geconcludeerd, dat de variabiliteit van voor de plant beschikbaar bodemvocht, uitgedrukt door de actuele transpiratie, een belangrijke bepalende factor is voor de oogstvariabiliteit.

Twee manuscripten in hoofdstuk drie gaan in op het toepassen van een gecombineerd stromings- en gewasopbrengstmodel om het ruimtelijk variërend effect van

bemestingsscenarios te evalueren. De ruimtelijke interpolatiemethode *Disjunctive Kriging* werd toegepast om de ruimtelijke variabiliteit van gesimuleerde nitraatuitspoeling te vertalen in kaarten waarin de kans op overschrijding van een normwaarde is aangegeven. Tevens werd onderzocht of door toepassing van *Disjunctive CoKriging* het aantal simulaties kon worden verminderd door reeds aanwezige ruimtelijke informatie te gebruiken. Uit de resultaten van de simulaties werd geconcludeerd, dat de verschillende bodemeenheden binnen een perceel verschillend reageren op een identieke (kunst-) mestgift, zowel voor wat betreft de nitraatuitspoeling als de gewasopbrengst. Ook werd geconcludeerd, dat de variabiliteit van de oogst zal toenemen als het bemestingsniveau toeneemt.

CURRICULUM VITAE

Peter A. Finke werd op 29 november 1960 geboren te Zaandam. Na de lagere school met succes te hebben doorlopen begon hij in 1972 met de middelbare-school opleiding aan het St. Michaëlcollege te Zaandam, waar hij in 1979 het diploma Atheneum-8 behaalde. In datzelfde jaar begon hij met de studie Fysische Geografie aan de Universiteit van Amsterdam, waar hij in 1988 cum laude afstudeerde. De doctoraalvakken waren Bodeminventarisatie, Bodemvorming en Verwering, Simulatie van Geomorfologische Processen en Hoofdstukken uit de Informatica.

Per 1 juni 1988 trad hij als Assistent In Opleiding in dienst bij de Landbouwniversiteit te Wageningen bij de vakgroep Bodemkunde en Geologie, met als onderzoeksopdracht de karakterisering van de bodemstructuur op perceelsnivo ten behoeve van de simulatie van nutriëntstromen. Een belangrijk deel van dit onderzoek vond plaats in de context van het EG-onderzoeksproject 'Nitrate in Soils'.

In 1991 trouwde hij met Brit Scheeren. Zij hebben een zoon: Tim.